CHAPTER 1. INTRODUCTION

Vehicle fuel consumption and emissions are two critical aspects considered in the transportation planning process of highway facilities. Horowitz categorized the four major sources of polluting emissions from man-made sources as transportation, stationary fuel combustion, industrial processes, and solid waste disposal (Horowitz, 1982). Among these sources, pollutants from motor vehicle transport are generally referred to as mobile-source emissions. These emissions are the focus of this study (NRC, 1995).

According to a study, today's cars and trucks account for nearly 50% of the emission of ozone precursors (HC and NOx), and 90% of the CO emissions in urban areas (Heinsohn *et al*., 1999). Highway vehicles, which contribute more than one-third of the total nationwide emissions, are the largest source of transportation-related emissions (Nizich *et al*., 1994). Nationwide, motor vehicles are the source of more than 75 percent of the total CO emissions, and about 35 percent of emissions of HC and NOx (Nizich *et al*., 1994).

Light duty vehicles are further responsible for approximately 40 percent of all US oil consumption. However, according to a report, average new light duty vehicle fuel economy sold in US has to declined from 9.3 kpl (22.1 mpg) in 1987 and 1988 to 8.6 kpl (20.4 mpg) in 2001 (Hellman and Heavenrich, 2001). The decline could be due to the increasing market share of less efficient light duty trucks, increased vehicle weight, and increased vehicle performance.

1.1 PROBLEM DEFINITION

The 1990 Clean Air Act Amendments (CAAA) require states to attain and maintain ambient air quality standards. The requirements of the CAAA establish significant restrictions on the transportation sector, constraining in particular highway projects that expand capacity for their potential to increase motor vehicle traffic and emissions. These regulations give heavy burdens to local transportation planners and engineers who have responsibility to improve local traffic problems.

Current state-of-the-art models estimate vehicle emissions based on typical urban driving cycles. Most of these models offer simplified mathematical expressions to compute fuel and emission rates based on average link speeds without regarding transient changes in a vehicle's speed and

acceleration as it travels on a highway network (EPA, 1993c). Moreover, most models use an aggregate modeling approach where a 'characteristic' vehicle is used to represent dissimilar vehicle populations. While this approach has been accepted by transportation planners for the evaluation of network-wide highway impacts on the environment, it is not suited for the evaluation of energy and environmental impacts of operational-level projects. Instead, it can be argued that modeling individual vehicle fuel consumption and emissions coupled with the modeling of vehicle dynamics on a highway network could result in more reliable evaluations of operational-level project impacts.

1.2 RESEARCH OBJECTIVE

The primary objective of this dissertation is to develop mathematical models to predict vehicle fuel consumption and emissions under various traffic conditions. Current state-of-the-art models that are utilized to estimate fuel consumption and emissions are predicting their measures of effectiveness (MOEs) based on typical driving cycles using average speed. However, this approach of using certain cycle's average speed is not suitable for the evaluation of fuel consumption and emission impacts of operational level projects since it is impossible to differentiate projects having same average speeds with different driving conditions. This approach has been accepted by transportation planners and federal agencies to estimate highway impacts on the environment.

This dissertation addresses this issue, presenting a mathematical model to predict fuel consumption and emissions for individual vehicles using instantaneous speed and acceleration as explanatory variables. Today, the availability of relatively powerful computers on the average desktop makes this approach feasible, even for large highway networks. The introduction of Intelligent Transportation Systems (ITS) further makes a compelling case to compare alternative ITS and non-ITS investments with emphasis on energy and emission measures of effectiveness. Until now, the benefits derived from ITS technology in terms of energy and emissions have not been systematically quantified. The ultimate use of these models would be their integration into traffic network simulators and their use to better understand the impacts of traffic policies, including the introduction of ITS technology, on the environment. Furthermore, these models can be utilized in conjunction with Global Positioning System (GPS) speed measurements to evaluate the energy and emission impacts of operational-level projects in the field.

1.3 RESEARCH CONTRIBUTIONS

The dissertation develops instantaneous fuel consumption and emission models for light-duty vehicles and trucks under hot stabilized conditions. These models use vehicle instantaneous speed and acceleration levels as independent input variables. It is anticipated that the microscopic modeling provided in this dissertation will have many practical and methodological implications to local transportation planners and traffic engineers who will be able to use this modeling to accurately estimate pollutants and fuel consumption and predict the impacts of operational-level projects. Furthermore, the output of such models can serve as input to utilize dispersion models for the evaluation of regional air quality impacts. More specifically, this research effort makes the following contributions.

- Develops microscopic energy and emission models for normal light-duty cars and trucks under hot stabilized conditions,
- Develops a framework for modeling vehicle emissions microscopically,
- Develops procedures for estimating cold start impacts on vehicle emissions,
- Develops procedures for characterizing high emitting vehicles, and
- Develops microscopic emissions models for high emitting vehicles.

1.4 DISSERTATION LAYOUT

This dissertation is organized into eight chapters. The second chapter provides a review of current state-of-the-art energy and emission models. The literature review discusses the contribution of motor vehicle transportation to air pollution and energy consumption, including those factors affecting fuel consumption and emissions. Furthermore, regulations such as the air quality standards, Clean Air Act Amendments, conformity analysis, and the air-quality related planning process are discussed. Various existing fuel consumption and emissions models are also described. The third chapter presents an overview of the research methodology in terms of estimating hot stabilized vehicle emissions, cold start vehicle emissions, and the modeling of high emitters. Chapter 4 shows the development of fuel consumption and emission model, and describes mathematical approaches proposed for modeling highway vehicle energy consumption and emissions, as well as some validation results using field data and other emission model. Chapter 5 compares the model with various state-of-the-art models. Chapter 6 continues by

presenting a framework for developing microscopic emission models utilizing data obtained from the U.S. Environmental Protection Agency (EPA). In chapter 7, the dissertation investigates high emitter emission behaviors and derives multiplicative factors for newly developed EPA driving cycles. The chapter also describes high emitter modeling procedures. Subsequently, microscopic cold start emission behaviors and cold engine start emission modeling is presented in Chapter 8. Finally, chapter 9 provides a summary of the findings and the conclusions of the research effort.

CHAPTER 2. LITERATURE REVIEW

In order to provide a background for the research that is presented in this dissertation, a number of topics are discussed in this chapter. First, the US Federal air quality requirements are presented because these provide the motivation for this research effort. Secondly, vehicle, traffic, and driver related variables that impact vehicle emission levels are discussed. These key variables are critical for the development of comprehensive energy and emission models. Third, the current state-of-the-art energy and emission models are presented. In addition, the assumptions, domain of application, and shortcomings of these models are discussed. Finally, based on the limitations of the current state-of-the-art models, research recommendations are identified.

2.1 TRANSPORTATION POLLUTANTS

Transportation is one of the major contributors to man-made polluting emissions. According to a literature, transportation sources are responsible for about 45 percent of US nationwide emissions of the EPA defined pollutants (NRC, 1995). Most emissions that are produced by vehicles are generated in the combustion process and from evaporation of the fuel itself. Gasoline and diesel fuels are comprised of hydrocarbons and compounds of hydrogen and carbon atoms. In a perfect combustion, all the hydrogen in the fuel is converted into water, and the carbon is changed to carbon dioxide. Unfortunately, a perfect combustion process is impossible to achieve in the real word, and many pollutants result as by-products of this incomplete combustion process and from the evaporation of the fuel itself (EPA, 1994a).

The principal pollutants emitted from typical motor engines are carbon monoxide, hydrocarbon and oxides of nitrogen. Carbon monoxide (CO), a product of an incomplete combustion, is a colorless, odorless and poisonous gas. CO reduces the flow of oxygen in the bloodstream and is harmful to every living organism. In some urban areas, the motor vehicle contribution to carbon monoxide emissions can exceed 90 percent (EPA, 1993a).

Hydrocarbon (HC) emissions result from fuel that does not burn completely in the engine. It reacts with nitrogen oxides and sunlight to form ozone, which is a major component of smog. Ozone is one of EPA's defined pollutants known to cause irritations of the eyes, damage to the

lung tissue and affect the well being of the human respiratory system. Furthermore, hydrocarbons emitted by vehicle exhaust systems are also toxic and are known to cause cancer in the long term (EPA, 1994a).

While CO and HC are the product of incomplete combustion of motor fuels, oxides of nitrogen (NOx) are formed differently. NOx is formed by the reaction of nitrogen and oxygen atoms during high pressure and temperature chemical processes that occur during the combustion. NOx also leads to the formation of ozone and contribute to the formation of acid rain (EPA, 1994a).

The air/fuel (A/F) ratio is one of the most important variables affecting the efficiency of catalytic converters and the level of exhaust emissions (Johnson, 1988). The highest CO and HC are produced under fuel-rich conditions and the highest NOx is emitted under fuel-lean conditions. Generally, fuel-rich operations occur during cold-start conditions, or under heavy engine loads such as during rapid accelerations at high speeds and on steep grades. Therefore, high levels of CO and HC are generated on congested highways and in other high traffic density areas.

2.2 US FEDERAL LAW EMISSION REQUIREMENTS

The first significant legislation to recognize the harmful effects of air pollution on pubic health was the Clean Air Act Amendments (CAAA) of 1970. The CAAA established the U.S. Environmental Protection Agency (EPA) and mandated the EPA to set health-based national ambient air quality standards (NAAQS) for six pollutants: carbon monoxide (CO), lead (pb), nitrogen dioxide (NO_2), ozone (O_3), particulate matter (PM-10) and sulfur dioxide (SO_2) (NRC 1995). The Amendment further imposed automobile standards for 1975 models to achieve clean air by setting the 0.41 gram per mile HC standard and the 3.4 grams per mile CO standard. However, these standards were not achieved and the government delayed the HC standard until 1980 and the CO standard until 1981 in the Clean Air Act of 1977. In the amendment, the NOx standard was relaxed to 1 gram per mile and the deadline was extended until 1981 (EPA, 1994b).

2.2.1 1990 Clean Air Act (CAA)

In 1990, the new Clean Air Act, placed a heavy burden on the transportation community. This legislation was amended by Congress to require further reductions in HC, CO, NOx, and

particulate emissions. It also introduced a comprehensive set of programs aimed at reducing pollution from vehicles. These included additional technological advances, such as lower tailpipe standards; enhanced vehicle inspection and maintenance (I/M) programs; new vehicle technologies and the use of clean fuels; transportation management provisions; and possible regulation of emissions from non-road vehicles (EPA, 1994b). The regulations of the 1990 amendments resulted in emission reductions as newer, cleaner vehicles replaced older ones and as technology-oriented programs were implemented. However, these actions may not be sufficient to offset the growth in emissions from motor vehicle travel due to the rapid increase of annual vehicle mile traveled (VMT). In particular, EPA estimates that tail pipe emission gains could be offset by 2002 for CO and HC and by 2004 for NOx. Therefore, the CAAA requires the limitation of automobile trips and VMT growth in nonattainment areas (NRC, 1995).

The act defined deadlines to attain the goals that are set based on the severity of air quality conditions. According to the severity of condition, urban areas are classified as marginal, moderate, serious, severe and extreme. For ozone, forty areas that were ranked as marginal had 3 years from the baseline year, 1990, to attain the EPA standard. 29 areas for ozone and 37 for CO were classified as moderate and had 6 years to achieve the goal. There were twelve serious areas for ozone and one for CO with 9 years to establish compliance. There were nine severe cases for ozone with 15 years to achieve compliance. Only Los Angeles was classified as extreme for ozone and had 20 years to comply with the new standards. 83 areas for PM-10 have been designated as nonattainment areas. Los Angeles is also the only area that does not satisfy the NOx regulation (NRC, 1995; NRC, 1997).

The requirements were also different with one another according to the rank of air quality severity. Areas of moderate or worse ozone classification must submit revisions to State Implementation Plans (SIPs) showing that, during the period, ozone will be reduced by at least 15 percent. These areas must reduce by 3 percent the ozone emissions per year until attainment is achieved. Moreover, areas classified as severe or extreme are required to adopt transportation control measures (TCMs). TCMs are activities intended to decrease motor travel or otherwise reduce vehicle emissions. Areas with carbon monoxide specification are required to forecast vehicle miles traveled (VMT) annually, and if actual VMT exceeds expected VMT, they are

required to adopt TCMs that must be included in their SIPs. Furthermore, areas designated as serious for CO emissions are required to adopt TCMs (NRC, 1995).

The amendment of 1990 further defined sanctions for noncompliance. For failure to submit a SIP, EPA disapproval of a SIP, failure to make a required submission, or failure to implement any SIP requirement, highway projects assisted by federal government could be withheld. Additionally, if sanctions were commanded, the department of transportation (DOT) can only approve highway projects that would not increase single-vehicle trips (NRC, 1995).

2.2.2 Intermodal Surface Transportation Efficiency Act (ISTEA)

ISTEA supplements the CAAA by reinforcing air quality conformity requirements. The act allows to transfer highway funds to transit and other cleaner modes and enhances the planning responsibilities of MPOs that are responsible for conformity analyses. The legislation also provides authorizations for highway construction, highway safety, and mass transportation expenditures. The ISTEA created a new program, Congestion Mitigation and Air Quality Improvement (CMAQ), which provides funds to projects and programs in nonattainment areas in order to help achieve the NAAQS. The ISTEA provides major changes in the makeup of the nation's surface transportation systems, their priority goals, and how they are funded and administered.

2.2.3 State Implementation Plan Submissions (SIPs)

The federal CAA places most of the responsibility on the states to prevent air pollution and control air pollution at its source. In order for a state to conduct an air quality program, the state must adopt a plan and obtain approval of the plan from the EPA. Federal approval provides for some consistency in different state programs and ensures that a state program complies with the requirements of the CAA and EPA rules. A SIP adopted by a state government and approved by the EPA is legally binding under both state and federal law and may be enforced by either government (Minnesota Pollution Control Agency, 1998).

SIPs are a collection of regulations that demonstrate how a state will reduce pollution from the contaminated areas under the Clean Air Act. The states must obtain the approval from the public

before an SIP is consummated. EPA approves each SIP, and if it is not acceptable, the EPA can assume responsibility for enforcing the Clean Air Act in that state (EPA, 2001b).

SIPs focus on attainment and maintenance of the national ambient air quality standards (NAAQS). SIPs include state air quality rules, control strategies to attain and maintain the NAAQS, compliance schedules to attain the visibility protection. There are other state programs that require a plan and approval by the EPA, however, they are not termed "SIPs". For example, the CAA amendments of 1990 required state submittal of an operating permit program, and gives states the option of submitting an air toxics program.

In SIPs, air quality modelers must project mobile source emission inventories and calculate the differences in emissions between the Build and No-Build conditions of transportation plans, programs, and projects.

2.2.4 Conformity Process

The conformity process is designed to ensure that a nonattainment area will keep transportation-related emissions within the bounds to bring the state into compliance with NAAQS. Other purposes are mentioned in the conformity regulations as well, including establishment of a procedural framework and incentives for analyzing transportation related pollution, improvements in both transportation and air planning processes and establishment of tighter connections between the two, and improvements in public deliberations and decisions on transportation and air quality issues. Furthermore, It is believed that the conformity process promotes transit enhancements, other transportation control measures (TCMs), and increased land use regulation (Howitt *et al.*, 1999).

Conformity requires that Metropolitan Planning Organization (MPO) and DOT transportation plans, programs, and projects in nonattainment areas be in accordance with the compliance standards contained in the SIPs. Under the CAAA, the new conformity rules require MPOs and DOT to demonstrate that transportation activities will not cause or contribute to any new violations, or delay timely attainment of standards (NRC, 1995).

The notable feature of the conformity process is the project level review. MPOs in nonattainment and maintenance areas must demonstrate that (a) all federally funded and regionally significant

projects, including nonfederal projects, in regional transportation improvement programs (TIPs) and plans will not produce higher levels of emissions than in a 1990 baseline year; and (b) when these projects are built, emissions will be lower than if the projects are not built. Also, MPOs must explain using a regional analysis that the emissions produced by the implementation of transportation plans and TIPs will not exceed target levels or emission budgets for motor vehicle emission sources from nonattainment and maintenance areas contained in the SIPs (NRC, 1995). Emission budget is the maximum amount of pollution of a particular type, e.g., from mobile source, allowable under an SIP (Howitt *et al.*, 1999). If modeled transportation pollutant estimates exceed SIP emission budgets, the MPO must alter its transportation land and programs to meet the budget constraints. Furthermore, MPOs must demonstrate timely implementation of TCMs in their SIPs. Each MPO must also accomplish the Intermodal Surface Transportation Efficiency Act (ISTEA) "fiscal constraint" requirement for TIPs and plans by showing that the financial resources are to be available to carry out the state's plan and programs (Howitt *et al.*, 1999).

In order to comply with the conformity regulations, MPOs must adjust emission estimates from TIPs and plans with those contained in the motor vehicle emission budgets in SIPs. Also, MPOs must conduct periodic testing to determine whether actual emissions are in line with estimates, and take corrective action if they are not (NRC, 1995).

2.2.5 Transportation Control Measures (TCMs)

TCMs are an important component of an overall strategy for reducing mobile source emissions. The CAAA and the ISTEA both discuss TCMs as a transportation strategy to be integrated into transportation and environmental planning and programming. Many MPOs count heavily on emission alleviation from TCMs that are often focused on the commuting trip because these trips typically have lower vehicle occupancies, occur daily, and tend to be concentrated during the congested peak hours. Experience has show how employers can significantly influence the commuting pattern of their employees and many TCMs are thus utilizing employer-based commuter programs. Specifically these TCM activities include the distribution of commuter marketing materials; telecommuting programs; flexible, staggered work hours; transit pass and rideshare subsidies; rideshare matching information and services; and bicycle amenities, such as showers, clothing lockers, and safe storage for bikes. More extensive TCM programs include

parking pricing, carpool parking, carpool coordination support, and a guaranteed ride home program (NRC, 1997).

2.3 TRANSPORTATION ENERGY CONSUMPTION

Major legislation has not been issued in the fuel energy sector since Congress passed the Energy Policy and Conservation Act (EPCA) of 1975, which set the fuel economy standard for new manufactured automobiles. The EPCA require that auto makers increase the corporate average fuel economy (CAFE) of automobiles and light trucks sold in the United States to 11.7 km/h (27.5 mpg) in the 1985 model year and thereafter. Between 1970 and 1992, in-use fuel economy for average passenger cars improved from an average of 5.7 km/h (13.5 mpg) to 9.2 km/h (21.6 mpg), which is a 60 percent enhancement. These improvements are attributed to the introduction of CAFE standards, technology improvements such as electronic fuel injection and more efficient engines and transmissions, and the reduced weight of passenger vehicles. However, although vehicle fuel economy has been improved, during the past decade the low price of gasoline, growing motor vehicle ownership and increased motor vehicle travel have resulted in a steady increase of transportation's share of total petroleum consumption in the United States. For example, in 1992, the transportation sector was responsible for 65 percent of total gasoline consumption. Consequently, energy officials have investigated and continue to search for means to improve fuel efficiency and reduce vehicle travel to reduce energy consumption (NRC 1995).

2.4 FACTORS AFFECTING TRANSPORTATION POLLUTANTS

Emissions that result from transportation sources are caused by several variables. These variables have been categorized (NRC 1995) as follows:

- travel-related factors,
- driver-related factors,
- highway network characteristics, and
- vehicle characteristics and other factors.

The following paragraphs describe in detail these factors.

2.4.1 Travel-Related Factors

Pollutants emitted from motor vehicles are dependent on the number of trips, distance traveled, and the portion of different vehicle operating modes. Emissions from vehicle include exhaust emissions and evaporative emissions. The former includes start-up emissions, which are classified as cold start or hot start depending on how long the vehicle has been turned off, and running emissions, which are emitted during a hot stabilized mode. The latter comprise running losses and hot soak emissions produced from fuel evaporation when an engine is still hot at the end of a trip, and diurnal emissions, which results from evaporation from the gasoline tank regardless of whether the vehicle is operated or not. (NRC 1995).

Speed, acceleration and engine load of a vehicle are also significant factors that impact emission rates. According to current model estimates such as MOBILE5a developed by EPA and EMFAC7F developed by the California Air Resources Board (CARB), emissions are generally high in low speed, congested driving conditions. Emissions fall at intermediate speed, low density traffic conditions. On the other hand, NOx has a different attribute showing the highest point at high speed (NRC 1995). However, these estimates have some problems. For example, sharp acceleration, which contribute high emission rates, is not explained in existing emission models. Acceleration, which causes a vehicle to operate in a fuel-rich mode, must be used as an input factor to estimate accurate emission rates in these models.

2.4.2 Driver-Related Factors

Smoothness and consistency of vehicle speed, which are heavily affected by driving behavior and traffic conditions, are important elements that affect vehicle emissions. Sharp acceleration caused from passing, changing lanes, merging onto a freeway from a ramp, or leaving a signalized intersection impose heavy loads on the engine and result in high emission levels. Aggressive driving may result in CO emission levels 15 times higher, and VOC levels 14 times higher, than those resulting from "average" driving. These results were attained by comparing time-space-emission traces for the same 11 km (7 mi) trip from downtown to an outlying area (NRC 1995).

2.4.3 Highway-Related Factors

Emission rates of motor vehicles also depend on the geometric design of the highway. Highways with facilities such as signalized intersections, freeway lamps, tool booths and weaving sections may increase the emission levels due to the engine enrichment from accelerations. Grade on highways is one of the large contributors affecting emission rates. On a steep grade, vehicles require more engine power. That requires high A/F ratio (high enrichment statues) to maintain the same speeds. Road conditions are also considered in estimating emissions.

2.4.4 Vehicle-Related And Other Factors

Vehicle characteristics such as engine size, horsepower and weight are also factors influencing emission rates on highways. Generally, vehicles with large engine sizes emit more pollutants than vehicles with small engines, and large engine sizes are commonly accompanied with high maximum horsepower and heavier vehicle.

Emission rates also vary with vehicle age. Older vehicles produce higher emission rates than newer fuel-injected vehicles during normal operation and vehicle starts (Enns *et al.*, 1993). Furthermore, older vehicles were not designed for the more restrictive emission standards that are currently in place. According to known data, 1975-model vehicles emit CO and HC emissions three times more than 1990-model vehicles (US DOT and EPA, 1993).

Vehicle-to-vehicle and vehicle-to-control interaction can be significant impacts to the vehicle emissions. These factors can be designated as the traffic-related factors.

Ambient temperature is an important parameter affecting both exhaust and evaporative emissions. The engine and emission control system take longer to warm up at cold temperature increasing cold start emissions. Moreover, as the temperature increases, evaporative emissions increase with higher emission rates.

2.5 Factors Affecting Transportation Energy Consumption

The primary energy source for the transportation sector is petroleum. The sector consumes nearly two-thirds of the petroleum used in the United States. The highway traffic is responsible

for nearly three-fourths of the total transportation energy use, with about 80 percent from automobiles, light trucks, and motorcycles and about 20 percent from heavy trucks and buses (Davis, 1994). The principal factors affecting fuel consumption are highly related to those affecting emissions. These include travel-related factors, highway conditions and other vehicle factors.

2.5.1 Travel-Related Factors

Fuel consumption is highly dependent on many different traffic characteristics. Speed and acceleration are significant factors affecting fuel consumption rates. Generally, fuel consumption rates increase as speed and acceleration increase. Also, fuel consumption rates are increased by engine friction, tires and accessories such as power steering and air conditioning at low speeds and dominated by the effect of aerodynamic drag on fuel efficiency at high speeds (An and Ross, 1993a).

The modal operation of the vehicle also affects fuel consumption. Engines typically take several minutes to reach their normal operation. The cold start fuel consumption experienced during the initial stages of the trip results in lower fuel efficiency than when the engines are fully warmed up (Baker, 1994).

2.5.2 Driver-Related Factors

Driving behavior, such as accelerations, braking, and gear shifting, is an important element that affects the fuel economy. Aggressive behaviors, sharp acceleration and braking, both negatively affect fuel economy when compared to cruise-type driving. According to An *et al.*(1993c), repeated braking behavior can cost up to 15 percent of fuel use in an urban driving trip and, in a congested urban area, aggressive driving with quick accelerations may result in a 10 percent increase in fuel use. Therefore, highway capacity additions, advanced traffic control devices, and traffic smoothing strategies that affect both traffic conditions and driver behavior can improve fuel economy.

2.5.3 Highway-Related Factors

Highway related factors such as steep grades and poor road surface conditions also reduce fuel efficiency. On steep grades, vehicles expand additional power to overcome grade resistance,

thus consuming more fuel than under normal conditions. Also, rough roads can lead to significant increments in fuel consumption by influencing the rolling resistance. At typical highway speeds, a vehicle tested on a rough road increased its fuel consumption by five percent over a vehicle tested on a normal quality road (Baker, 1994).

2.5.4 Vehicle-Related And Other Factors

Vehicle characteristics such as weight, engine size, and technologies are the primary factors affecting fuel economy. Generally, larger and heavier vehicles, vehicles with automatic transmissions, and vehicles with more power accessories (e.g., power seats and windows, power brakes and steering, and air conditioning) require more fuel than vehicles lacking these systems (Murrell, 1980).

Without proper vehicle maintenance, fuel consumption can increase by as much as 40 percent (Baker, 1994). According to this literature, improper engine tuning can increase average fuel consumption by about 10 percent and wheel misalignment as small as 2 mm can cause an increase of fuel consumption by about 3 percent due to increases in rolling resistance between the vehicle tires and the pavement surface (Baker, 1994).

Finally, the influence of weather conditions contributes to the fuel economy. Fuel consumption rates worsen at low temperatures and high winds, which result in aerodynamic losses (Murrell, 1980). For example, in Europe, fuel consumption in winter is worse than in summer by about 15 to 20 percent (Baker, 1994).

2.6 State-of-the-Art Energy and Emission Models

This section describes the various state-of-the-art energy and emission models as a background before comparing the models. These models are categorized as macroscopic and microscopic models. Macroscopic models use average aggregate network parameters to estimate network-wide energy consumption and emission rates. Alternatively, microscopic models estimate instantaneous vehicle fuel consumption and emission rates that are aggregated to estimate network-wide measures of effectiveness.

2.6.1 Macroscopic Emission Models

The EPA's MOBILE model and the California Air Resources Board's (CARB's) EMFAC model are two emission models that are commonly utilized in the United States. These models have been authorized by the EPA to perform conformity analysis. The EMFAC model is currently utilized in the state of California while the MOBILE model is utilized in all other states. Both models produce activity-specific emission rates that are a function of vehicle type and age, average speed, temperature, altitude, vehicle load, air conditioning usage, and vehicle operating mode. These emission rates are multiplied by vehicle activities such as vehicle miles-traveled, number of trips and vehicle-hours traveled in order to estimate total emission levels. The MOBILE model estimates three pollutants: hydrocarbons (HC), carbon monoxide (CO), and oxides of nitrogen (NO_x), while the EMFAC model produces composite emission factors for these three pollutants plus particulate matter.

Current estimates of emission rates produced by the MOBILE and EMFAC models are expressed as functions of average speeds and are based on vehicle testing on a limited number of driving cycles. Emission rates at average speeds other than the basic case are multiplied by the appropriate speed correction factor (SCF) associated with a vehicle class and operating speed. SCFs are derived from emissions data from tests over several driving cycles of different average speeds. The range of average speed for SCFs is 4.0 to 105 km/h (2.5 to 65 mph). The SCFs are estimated using the average cycle speed as an independent variable and the emission rates as a dependent variable. Therefore, speed-corrected emission rates used in macroscopic emission models are highly dependent on the average cycle speed.

The use of SCFs for estimating vehicle emissions suffers from a number of limitations, as discussed in the following sections. First, a limited set of driving cycles, which insufficiently represent the entire range of specific traffic flow conditions, are used to estimate emission rates in current models. Many of the driving cycles are also out of date (the FTP is more than 20 years old), and, thus, may not represent current real world driving conditions. Second, current emission models predict emission rates on a single traffic-related variable, namely the average speed. Average trip speeds are not equivalent to link-specific speeds for all portions of vehicle trips. This method of using average speeds cannot represent the distribution of speeds and accelerations of a trip, which vary by type of facility and level of congestion. For example,

existing emission models cannot compare between a highly congested freeway and normal density arterial with the same average speed, though each trip involves a different distribution of vehicle speed and acceleration levels causing distinct emission differences.

2.6.2 Microscopic Energy and Emission Models

Instantaneous fuel consumption and emission models are derived from a relationship between instantaneous fuel consumption and emission rates and instantaneous measurements of explanatory variables such as vehicle power, tractive efforts, acceleration, speed, etc. Second-by-second vehicle characteristics, traffic conditions, and roadway conditions are required in order to estimate the expected vehicle fuel consumption and emission rates. Due to the detailed characteristic of fuel consumption and emission data, these models are usually implemented to evaluate individual transportation projects such as signal re-timing, the modeling of toll plazas, the modeling of highway sections, etc. This section first describes the widely used microscopic fuel consumption models, followed by a description of the widely used Comprehensive Modal Emission Model (CMEM). Finally, a description of the Virginia Tech microscopic energy and emission models are presented.

2.6.2.1 Fuel Consumption Models

From Newton's second law the net force on a vehicle in the direction of motion is proportional to its acceleration. The total includes both the net force and the force that is required to overcome the aerodynamic, rolling resistance and grade resistance. Assuming that the fuel consumption is proportional to the power exerted (product of force and speed), the approach requires that the total force be estimated from the tractive and resistance forces. A more detailed description of this modeling approach is described in the following sub-sections.

2.6.2.1.1 Post Model

Post *et al.* (1984) developed a fuel consumption model based upon the instantaneous power demand undergone by a vehicle. The model was built from chassis dynamometer experiments on 177 in-use vehicles. On-road instantaneous power demand was derived from the total force required to overcome the aerodynamic, rolling, and grade resistance forces for the traction of the vehicle. The instantaneous fuel consumption was computed using the vehicle power as a single independent variable as expressed in Equation 2-1.

$$F = \begin{cases} a + bP_{tot} & \text{for } P_{tot} \geq 0 \\ a & \text{for } P_{tot} < 0 \end{cases} \quad [2\text{-}1]$$

Where:

F = Instantaneous fuel consumption rate (ml/s),

a = Vehicle parameter, Idle fuel consumption rate (ml/s),

b = Vehicle parameter, and

P_{tot} = Instantaneous total power (kW).

Vehicle parameters a and b were found to vary with time as the vehicle's condition and state of tune altered. The zero power fuel consumption rate (a) was found to correlate strongly with the vehicle's engine capacity. However, the parameter was found to vary with time in the range of 10 percent due to instability of idling rpm or idling fuel/air ratio mixture. The fuel consumption rate per kW (b) was found to vary as a result of ignition time changes, air cleaner blockages, and other phenomena. The on-road instantaneous total power (P_{tot}) was computed as the sum of drag power, inertial power, and gradient power. Consequently, the instantaneous total power demand (P_{tot}) is a function of speed, speed squared, speed cubed, and the product of speed and acceleration, as summarized in Equation 2-2.

$$P_{tot} = f\left(u, u^2, u^3, ua\right) \quad [2\text{-}2]$$

Where:

P_{tot} = Instantaneous total power (kW),

u = Instantaneous vehicle speed (km/h), and

a = Instantaneous vehicle acceleration (m/s^2).

2.6.2.1.2 ARRB (Akcelik) Model

The Australian Road Research Board (ARRB) model was developed from the Post *et al*. model that was described earlier (Akcelik, 1989). The major difference between the ARRB and the Post model is a detailed examination of the b parameter. According to Akcelik, an average b value does not provide accurate results because the b value varies as a function of vehicle's instantaneous speed and acceleration rate. In order to improve the accuracy of the Post model in predicting fuel consumption during constant-speed driving as well as acceleration behaviors, the

authors adopted two efficiency parameters, b_1 and b_2, and allowed for an engine/internal drag component to be part of the total drag power. Equation 2-3 shows the general form of the ARRB model.

$$F = a + b_c P_c + b_a P_a \quad [2\text{-}3]$$

Where:

P_c = P_D+P_{ec}

P_a = P_I+P_{ea}

F = Instantaneous fuel consumption rate (ml/s),

a = Vehicle parameter, idle fuel consumption rate (ml/s),

b_c, b_a = Vehicle parameter (ml/s/kW),

P_c = Total drag power during constant-speed driving (kW),

P_a = Total engine/inertia drag power (kW),

P_D, P_I = Coast-down drag and inertia powers (kW), and

P_{ec}, P_{ea} = Power associated with engine/internal drag during constant speed driving and acceleration (kW).

2.6.2.2 Microscopic Fuel Consumption and Emission Model

Several microscopic emission models are described in the literature, however; only the Comprehensive Modal Emissions Model (CMEM) and the Virginia Tech Microscopic energy and emissions model (VT-Micro) were available for public third party use at the time that this research was conducted. Consequently, the CMEM and VT-Micro models are utilized as part of the validation/comparison effort that is presented in the study. Since a more detailed description of the VT-Micro model is presented in Chapter 4, the CMEM model is explained in this section.

The Comprehensive Modal Emissions Model (CMEM), which is one of the newest power demand-based emission models, was developed by researchers at the University of California, Riverside (Barth *et al.*, 2000). The CMEM model estimates LDV and LDT emissions as a function of the vehicle's operating mode. The term "comprehensive" is utilized to reflect the ability of the model to predict emissions for a wide variety of LDVs and LDTs in various operating states (e.g., properly functioning, deteriorated, malfunctioning).

The development of the CMEM model involved extensive data collection for both engine-out and tailpipe emissions of over 300 vehicles, including more than 30 high emitters. These data were measured at a second-by-second level of resolution on three driving cycles, namely: the Federal Test Procedure (FTP), US06, and the Modal Emission Cycle (MEC). The MEC cycle was developed by the UC Riverside researchers in order to determine the load at which a specific vehicle enters into fuel enrichment mode. CMEM predicts second-by-second tailpipe emissions and fuel consumption rates for a wide range of vehicle/technology categories. The model is based on a simple parameterized physical approach that decomposes the entire emission process into components corresponding to the physical phenomena associated with vehicle operation and emission production. The model consists of six modules that predict engine power, engine speed, air-to-fuel ratio, fuel use, engine-out emissions, and catalyst pass fraction. Vehicle and operation variables (such as speed, acceleration, and road grade) and model calibrated parameters (such as cold start coefficients, engine friction factor) are utilized as input data to the model.

Vehicles were categorized in the CMEM model based on a vehicle's total emission contribution. Twenty-eight vehicle categories were constructed based on a number of vehicle variables. These vehicle variables included the vehicle's fuel and emission control technology (e.g. catalyst and fuel injection), accumulated mileage, power-to-weight ratio, emission certification level (tier0 and tier1), and emitter level category (high and normal emitter). In total 24 normal vehicle and 4 high emitter categories were considered (Barth *et al*., 2000).

2.7 SUMMARY

This chapter has explained the major pollutants generated vehicle sources and also highlighted the US federal government attempts at reducing vehicle emissions through various regulatory procedures. In addition, the chapter described the factors affecting fuel consumption and emissions. These factors are categorized as travel, driver, highway network, and vehicle related factors. Furthermore, various approaches and modeling efforts for quantifying transportation fuel consumption and emission impacts were presented. In general, apart from the CMEM model, these models lack the level of resolution that is required to evaluate alternative traffic-operational projects on the environments. This dissertation is an attempt at responding to this need, as will be demonstrated in the forthcoming chapters.

CHAPTER 3. RESEARCH METHODOLOGY

The previous chapter identified the need for comprehensive energy and emission models. This chapter introduces the proposed research approach in developing a comprehensive model.

3.1 INTRODUCTION

This chapter describes the research methodology that is proposed to estimate mobile source fuel consumption and emissions. There are many methods and techniques utilized to predict accurate fuel consumption and emissions. For automobile energy consumption modeling, relatively simple methodologies such as average speed methods are utilized and it has been proved that the models estimate reasonably well fuel consumption. However, it is a different problem to predict mobile-source emissions. Emission models consider engine start emissions, soak time emissions, evaporation, high emitters, emission technologies which significantly influence to approximate precise automobile emissions. To describe these methodologies, several models are briefly investigated including the study of their assumptions, limitations and strengths. In the following sections, a simple proposed methodologies to assess mobile source emissions and fuel consumptions (if applicable) are presented.

3.2 METHODOLOGIES

The research approaches include four basic tasks, as follows:

1. Identification of the optimum model approach and structure for hot stabilized condition,
2. Development of a framework for modeling vehicle emissions
3. Development of new high emitter cut-points for newly developed EPA drive cycles and high emitter emission models, and
4. Development of a framework for estimating instantaneous vehicle start emissions.

3.2.1 Identification Of The Optimum Model Approach and Structure For Hot Stabilized Condition

In order to estimate instantaneous emissions and fuel consumption, several methods are examined in this study. First, the modeling approach is executed to find out the relationships between the instantaneous vehicle engine tractive force and vehicle emissions and fuel consumption using the data collected Oak Ridge national laboratory (ORNL). It is believed that

the instantaneous vehicle engine tractive force is proportional to vehicle emissions and fuel consumption rates. As mentioned in Chapter 2, Post (1984) and Akcelik (1989) developed fuel consumption models based on the instantaneous vehicle engine tractive force. However, these models do not estimate fuel consumption and emissions accurately during the deceleration mode. When a vehicle is operated in deceleration mode, the vehicle does not generate any tractive force. However, during this mode, the vehicle emits emissions and consumes fuel. Generally vehicle emissions and fuel consumption rates are increased as speed increase even though the vehicle is under deceleration mode. Most power-based models assume that vehicles consume constant fuel rate during deceleration and idling modes. This problem is very critical in microscopic emissions and fuel consumption modeling because a typical driving cycle (FTP cycle) shows that 34.5% of driving mode is deceleration condition and 17.9 % of driving mode is idling condition. Therefore, 52.9% among the total driving mode emits same amount of emission rates and consumes same amount of fuel rate because the negative force is assumed to idling condition, which is unrealistic. Consequently, in order to overcome these problems, deceleration and idle modes should be explained in the model.

Secondly, in order to decide the optimum model structure, more variables, besides the model variables derived from the relationships between the instantaneous vehicle engine tractive force and vehicle emissions and fuel consumption, are introduced and examined for the emissions and fuel consumption modeling. Many experimental combinations of speed and acceleration using linear, quadratic, cubic, and quartic terms are tested to decide the optimum model structure. Another procedure introduced to the modeling is to utilize the data transformation technique using a logarithmic function for the fuel consumption and emission data. A logarithm transformation can capture the large nonlinear behaviors observed for most energy and emission data.

Finally, hybrid models are examined to increase the model accuracy. Emission data show that positive acceleration emission data has significant difference with negative acceleration emission data. Positive acceleration emission data have smooth variations at higher speed regime while negative acceleration data have more decent movements. Those behaviors cannot be captured in one regime model properly. Therefore, positive acceleration data and negative acceleration data are modeled separately to reduce the model errors.

3.2.2 Development of a Framework for Modeling Vehicle Emissions

The original fuel consumption and emission models are derived from ORNL emission data. The ORNL data contained only nine normal emitting vehicles, specifically six light duty automobiles and three light duty trucks. These vehicles were selected in order to produce an average vehicle that was consistent with average vehicle sales in terms of engine displacement, vehicle curb weight, and vehicle type for the year 1995. However, It was blamed that those nine vehicles are not enough to represent the characteristics of current on road fleet. More vehicle emission data is desired to estimate more accurate emissions. In order to expand the model, the dissertation develops a framework for modeling vehicle emissions. The framework utilizes statistical techniques for aggregating vehicles into homogenous categories and accounts for temporal lags between vehicle operational variables and vehicle emissions. Finally, the framework is utilized to develop new emission models utilizing second-by-second chassis dynamometer emission data collected from EPA.

3.2.3 Development of New High Emitter Cut-points for Newly Developed EPA Drive Cycles and High Emitter Emission Models

In this part of the research, efforts are concentrated on studying high emitter criteria and high emitter characteristics. High emitter criteria are important elements to estimate accurate emissions as they allow vehicles to be classified as normal emitters or high emitters. This part of the research compares high emitter classifications proposed by several entities, such as EPA and Georgia Tech. It also investigates the second-by-second behaviors of high emitting and normal emitting vehicles. The research concentrates on examining the aggressiveness of several driving cycles. After the comparison of emissions collected during each cycle, new high emitter emission standards (cup-points) for different cycles are established.

Similar to the microscopic fuel consumption and emission modeling, high emitter modeling is developed in a micro-scale modeling process. However, due to insufficient emission data, few vehicle data is available to compare emissions in normal conditions and high emitting conditions and fully evaluate the resulting model. Various types of high emitters vehicles are categorized by their emitting behavior characteristics. The same framework utilized at section 3.2.2 is employed for high emitter vehicles.

3.2.4 Development of a Framework for Estimating Instantaneous Vehicle Start Emissions

This section describes the modeling of engine start which has significant effects on fuel consumption and emissions. Most existing models combine the effects of engine starts and transient driving into a single estimate of additional exhaust emissions. This approach is possible when using macroscopic approaches such as in the MOBILE model, However, it is difficult to adjust the number of trips associated with various driving distances and impossible to estimate micro-scale impact for cold engine starts due to the aggregate characteristic. In the instantaneous emission modeling presented in this thesis, an engine start module is incorporated with second-by-second engine start emission rate. In response to these needs, the engine start module is planned to have a separate estimate for emissions from vehicle driving and engine start. In order to model the engine start emissions, the following concepts are utilized for modeling:

- The magnitude of start emissions will not depend on speeds or driving cycles. The total extra emissions for single trip cold engine start impacts depend on the duration of soak time period.
- Engine start emissions will be handled as instantaneous emissions in second-by-second basis.
- Impact of engine start emissions is decreased on a certain time after engine starting and finally vanished.

In order to verify the impact of engine start operation, a relationship between engine start emissions and the hot stabilized condition emissions derived from same driving cycles should be utilized. Using these emissions, it is possible to develop a general relationship to estimate the cold start emissions. Specifically, since the extra engine start emissions are the portion of the cold start emission, if the duration of engine start operation and extra emissions generated from an engine start operation are known, simple linear decay function can be established to estimate the microscopic cold start emissions.

3.3 SUMMARY

Various research approaches utilized in this dissertation have been examined in this chapter. The research identifies the optimum model approach and structure for hot stabilized condition. The modeling approach is executed to find out the best regression model structure using relationships

between the instantaneous vehicle engine tractive force and vehicle emissions and fuel consumption. Data transformation technique using a logarithmic function for the emission data is utilized. Hybrid models are examined to increase the model accuracy. The development of a framework to estimating emissions microscopically is discussed to expand the emission models using second-by-second EPA data. Also, high emitter criteria are investigated to review what constitutes a high emitter. Depending to the definition, some vehicles can be classified as high emitters or normal vehicles. Those results can affect significant total emission estimations in macroscopic models. Finally, a microscopic engine start emission model is discussed. In engine start modeling, a simple cold emission decay function is applied to account for cold start impacts. The decay function is established using extra start emissions and the engine start duration.

CHAPTER 4. ESTIMATING VEHICLE FUEL CONSUMPTION AND EMISSIONS BASED ON INSTANTANEOUS SPEED AND ACCELERATION LEVELS: VT-MICRO MODEL DEVELOPMENT

Several hybrid regression models (known as the Virginia Tech Microscopic Energy and Emission Model: VT-Micro) that predict hot stabilized vehicle fuel consumption and emission rates for light-duty vehicles and light-duty trucks are presented in this chapter. Key input variables to these models are instantaneous vehicle speed and acceleration measurements. The energy and emission models described in this research utilize data collected at the Oak Ridge National Laboratory that included fuel consumption and emission rate measurements (CO, HC, and NO_x) for five light-duty vehicles and three light-duty trucks as a function of the vehicle's instantaneous speed and acceleration levels.

4.1 INTRODUCTION

Estimating accurate fuel consumption and emissions has been considered a significant problem in transportation planning process. However, it is argued that predictions from current state-of-the-art models are not suitable for the reliable evaluation of fuel consumption and emission impacts of operational level projects. The following section describes several problems in estimating fuel consumption and emissions, and the specific objectives of the study.

4.1.1 Problem Definition

Vehicle fuel consumption and emissions are two significant considerations in the transportation planning process of highway facilities. For instance, recent studies indicate that as much as 45% of the pollutants released in the U.S. are a direct consequence of vehicle emissions (National Research Council, 1995). Also, various Intelligent Transportation Systems (ITS) technologies has been introduced to improve the traffic flow in urban areas. Comparing alternative ITS and non-ITS investments with emphasis on energy and emission impacts has been considered critical aspects in the ITS implementation process. Until now, the benefits derived from the implementation of ITS technologies in terms of energy and emissions have not been systematically quantified.

Current state-of-the-art models estimate vehicle emissions based on average link speeds without regarding transient changes in a vehicle's speed and acceleration as it travels on a highway network. Most of these models calculate fuel and emission rates based on simplified mathematical expressions derived from typical urban driving cycles. While this approach has been accepted by transportation planners for the evaluation of network-wide highway impacts on the environment, it is not suited for the evaluation of energy and environmental impacts of operational-level projects.

4.1.2 Research Objective

In an attempt to overcome the limitations of current energy and emission models, this chapter develops mathematical models that predict vehicle fuel consumption and emissions using instantaneous speed and acceleration as explanatory variables. The ultimate use of these models would be their integration into traffic network simulators to better understand the impacts of traffic policies, including the introduction of ITS technologies, such as signal coordination, incident management, and electronic payment systems, on the environment.

4.1.3 Chapter Layout

This chapter is organized in six sections. The first section introduces the problem statement. The next section describes the significance of the proposed models. The third section describes the data sources that were utilized to develop the proposed modeling approach. The fourth section describes several mathematical approaches for the evaluation of vehicle fuel consumption and emission impacts. Furthermore, the proposed model is compared to the alternative approaches in order to demonstrate the merit of the proposed models. The fifth section describes how the model was validated against real world field data and current state-of-the-art emission models. Finally, the last section of the chapter provides a summary of the findings.

4.2 SIGNIFICANCE OF PROPOSED MODELS

Numerous variables influence vehicle energy and emission rates. These variables can be classified into six broad categories, as follows: travel-related, weather-related, vehicle-related, roadway-related, traffic-related, and driver-related factors. The travel-related factors account for the distance and number of trips traveled within an analysis period while the weather-related

factors account for temperature, humidity, and wind effects. Vehicle-related factors account for numerous variables including the engine size, the condition of the engine, whether the vehicle is equipped with a catalytic converter, whether the vehicle's air conditioning is functioning, and the soak time of the engine. The roadway-related factors account for the roadway grade and surface roughness while the traffic-related factors account for vehicle-to-vehicle and vehicle-to-control interaction. Finally, the driver-related factors account for differences in driver behavior and aggressiveness.

The state-of-the-art emission models such as MOBILE6 developed by the US Environmental Protection Agency (EPA) and EMFAC 2000 developed by the California Air Resources Board (CARB) attempt to account for travel-related, weather-related, and vehicle-related factors on vehicle emissions. However, these models generally fail to capture roadway, traffic, and driver related factors on vehicle emissions. Specifically, the models use average speed and vehicle miles traveled to estimate vehicle emissions. Implicit in each facility average speed is a driving cycle. Consequently, the current state-of-the-art emission models are unsuitable for evaluating the environmental impacts of operational-level projects where changes in traffic behavior between a before and after scenario are critical.

The models developed in this chapter attempt to overcome the shortcomings of the state-of-the-art models by quantifying traffic and driver related factors on vehicle emissions in addition to travel related factors. Specifically, the models use the vehicle's instantaneous speed and acceleration levels to estimate vehicle emissions. Further refinements to the model include accounting for vehicle and weather related factors.

4.3 VEHICLE ENERGY AND EMISSION DATA SOURCE DESCRIPTION

The data that were utilized to develop the fuel consumption and emission models that are presented in this research were collected at the Oak Ridge National Laboratory (ORNL). Specifically, test vehicles were driven in the field in order to verify their maximum operating boundary. Subsequently, vehicle fuel consumption and emission rates were measured in a laboratory on a chassis dynamometer within the vehicle's feasible vehicle speed and acceleration envelope. Data sets were generated that included vehicle energy consumption and emission rates as a function of the vehicle's instantaneous speed and acceleration levels. Several measurements

were made in order to obtain an average fuel consumption and emission rate (West *et al.*, 1997). The emission data that were gathered included hydrocarbon (HC), oxides of nitrogen (NO_x), and carbon monoxide (CO) emission rates.

The eight normal emitting vehicles included five light-duty automobiles and three light duty trucks, as summarized in Table 4-1. These vehicles were selected in order to produce an average vehicle that was consistent with average vehicle sales in terms of engine displacement, vehicle curb weight, and vehicle type (West *et al.*, 1997). Specifically, the average engine size was 3.3 liters, the average number of cylinders was 5.8, and the average curb weight was 1497 kg (3300 lbs) (West *et al.*, 1997). Industry reports show that the average sales-weighted domestic engine size in 1995 was 3.5 liters, with an average of 5.8 cylinders (Ward's Communications, 1996; Ward's Communications, 1995).

The data collected at ORNL contained between 1,300 to 1,600 individual measurements for each vehicle and Measure of Effectiveness (MOE) combination depending on the envelope of operation of the vehicle. Typically, vehicle acceleration values ranged from –1.5 to 3.7 m/s^2 at increments of 0.3 m/s^2 (-5 to 12 ft/s^2 at 1 ft/s^2 increments). Vehicle speeds varied from 0 to 33.5 m/s (0 to 121 km/h or 0 to 110 ft/s) at increments of 0.3 m/s. A sample data set for one of the test vehicles is presented in Figure 4-1 for illustration purposes. The figure clearly demonstrates the large nonlinear behavior in all MOEs as a function of the vehicle speed and acceleration. Specifically, ‘peaks’ and ‘valleys’ are prevalent as a result of gear shifts under various driving conditions. In addition, it is evident that as acceleration and speed increases the MOEs generally tend to increase. Furthermore, it is noted that the gradient of the MOEs in the negative acceleration regime (-1.5 to 0 m/s^2) is generally smaller than that in the positive acceleration regime (0 to 3.7 m/s^2).

It is interesting to note that the ORNL data represents a unique vehicle performance envelope. For example, low weight-to-power ratio vehicles have better acceleration characteristics at high speeds than their high weight-to-power ratio counterparts. This inherent performance boundary is extremely important when these models are used in conjunction with microscopic traffic flow models as they represent a physical kinematic constraint in the car-following equations of motion. A typical speed-acceleration performance boundary is illustrated in Figure 4-2 for a hypothetical

composite vehicle. The composite vehicle was derived as an average of the eight test vehicles to reflect a typical average vehicle.

4.4 DEVELOPMENT OF MODELS

This section describes the background of modeling procedure, model development, and model limitations.

4.4.1 Background

Several regression model structures were evaluated as part of the research effort that is presented in this study. The first of these models attempted to establish the relationship between the tractive effort and vehicle fuel consumption and emissions. The use of tractive effort as an independent variable for estimating vehicle fuel consumption was first proposed by Akcelik *et al*. (1983) and further enhanced by Biggs and Akcelik (1986). Post *et al*. (1984) extended these models to develop power demand models for the estimation of vehicle fuel consumption and emissions of hydrocarbons and nitrogen oxides. The presumption was that the instantaneous engine tractive force was proportional to vehicle emissions and fuel consumption rates. It should be noted that the model presented by Biggs and Akcelik (1986) assumed idling conditions for negative tractive effort conditions (deceleration mode). However, the ORNL data indicate that vehicle emissions and fuel consumption rates increase as speed increases even though the vehicle is in a deceleration mode.

While the comparison of these models is beyond the scope of this research effort, a subsequent chapter will present a detailed comparison of the various models to the models that are proposed in this chapter. It is sufficient to mention at this point, however, that the Federal Test Procedure (FTP) drive cycle involves a decelerating drive mode for 34.5 percent of the time, and idling mode for 17.9 percent of the time. Consequently, these models would indicate identical vehicle emission rates for 52.9 percent of the entire cycle, which results in significant errors in estimating vehicle emissions.

4.4.2 Model Development

The derivation of the final models involved experimentation with numerous polynomial combinations of speed and acceleration levels. Specifically, linear, quadratic, cubic, and quartic

terms of speed and acceleration were investigated. The final regression models included a combination of linear, quadratic, and cubic speed and acceleration terms because it provided the least number of terms with a relatively good fit to the ORNL data (R^2 in excess of 0.70 for most MOEs). These models fit the ORNL data accurately for high speed and acceleration levels, however the models are less accurate at low speed and acceleration levels.

The final model included a third degree polynomial based on Equation 4-1. This model produced reasonable fits to the ORNL data except in a few instances where the models produced negative dependent variable values. To solve this problem, a data transformation technique was adopted to the model that is presented in Equation 4-1 resulting in the model that is presented in Equation 4-2. First, independent variables were transformed using the natural logarithm. Second, regression models were fitted to the transformed data. Finally, the predicted values were then transformed back by utilizing an exponential function. The coefficient of determination of the MOE estimates using Equation 4-2 ranged from 0.72 to 0.99, as summarized in Table 4-2. The statistical results indicate a good fit for fuel consumption estimates ($R^2 = 0.996$), an average fit for NO_x estimates ($R^2 = 0.805$), and a relatively poor fit for HC and CO emission estimates ($R^2 = 0.72$ and 0.75, respectively).

In order to isolate and identify the shortcomings of the log-transformed polynomial regression models, Figure 4-3 illustrates graphically the quality of fit between the regression models and the ORNL data. It is noted from Figure 4-3 that the errors in the HC and CO model estimates are high in the high acceleration region (overestimates HC emissions by up to 25 percent and CO emissions by 100 percent). These errors in the regression model are caused by the significant sensitivity of the dependent variable to the independent variables at high accelerations compared with the marginal sensitivity of the dependent variable in the negative acceleration range. Differences in behavior for positive versus negative accelerations can be attributed to the fact that in positive accelerations the vehicle exerts power, while in the negative acceleration range the vehicle does not exert power.

Consequently, separate regression models were developed for positive and negative accelerations, as demonstrated in Equation 4-3. It should be noted that the intercept at zero speed and zero acceleration was estimated for positive accelerations and fixed in the negative acceleration

formulation in order to ensure a continuous function between the two regression regimes. The final models that were developed resulted in good fits to the ORNL data (R^2 in excess of 0.92 for all MOEs), as summarized in Table 4-2. Figure 4-4 further illustrates the effectiveness of the hybrid log-transformed models in predicting vehicle fuel consumption and emission rates as a function of a vehicle's instantaneous speed and acceleration levels. A comparison of Figure 4-3 and Figure 4-4 clearly demonstrates the enhancement in model predictions as a result of separating positive and negative acceleration levels. It should be noted, however that the model estimates were less accurate than the polynomial model fits for high speed and acceleration combinations. Sample model coefficients for estimating HC emission rates for an average composite vehicle are summarized in Table 4-3.

The use of polynomial speed and acceleration terms may result in multi-colinearity between the independent variables as a result of the dependency of these variables. The Variance Inflation Factor (VIF), which is a measure of multi-colinearity, can be reduced by removing some of the regression terms with, however, a reduction in the accuracy of the model predictions. Consequently, a trade-off between reducing the model multi-colinearity should be weighed against a potential reduction in model accuracy. The existence of multi-colinearity results is model estimations of the dependent variable that are unreliable for dependent variable values outside the bounds of the original data. Consequently, the model was maintained with the caveat that the model should not be utilized for data outside the feasible envelope of a typical vehicle.

Even though this section demonstrates the regression models to estimate fuel consumption and emissions. Other modeling approach such as Artificial Neural Network (ANN) method has been tested as well. More detailed descriptions for ANN modeling approach are found in other literature (Ahn et al, 1998).

$$MOE_e = \sum_{i=0}^{3}\sum_{j=0}^{3}(K_{i,j}^{e} \times u^i \times a^j) \qquad [4\text{-}1]$$

$$MOE_e = e^{\sum_{i=0}^{3}\sum_{j=0}^{3}(K_{i,j}^{e} \times u^i \times a^j)} \qquad [4\text{-}2]$$

$$MOE_e = \begin{cases} e^{\sum_{i=0}^{3}\sum_{j=0}^{3}(L_{i,j}^{e} \times u^i \times a^j)} & \text{for } a \geq 0 \\ e^{\sum_{i=0}^{3}\sum_{j=0}^{3}(M_{i,j}^{e} \times u^i \times a^j)} & \text{for } a < 0 \end{cases} \quad [4\text{-}3]$$

Where:

MOE_e = instantaneous emission rate (mg/s),

$K^e_{i,j}$ = Model regression coefficient for MOE "e" at speed power "i" and acceleration power "j",

$L^e_{i,j}$ = Model regression coefficient for MOE "e" at speed power "i" and acceleration power "j" for positive accelerations,

$M^e_{i,j}$ = Model regression coefficient for MOE "e" at speed power "i" and acceleration power "j" for negative accelerations,

u = Instantaneous vehicle speed (km/h), and

a = Instantaneous vehicle acceleration (m/s^2).

4.4.3 Model Domain of Application

As is the case with any mathematical model, the proposed models are applicable for a specified domain of application. First, the models are developed to estimate vehicle fuel consumption and emission rates for light duty vehicles and trucks. Second, the models estimate vehicle emissions for hot stabilized conditions and do not consider the effect of vehicle start effects. Third, the models are confined to speed and acceleration levels within the envelope of the ORNL data. The third limitation results from the inherent limitation of any model to extrapolate response values beyond the boundaries used in the model calibration procedure. While most vehicles can travel faster than 121 km/h (upper limit of the testing boundary), it is impossible to establish a reliable forecasting pattern for energy and emission rates at high speeds due to the heavy nonlinear nature of the response curves. It has been observed from the US06 cycle that some speed and acceleration profiles exceed the speed and acceleration boundary (13 out of 596 seconds). However, in these cases, authors recommend using boundary speed and acceleration levels in order to ensure realistic vehicle MOE estimates. Furthermore, it should be noted that these models have been successfully applied to Global Positioning System (GPS) speed measurements after applying robust smoothing techniques in order to ensure feasible speed measurements (Rakha *et al*., 2001).

4.5 MODEL VALIDATION

This section describes an aggregate model validation and an instantaneous model validation using field emission measurements.

4.5.1 Description of EPA Data Sets

In order to evaluate the accuracy of the proposed hybrid emission models, "real world" emission data were compared to regression model estimates. The field measurements were gathered by the Environmental Protection Agency (EPA) at the Automotive Testing Laboratories, Inc. (ATL), in Ohio and EPA's National Vehicle and Fuels Emission Laboratory (NVREL), in Ann Arbor, Michigan, in the spring of 1997. All the vehicles at ATL were drafted at Inspection and Maintenance lanes utilized by the State of Ohio and tested under as-received condition (without repairs). A total of 62 vehicles in East Liberty, Ohio and 39 vehicles in Ann Arbor, Michigan were recruited and tested. The sample of 101 vehicles included 3 heavy-duty trucks, 34 light-duty trucks, and 64 light-duty cars. The vehicle model years ranged from 1986 through 1996 (Brzezinski *et al*., 1999a).

All vehicles were tested using the standard vehicle certification test fuel. Vehicle emission tests were performed in random order to offset any possible order bias that could result in different ambient conditions for the tested cycles. The emission results were measured as composite "bags" and in grams on a second-by-second basis for HC, CO, NO_x, and CO_2 emissions.

4.5.2 Description of EPA Drive Cycles

The MOBILE5a model was developed based on vehicle emission testing using the Federal Test Procedure (FTP) drive cycle. If the estimated average speed is different from the average speed of the FTP drive cycle (31.4 km/h or 19.6 mph), speed correction factors are used to adjust the emissions measured using the FTP drive cycle. However, these speed correction factors are utilized regardless of the roadway type or traffic conditions. For example, the MOBILE5 model cannot compare a highly congested freeway and a normal density arterial with the same average speed, though each may involve a significant different distribution for speeds and accelerations causing distinct emission levels.

In order to address these problems, EPA has developed new facility-specific and area-wide driving cycles, based on real-world driving studies to incorporate within EPA's new MOBILE6 model (Brzezinski *et al*., 1999a). Table 4-4 provides a brief description of the new cycles and additional emission test cycles used for emission testing. It should be noted that the ST01 drive cycle was not utilized for the model validation because the cycle involves cold starts.

4.5.3 Aggregate Emission Model Validation

The EPA data that were described earlier were utilized to validate the proposed models. The initial validation effort involved an aggregate level comparison between EPA's aggregate emission measurements over 15 drive cycles using vehicles that were classified as clean with the proposed model estimates of vehicle emissions. In identifying clean vehicles, manufacture's standard emission rates were applied, which are 0.26 grams/km (0.41 grams/mile) for HC, 2.13 grams/km (3.4 grams/mile) for CO, and 0.63 grams/km (1.0 gram/mile) for NO_x for Bag 2 of the FTP City cycle. Based on these criteria a total of 51 vehicles of the 101 vehicles were classified as clean for HC emissions, 47 vehicles for CO emissions, and 60 vehicles for NO_x emissions.

Figure 4-5 shows the comparisons between simulated regression model results and EPA's "real world" data for different driving cycles. Figure 4-5 illustrates the variation in the 95^{th} percentile and 5^{th} percentile using vertical lines and mean values of EPA field measurements using small bar for the 16 drive cycles. The bar plots represent the proposed regression model emission estimates using an average composite vehicle. The emissions are computed as the sum of instantaneous vehicle emissions for each of the 15 drive cycles. Figure 4-5 clearly illustrates a good fit between the model estimates and the field measurements. Specifically, the predictions lie within the 95^{th} percentile and the 5^{th} percentile confidence limits. Furthermore, the model estimates generally follow the average field emission values of the clean vehicle fleet. Also, it is noted that the average HC and CO values of the ARTE and FNYC cycle are high compared to the model estimates, as a result of a few emission measurements that are extremely high. The simulation results for NO_x appear to follow the average values almost perfectly.

4.5.4 Instantaneous Emission Model Validation

The next step in validating the proposed models was to compare second-by-second field HC, CO, and NO_x measurements against instantaneous model estimates with the objective of identifying

any shortcomings in the proposed models. In order to ensure consistency in the comparison, the Subaru Legacy was selected for comparison purposes because both the ORNL data set and the EPA data set included a Subaru Legacy vehicle. Specifically, the ORNL included a1993 model and the EPA data included a 1992 model.

Figure 4-6 illustrates the speed and acceleration profiles of the ARTA drive cycle, which involves several full and partial stops in addition to travel at a fairly high speed (in the range of 100 km/h). The figure clearly demonstrates that the ARTA drive cycle involves a more aggressive and realistic driver behavior compared to the FTP City cycle. In addition, Figure 4-6 illustrates the variation in the instantaneous vehicle emissions of HC as measured on a dynamometer as it travels through the drive cycle. Superimposed on the figure are the hybrid log-transformed model estimates of vehicle emissions based on instantaneous vehicle speed and acceleration levels.

The total vehicle emissions of HC as measured in the laboratory was 0.86 grams, while the estimated HC emissions based on the proposed hybrid model was 1.06 grams, which corresponds to a 19 percent difference in overall emissions for the entire cycle. The figure illustrates that in general the model prediction almost perfectly follows the EPA vehicle emission measurements, demonstrating the uniqueness of the model for assessing traffic improvement projects, including ITS technology, on the environment. Figure 4-6 demonstrates that the EPA emission rates are slightly shifted to right side relative to the model estimates. The offset in vehicle emissions results from a time lag between vehicle accelerations and their corresponding emissions through the tailpipe. It is noted that the time lags between vehicle accelerations and vehicle emissions typically range between 5 and 10 seconds.

4.5.5 Comparison with MOBILE5a

The hybrid log-transformed polynomial models were validated against MOBILE5a because MOBILE6 was not commercially available at the time the models were developed. The comparison is made for the FTP City cycle, also known as LA4, and the Highway Economy cycle because these cycles are reflected in the MOBILE5a.

In conducting the comparison, the following constraints were implemented within the MOBILE5a input parameters. First, vehicle compositions were set to be consistent with the ORNL vehicle composition (i.e. 5/8 were light duty vehicles and 3/8 were light duty trucks). Second, the model year distribution was made consistent with the ORNL vehicle sample. Third, the vehicle mileage was set to be less than 50,000 miles to be consistent with the ORNL data. Finally, only hot stabilized conditions were modeled without the inclusion of high emitters.

The results of the model comparisons are illustrated in Figure 4-7. The composite vehicle emission estimates are represented by the rectangles in Figure 4-7 while the 95^{th} percentile and 5^{th} percentile emission estimates for individual ORNL eight vehicles are represented by the extents of the vertical lines. The MOBILE5a results reflect different annual vehicle mileage compositions with the rectangles reflecting the composition that is consistent with the ORNL data. Figure 4-7 clearly demonstrates consistency in the vehicle emissions between the instantaneous emission models and MOBILE5a for both the LA4 and Highway Economy drive cycles. Furthermore, the results indicate similar relative differences across the different drive cycles.

4.6 SUMMARY

The research presents microscopic fuel consumption and emission models (VT-Micro) that require instantaneous vehicle speed and acceleration levels as input variables. The models, that were developed using the ORNL data, estimate hot stabilized vehicle emissions for normal light duty vehicles. The models are found to produce vehicle emissions that are consistent with the ORNL data (coefficient of determination is excess of 90 percent).

The development of these models attempts to bridge the existing gap between traffic simulation models, traditional transportation planning models, and environmental impact models. The models presented in this research are general enough to be incorporated within microscopic traffic simulation models. It is believed that given the current power of desktop computers, the implementation of any of the models presented in this study adds an acceptable computational overhead to a microscopic simulation model. The benefit of this integration would be substantial if one considers that current environmental models are quite insensitive to traffic and driver related factors on vehicle emissions. Currently, the models developed in this study have been

incorporated within the microscopic traffic simulation tool INTEGRATION to further demonstrate their application and relevance to traffic engineering studies (Rakha *et al*., 2000b).

The models can also be applied directly to estimate vehicle fuel consumption and emissions using instantaneous GPS speed measurements (Rakha *et al*., 2000a).

Table 4-1. ORNL Test Vehicle Characteristics

Year	Make/Model	Engine & Transmission	Curb Weight (kg)	Rated Power (hp)
Light-Duty Cars				
1988	Chevrolet Corsica	2.8L pushrod V6,PFI, M5	1209	130
1994	Oldsmobile Cutlass Supreme	3.4L DOHC V6, PFI, L4	1492	210
1994	Oldsmobile 88	3.8L pushrod V6, PFI, L4	1523	170
1995	Geo Prizm	1.6L OHC I4, PFI, L4	1116	105
1993	Subaru Legacy	2.2L DOHC flat 4, PFI, L4	1270	130
	ORNL LDV average	2.8L, 5.2 cyl.	1322	149
1995	LDV industry average	2.9L, 5.4 cyl.	1315	
Light-Duty Trucks				
1994	Mercury Villager Van	3.0L pushrod V6, PFI, L4	1823	151
1994	Jeep Grand Cherokee	4.0L pushrod I6, PFI, L4	1732	190
1994	Chevrolet Silverado Pickup	5.7L pushrod V8, TBI, L4	1823	200
	ORNL LDT average	4.2L, 6.7 cyl	1793	180
1995	LDT industry average	4.6L, 6.5 cyl		
	8-vehicle average	**3.3L, 5.8 cyl**	1497	160
1995	**LDV+LDT, industry avg.**	**3.5L, 5.8 cyl**		

Table 4-2. Regression Model Comparison

	Correlation of Determination			
	Fuel	**HC**	**CO**	**NOx**
Force model with log transformation	0.870	0.319	0.870	0.667
Polynomial regression model with log transformation	0.996	0.716	0.748	0.805
Hybrid regression model with log transformation	0.998	0.974	0.918	0.982

Table 4-3. Sample Coefficients of Hybrid Regression Model (HC Emissions for Composite Vehicle)

Positive Acceleration Coefficients	Constant	Speed	$Speed^2$	$Speed^3$
Constant	-0.87605	0.03627	-0.00045	2.55E-06
Acceleration	0.081221	0.009246	-0.00046	4.00E-06
$Acceleration^2$	0.037039	-0.00618	2.96E-04	-1.86E-06
$Acceleration^3$	-0.00255	0.000468	-1.79E-05	3.86E-08
Negative Acceleration Coefficients	Constant	Speed	$Speed^2$	$Speed^3$
Constant	-0.75584	0.021283	-0.00013	7.39E-07
Acceleration	-0.00921	0.011364	-0.0002	8.45E-07
$Acceleration^2$	0.036223	0.000226	4.03E-08	-3.5E-08
$Acceleration^3$	0.003968	-9E-05	2.42E-06	-1.6E-08

(Speed: km/h, Acceleration: km/h/s, HC Emission Rate: mg/s)

Table 4-4. EPA's New Facility-Specific Drive Cycle Characteristics

Cycle	Average Speed (km/h)	Maximum Speed (km/h)	Max. Acceleration (km/h/s)	Duration (Seconds)	Length (km)
Freeway, High Speed	101.12	119.52	4.32	610	17.15
Freeway, LOS A-C	95.52	116.96	5.44	516	13.68
Freeway, LOS D	84.64	112.96	3.68	406	9.54
Freeway, LOS E	48.8	100.8	8.48	456	6.18
Freeway, LOS F	29.76	79.84	11.04	442	3.66
Freeway, LOS G	20.96	57.12	6.08	390	2.27
Freeway Ramps	55.36	96.32	9.12	266	4.10
Arterial/Collectors LOS A-B	39.68	94.24	8	737	8.11
Arterial/Collectors LOS C-D	30.72	79.2	9.12	629	5.38
Arterial/Collectors LOS E-F	18.56	63.84	9.28	504	2.59
Local Roadways	20.64	61.28	5.92	525	2.99
Non-Freeway Area-Wide Urban Travel	31.04	83.68	10.24	1348	11.60
LA04	31.36	90.72	5.28	1368	11.92
Running 505	40.96	90.72	5.28	505	5.744
LA 92	39.36	107.52	11.04	1435	15.696
ST01	32.32	65.6	8.16	248	2.224
New York Cycle	11.36	44.32	9.6	600	1.888

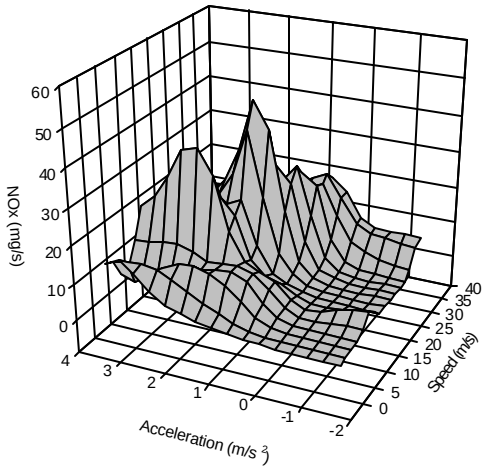

Figure 4-1. ORNL NOx Emissions Rates (Mercury Villager)

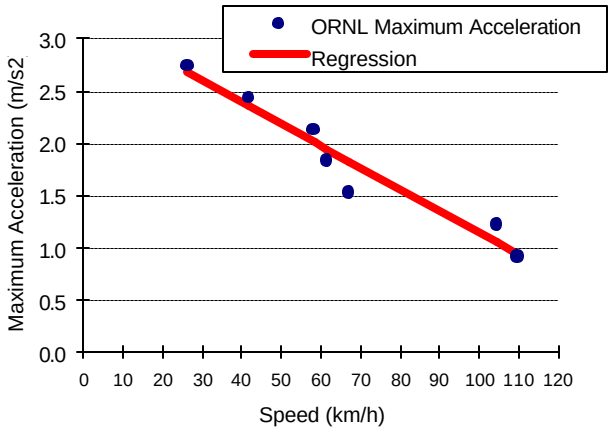

Figure 4-2. Maximum Acceleration as a Function of Vehicle Speed (Composite Vehicle)

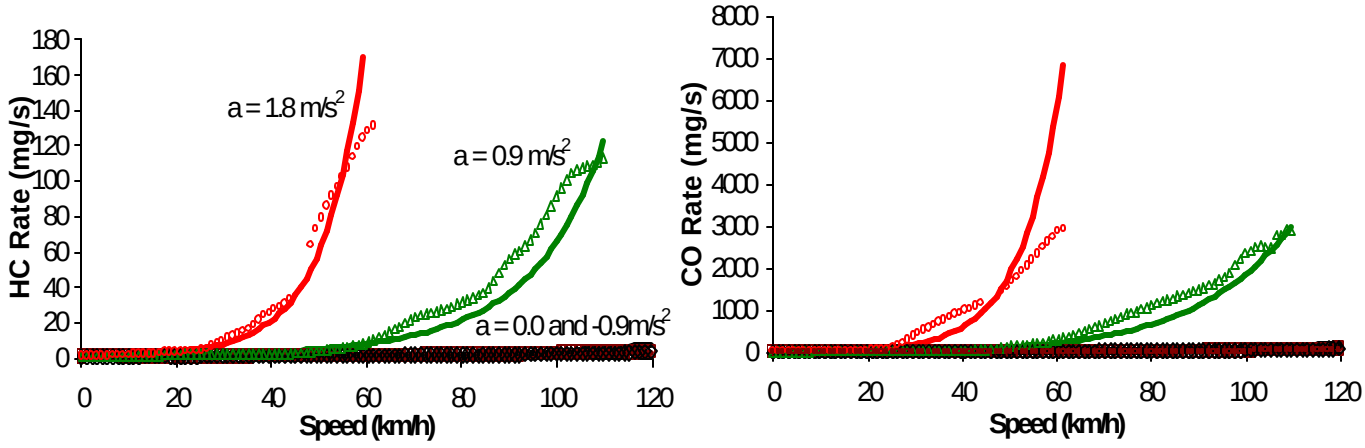

Figure 4-3. Regression Model Predictions (Composite Vehicle – Log-Transformed Polynomial Model)

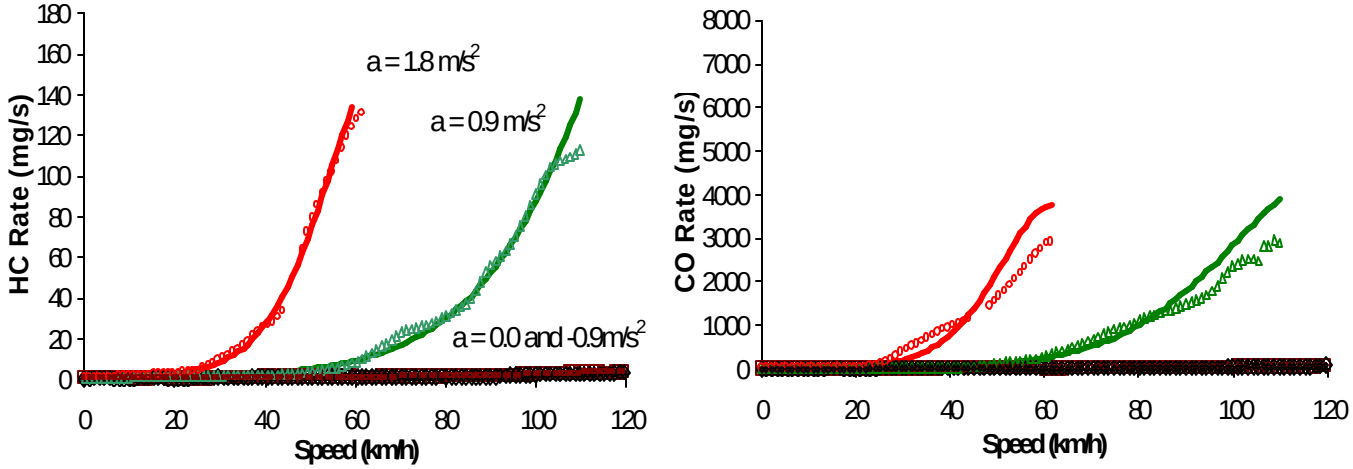

Figure 4-4. Regression Model Predictions (Composite Vehicle – Log-Transformed Hybrid Polynomial Model)

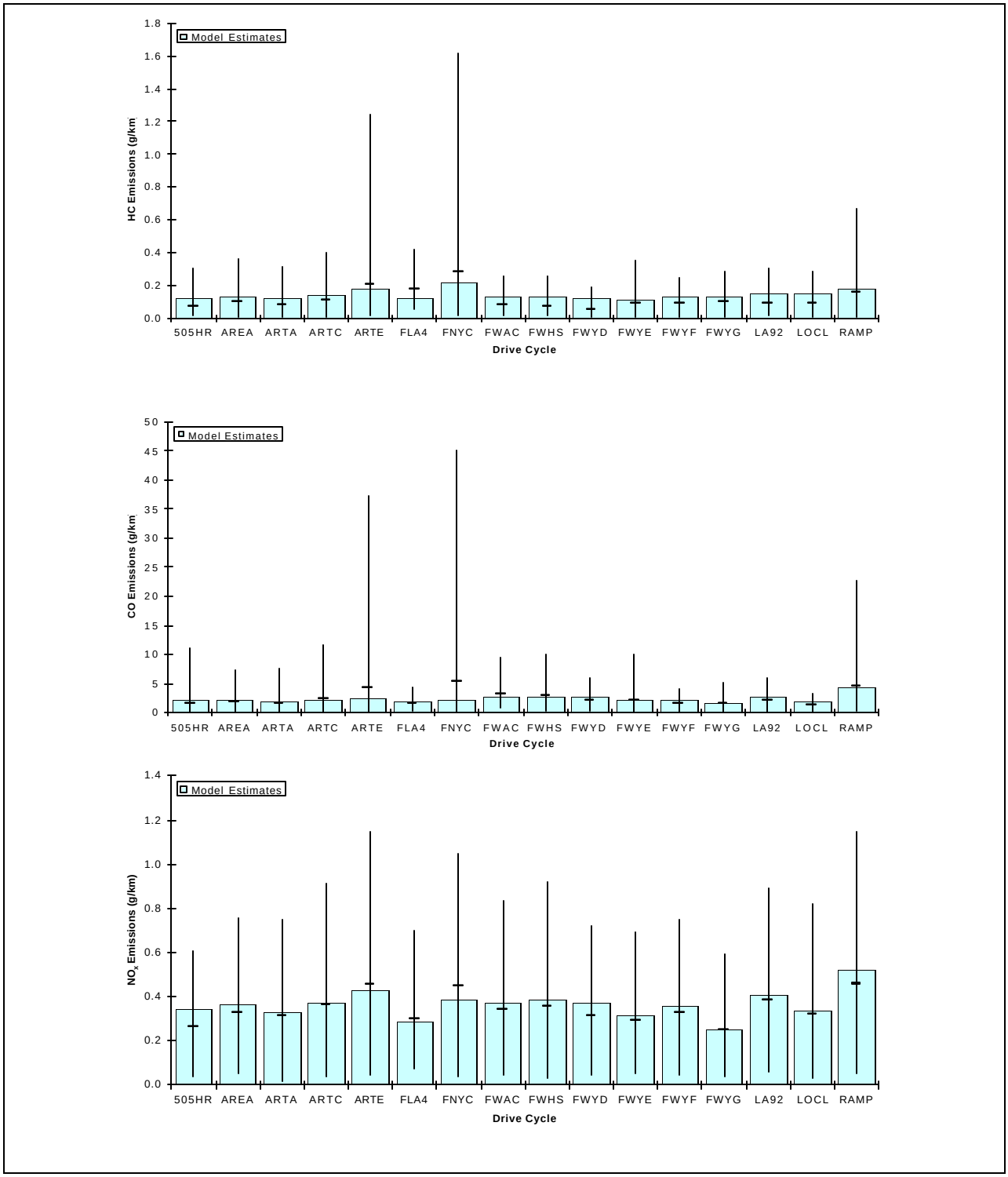

Figure 4-5. Simulated Emissions for Different Driving Cycles

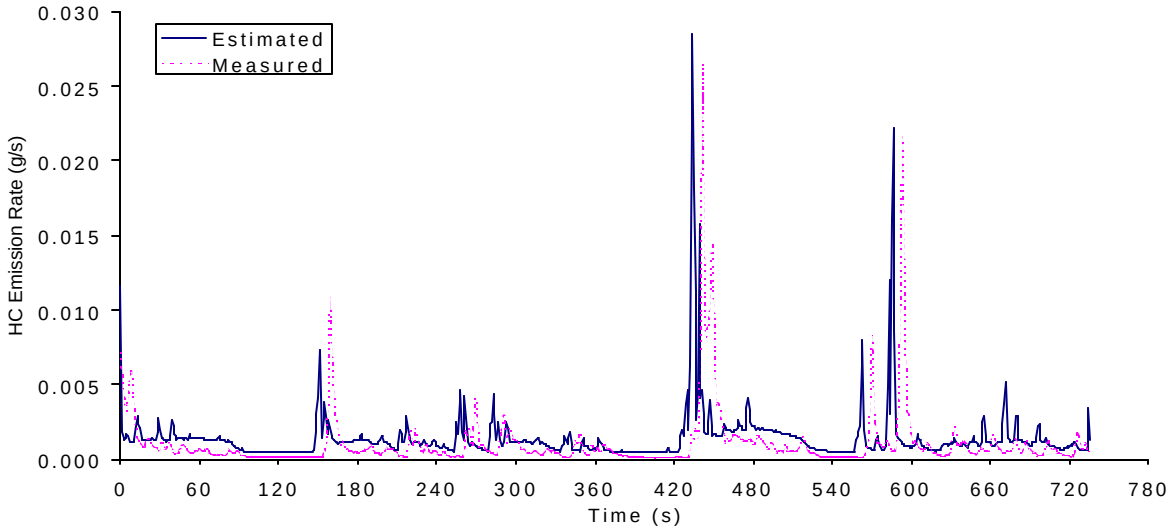

Figure 4-6. HC Emission Comparison for the ARTA Driving Cycle

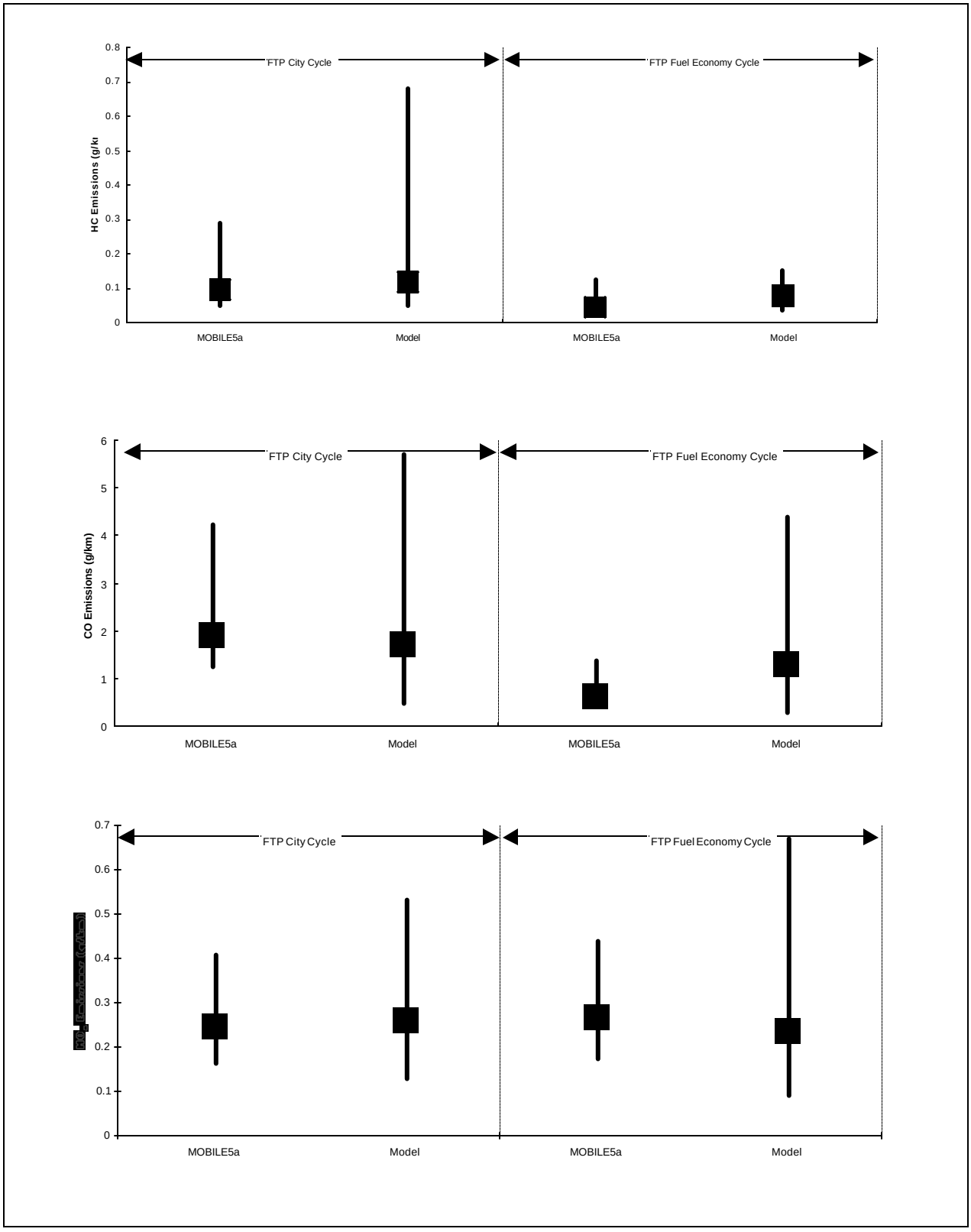

Figure 4-7. Model Comparison to MOBILE5a

CHAPTER 5. COMPARISON OF MOBILE5A, VT-MICRO, AND CMEM MODELS FOR HOT-STABILIZED LIGHT DUTY GASOLINE VEHICLES

This chapter compares fuel consumption and emission results from MOBILE5a, VT-Micro, and CMEM models. The study quantifies the accuracy of the various state-of-the-art energy and emission models for both aggregate trip estimates and instantaneous estimates and identifies under what conditions (speed and acceleration levels) the models provide accurate energy and emission estimates.

5.1 INTRODUCTION

Numerous energy and emission models have been developed over the past decade. Typically, these models differ in their modeling approach, modeling structure, and in the data that were utilized to develop the models. Consequently, there is a need to validate and compare these models in a systematic fashion.

5.1.1 Objectives of Research

The objective of this study is to compare the various energy and emission models that have been described extensively in the literature in an attempt to identify any similarities and/or differences in model predictions. Furthermore, the study attempts to identify the conditions that result in similar and/or different model estimates and potential reasons for these differences.

5.1.2 Significance of Research

The research provides two significant contributions. First, the research quantifies the accuracy of the various state-of-the-art energy and emission models for both aggregate trip estimates and instantaneous estimates. Second, the research identifies under what conditions (speed and acceleration levels) the models provide accurate energy and emission estimates.

5.1.3 Chapter Layout

The chapter first compares and identifies the best model structure to be incorporated in the VT-Micro model. In order to ensure consistency in the model comparisons, the chapter utilizes the various model structures to develop model parameters using energy and emission data that were collected by the Oak Ridge National Laboratory. Subsequently, the VT-Micro model is

compared to the Comprehensive Modal Emission Model (CMEM) that was developed at the University of California, Riverside and the MOBILE5a output. Finally, the study summarizes the findings of the study and presents the main conclusions of this analysis.

5.2 IDENTIFICATION OF MOST SUITABLE MICROSCOPIC MODEL STRUCTURE

This section describes the procedures that were utilized to compare and identify the best model structure to be incorporated in the VT-Micro model by first describing the data that were utilized for the development of the models and the model selection procedure. Finally, the models are compared for a number of standard drive cycles. The same ORNL data were utilized to develop the VT-Micro model are used in this study.

5.2.1 Best Model Structure Selection

The first regression model that was tested included an enhancement to the Post and Akcelik models by introducing more variables, as demonstrated in Equation 4-1 (model 4 of Table 5-1). The model produced reasonable fits to the original data except in a few instances where the model produced negative dependent variable values. To solve this problem, a data transformation technique using the natural logarithm was adopted resulting in the new log-transformed model that is presented in Equation 4-2 (model 7 of Table 5-1). The coefficient of determination of the MOE estimates using Equation 4-2 ranged from 0.72 to 0.99, as demonstrated in Table 5-1. The statistical results indicated a good fit for fuel consumption (R^2 = 0.995) and NO_x estimates (R^2 = 0.960) and a relatively poor fit for HC and CO emission estimates (R^2 = 0.689 and 0.717, respectively).

In order to isolate and identify the shortcomings of the log-transformed polynomial regression models, Figure 5-1 illustrates graphically the quality of fit between the regression models and the ORNL data. It is noted from Figure 5-1 that the errors in the HC and CO model estimates are high at high acceleration levels (overestimates HC emissions by up to 25 percent and CO emissions by 100 percent). These errors in the regression model are caused by the significant sensitivity of the dependent variable to the independent variables at high accelerations compared with the marginal sensitivity of the dependent variable in the negative acceleration range. Differences in behavior for positive versus negative accelerations can be attributed to the fact

that in positive accelerations the vehicle exerts power, while in the negative acceleration range the vehicle does not exert power.

Consequently, separate regression models were developed for positive and negative accelerations, as demonstrated in Equation 4-3 (model 13 of Table 5-1). It should be noted that the intercept at zero speed and zero acceleration was estimated using the positive acceleration model and fixed in order to ensure a continuous function between the two regression regimes. The final models (Equation 4-3, model 13 of Table 5-1) that were developed resulted in good fits to the ORNL data, as demonstrated in Table 5-1 (R^2 in excess of 0.92 for all MOEs). Figure 5-2 further illustrates the effectiveness of the hybrid log-transformed model in predicting vehicle fuel consumption and emission rates as a function of a vehicle's instantaneous speed and acceleration levels. A comparison of Figure 5-1 and Figure 5-2 clearly demonstrates the enhancement in model predictions as a result of separating the positive and negative acceleration regimes. It should be noted, however that the model estimates were less accurate than the polynomial model fits without a logarithmic transformation for high speed and acceleration combinations. However, because the non-log transformed models produced negative MOE estimates, these models were not utilized.

5.2.2 Model Structure Comparison

This section describes how the various model structures were compared for a number of standard drive cycles. Prior to discussing the comparison results, the various drive cycles are initially presented and characterized.

5.2.2.1 Drive Cycle Characterization

EPA recently developed new facility-specific and area-wide driving cycles based on real-world driving studies to incorporate within EPA's new MOBILE6 model (Brzezinski *et al.*, 1999a). Table 5-2 provides a brief description of the new cycles, as well as additional emission test cycles used for emission testing.

The drive cycles listed in Table 5-2 include a number of high speed freeway cycles (cycles 1 and 2), four moderate and congested freeway cycles (cycles 3 through 6), a freeway ramp cycle (cycle 7), three arterial/collector cycles (cycles 8 through 10), a local roadway cycle (cycle 11),

and a number of standard cycles (cycles 12 through 17). The maximum speed in the cycles approaches 120 km/h (High Speed Freeway cycle) with a maximum acceleration of 11.04 km/h/s in the LA92 cycle.

It should be noted that apart from two observations out of all the 17 drive cycles all speed/acceleration combinations were within the feasible range of the ORNL average composite vehicle. Consequently, it appears that the ORNL range of coverage is consistent with field driving behavior.

5.2.2.2 Model Comparison using Standard Driving Cycles

In an effort to identify the best model structure for estimating vehicle fuel consumption and emission rates, emissions of HC, CO, and NO_x and fuel consumption were computed for four drive cycles using 14 different regression models (Table5-1) that were developed for an average composite vehicle. The models were simulated using the raw ORNL data. The four drive cycles that were considered included the standard FTP cycle (cycle 13), the Freeway LOS A-C (cycle 2), the New York cycle (cycle 17), and the Freeway Ramp cycle (cycle 7).

The error relative to the raw ORNL MOE estimates was computed for each of the four drive cycles. The raw emissions were estimated by inputting the speed-acceleration combination each second along the trip trajectory to ORNL lookup tables. These four cycles were selected in order to capture a wide range of driving behavior. Specifically, the FTP cycle is the regulatory urban driving cycle that is utilized by vehicle manufacturers for fuel consumption and emission standards. However, the FTP cycle is criticized for the fact that the accelerations in the cycle are fairly mild. Alternatively, the Freeway LOS A-C cycle represents a high-speed highway driving cycle at a relatively constant speed with minor acceleration and deceleration activities. The New York cycle involves traveling at low speeds under congested urban highway driving conditions, which result in significant stop and go driving behavior. Finally, the ramp cycle involves aggressive acceleration behavior, with potential engine enrichment and its impact on vehicle fuel consumption and emission rates.

In order to ensure consistency in the model comparisons, model coefficients were estimated for all 14 models using the ORNL data for an average composite vehicle. The model comparisons clearly demonstrate that the Post and Akcelik models (models 1 and 2) produce significant errors

for all four MOE estimates, as illustrated in Figure 5-3. Specifically, the majority of models estimate vehicle fuel consumption rates to within 10 percent of the ORNL lookup tables except for the Post and Akcelik models, which produce errors of 30 and 20 percent, respectively. Noteworthy is the fact that the Post and Akcelik models result in significant errors in MOE estimates (in excess of 20 percent) for the New York cycle, which involves driving in congested conditions in an urban environment.

Alternatively, emission predictions demonstrate significant differences between the various models. Furthermore, HC and CO emissions exhibit a similar trend demonstrating that the single-regime (models 6 through 8) and dual-regime (models 12 through 14) logarithmic models produce acceptable errors (errors within 10 percent). Alternatively, NO_x emission estimate errors exhibit a different trend. However, it should be noted that the dual-regime log-transformed models (12 through 14) all produce acceptable errors (within 10 percent).

In summary, Figure 5-3 illustrates that the proposed VT-Micro model (model 13) exhibited a good fit for all four cycles across all four MOEs.

5.2.2.3 Model Comparison for Full Speed-Acceleration Domain

After comparing the various model structures for a number of standard drive cycles, the next step was to compare the models for the envelope of operation of a typical light duty vehicle. As was done with the four-cycle comparison, the model estimates were compared against the ORNL measurements for each speed-acceleration combination. The data range covered speeds from of 0 to 121 km/h at 1.1 km/h increments and accelerations from –1.5 to 2.7 m/s^2 at 0.3 m/s^2 increments resulting in a total of 1305 observations.

Figure 5-4 illustrates the relative error between the model estimates and the ORNL raw data over the entire envelope of operation (1305 observations). The results of Figure 5-4 indicate that the single-regime models without a logarithmic transformation provide the best fit to the data, however, as was discussed earlier these models can produce negative MOE estimates. Alternatively, the dual-regime third order log-transformed model (model 13) ensures that all MOE estimates are positive and produces MOE estimates that are within 2 percent of the raw data.

Figure 5-5 compares the Root Mean Squared Error (RMSE) over the 1305 observations between the model estimates and the raw ORNL data. Figure 5-5 illustrates that the dual-regime multi-order polynomial regression models predict MOEs to a high degree of accuracy. Specifically, the dual-regime third order log-transformed model (model 13) estimates fuel consumption rates to within 0.1 ml/s of the raw data on average. Similarly, the model predicts HC, CO, and NOx emissions to within 5, 200, and 2 mg/s, respectively.

The comparisons that are presented in Figure 5-3, Figure 5-4, and Figure 5-5 demonstrate that the log-transformed dual-regime 3rd order polynomial model produces a best fit over the full range of cycles that were compared while estimating realistic MOE rates (non-negative MOEs). Consequently, only this model is compared against other state-of-the-art models, including the MOBILE5a and CMEM models in the remainder of this chapter.

5.3 COMPARISON OF VT-MICRO AND CMEM MODELS

The next step in the comparison effort was to compare the CMEM and VT-Micro model predictions for two sample drive cycles that included the FTP and Ramp cycle. Two CMEM model categories were considered, namely the low power/weight ratio vehicle category (CMEM-1, Category 6,10,17) and the high power/weight ratio vehicle category (CMEM-2, Category 7,11,17). These categories were constructed by generating a weighted composite vehicle of the same composition as the ORNL vehicles (no high emitters, mileages less than 50K). As expected, Figure 5-6 illustrates a high degree of consistency between the ORNL data and the VT-Micro model estimates for both drive cycles across all four MOEs. Alternatively, apart from the fuel consumption and NO_x emissions for the RAMP cycle large differences are observed between the VT-Micro and CMEM models. It is interesting to note that, apart from the CO emission estimates for the Ramp cycle, the CMEM low and high power categories produce almost identical MOE estimates.

In an attempt to isolate the differences between the VT-Micro and CMEM models, the various MOE estimates were predicted for the full envelope of operation of a typical vehicle (1305 speed-acceleration combinations), as was done in the previous section. It should be noted that each speed-acceleration observation was maintained for a duration of 5 seconds in order to ensure steady-state behavior when applying the CMEM model.

Figure 5-7 illustrates similar increasing trends in fuel consumption estimates between the VT-Micro and CMEM models for the cruising mode of operation. The low power/weight ratio vehicle categories are utilized for CMEM model simulations. However, the model predictions differ when the vehicle engages in a deceleration or acceleration mode of operation. Specifically, while the CMEM model predicts a constant emission rate as a function of vehicle speed when a vehicle is decelerating, the ORNL data and the VT-Micro model predict rates that increase with the vehicle speed. In addition, unlike the VT-Micro model, the CMEM model estimates a constant fuel consumption rate at a speed of 0 km/h regardless of the acceleration rate. Clearly, these observations do indicate some inherent limitations with the CMEM model predictions.

As was the case for the fuel consumption comparison, Figure 5-8 illustrates a similar behavior for HC emissions. Specifically, there appears to be consistency between the models for the cruise mode of operation, however inconsistencies are observed for the deceleration and acceleration modes of operation. In addition, it should be noted that, in general, the CMEM model tends to under-estimate vehicle HC emissions in comparison with the ORNL data and the VT-Micro model. Finally, the CMEM model estimates tend to respond marginally to increases in speeds in the range of 0 to 40 km/h and then increase rapidly for higher speeds for the acceleration mode of operation.

The CO emissions exhibit a similar trend of behavior as compared to the HC emissions, as illustrated in Figure 5-9. However, the CMEM model appears to predict higher CO emissions in the 0-to 20-km/h ranges than in the 20-to 40-km/h ranges for the same acceleration (2.4 m/s^2). It is not clear why this trend is observed given that the engine load increases with higher speeds and thus should result in higher CO emissions with higher speeds, as predicted by the ORNL data and the VT-Micro model. For example, the literature indicates that research suggests that sharp accelerations, which cause vehicles to operate in a fuel-rich mode, contribute significantly to high emission levels for CO and Volatile Organic Compounds (VOCs) or HCs (NRC, 1995).

In Figure 5-10, the ORNL data and VT-Micro models demonstrate a reduction in NO_x emissions at high engine loads, which is not the case for the CMEM model. This decrease in NO_x emissions at extremely high engine loads is consistent with what is described in the literature. For example a National Research Council (1995) report indicates that mild accelerations, which

do not cause fuel enrichment, increase NO_x emissions because of the higher loads placed on the engine. The literature suggests that under conditions of mild accelerations NO_x emissions can be 2 to 3 times higher than under cruise-type driving (NRC, 1995).

In Figures 5-7 to 5-10, during the deceleration mode or engine idling mode, it is investigated that fuel consumption and emissions increase as vehicle speeds increase. This can be explained that even though the engine is operated in idling mode, the vehicle power or tractive force, which is proportional to vehicle fuel consumption and emissions, still exist due to the vehicle rolling resistance and aerodynamic resistance. Since the vehicle rolling resistance and aerodynamic resistance are proportional to vehicle speeds, fuel consumption and emissions increase during engine idling condition when vehicle speeds increase.

5.4 MODEL VALIDATION AGAINST FIELD DATA AND MOBILE5A

The next step in the analysis was to validate the VT-Micro model against third-party field data that were collected on a chassis dynamometer and against the state-of-practice MOBILE5a model estimates. In addition, because of the discrepancies that were found between the VT-Micro and CMEM models, the CMEM model is also compared against the field data and MOBILE5a estimates.

Prior to discussing the specifics of the results it is important that the field data be described in some level of detail. These field data were collected by the Environmental Protection Agency (EPA) at the Automotive Testing Laboratories, Inc. (ATL), in Ohio and EPA's National Vehicle and Fuels Emission Laboratory (NVREL), in Ann Arbor, Michigan, in the spring of 1997. All the vehicles at ATL were drafted at Inspection and Maintenance lanes utilized by the State of Ohio and tested under as-received condition (without repairs). A total of 62 vehicles in East Liberty, Ohio, and 39 vehicles in Ann Arbor, Michigan were recruited and tested. The sample of 101 vehicles included 3 heavy-duty trucks, 34 light-duty trucks, and 64 light-duty cars. The vehicle model years ranged from 1986 through 1996 (Brzezinski *et al*., 1999b). All vehicles were tested using the standard vehicle certification test fuel. Vehicle emission tests were performed in random order to offset any possible order bias that could result in different ambient conditions for the tested cycles. The emission results were measured as composite "bags" and in grams on a second-by-second basis for HC, CO, NO_x, and CO_2 emissions.

For comparison purposes only normal vehicles (50 vehicles from the dataset) were considered by using the emission cut-points using 0.52 g/km (0.82 g/mi) for HC, 6.38 g/km (10.2 g/mi) for CO, and 1.25 (g/km) 2.0 g/mi for NOx (for the FTP bag emission results) to screen the high emitting vehicles from the vehicle fleet. The 95 percent confidence limits were then estimated for the normal vehicles for each of the three emissions (HC, CO, and NO_x) and used for comparison purposes.

In addition to the field data, the MOBILE5a model was utilized to estimate vehicle emissions for each cycle using the cycle's average speed and vehicle mileages in the range of 2k to 20k per year in order to be consistent with the ORNL vehicle sample. A vehicle composition of 67 percent light duty cars and 33 percent light duty trucks was considered in order to maintain the same vehicle distribution as the ORNL data. The minimum and maximum tail-pipe emission estimates for the different vehicle mileage configurations was estimated and illustrated in Figure 5-11.

Figure 5-11 demonstrates an excellent correspondence between the VT-Micro model and the field data. Specifically, the VT-Micro model estimates are within the mid-range of the field data, except for slight overestimations on HC emissions. Furthermore, the VT-Micro model estimates respond to the increase in HC emissions for the "ART E-F" and Ramp cycles in a fashion that is consistent with the field data. The figure shows that CO and NO_x estimates follows perfect fit to EPA mean values.

Figure 5-11 also illustrates some of the shortcomings of the MOBILE5a model. For example, while the field data and the VT-Micro models indicate an increase in vehicle emissions for the Ramp cycle, with its aggressive accelerations, the MOBILE5a model indicates a reduction in vehicle emissions. This limitation is attributed to the fact that the MOBILE5a model uses the average speed as a single traffic-related explanatory variable, which ignores the acceleration levels involved in the drive cycle. It would be interesting to compare MOBILE5a and MOBILE6 estimates for the full range of cycles when the MOBILE6 model is released, in order to evaluate whether this shortcoming has been resolved.

Figure 5-11 also describes CMEM model estimates for various cycles. In order to compare the models, 50 EPA normal vehicles are categorized by CMEM classifications (class 4 for 7 vehicles,

class 5 for 19, class 6 for 1, class 7 for 3, class 8 for 1, class 11 for 8, class 16 for 8, class 17 for 2, and class 18 for 1). Each CMEM category was simulated by 14 driving cycles and its weighted average was calculated for CMEM model estimates. CMEM model estimates appear to fall inside the bounds of the EPA 95/5 percentile and generally well follows EPA mean value patterns. However, it is discovered that the CMEM model generally underestimates NOx emissions and shows some variations at Fwy G, Art CD, Ramp cycles for CO emissions.

5.5 SUMMARY

The performance of various fuel consumption and emission models was assessed and validated using several evaluation techniques. The general conclusions of the study can be summarized as follows:

- The original power based models, namely the Post and Akcelik models, do not provide good MOE estimates when compared to field data.

- The log-transformed dual-regime 3rd order polynomial model structure, which is utilized within the VT-Micro model, predicts fuel consumption and emissions within an acceptable error range with respect to field data (coefficient of determination greater than 92 percent for all MOEs).

- The CMEM model exhibits some abnormal behaviors. First, the model estimates identical MOE estimates for speeds of 0 km/h regardless of the acceleration rate. Second, the model estimates constant MOE estimates during deceleration maneuvers. Third, the model generally underestimates MOEs for acceleration maneuvers comparing to EPA field data. Fourth, the CO emission estimates exhibit strange behavior at low speeds and high acceleration levels (sudden drops of emissions). Finally, the NO_x emissions do not exhibit the typical decay in emission rates at high engine loads.

- The proposed VT-Micro model has been demonstrated to be valid in terms of absolute light-duty hot stabilized normal vehicle tailpipe emissions. Specifically, the emission estimates were found to be within the 95 percent confidence limits of field data and within the same level of magnitude as the MOBILE5a model.

- The proposed VT-Micro model was found to reflect differences in drive cycles in a fashion that was consistent with field observations. Specifically, the model accurately captures the increase in emissions for the Ramp cycle, with its associated aggressive acceleration maneuvers, in comparison with other drive cycles.

Table 5-1. Proposed Instantaneous Energy and Emission Model Structures

Seq.	Model	No. of Parameters	Model Structure (Spd = u, Accel = a, Const = c)	R^2
1	Post	5	c, u, u^2, u^3, ua	Fuel: 0.983, HC: 0.784 CO: 0.828, NO_x: 0.904
2	Akcelik	5	c, u, u^3, ua, ua^2	Fuel: 0.987, HC: 0.779 CO: 0.822, NO_x: 0.902
3	2nd order polynomial	9	c, u, u^2, a, ua, u^2a, a^2, ua^2, u^2a^2	Fuel: 0.994, HC: 0.858 CO: 0.890, NO_x: 0.928
4	3rd order polynomial	16	c, u, u^2, u^3, a, ua, u^2a, u^3a,a^2, ua^2, u^2a^2, u^3a^2, a^3, ua^3, u^2a^3, u^3a^3,	Fuel: 0.997, HC: 0.963 CO: 0.985, NO_x: 0.951
5	4th order polynomial	25	c, u, u^2, u^3, u^4, a, ua, u^2a, u^3a, u^4a, a^2,ua^2, u^2a^2, u^3a^2, u^4a^2, a^3,ua^3, u^2a^3, u^3a^3, u^4a^3, a^4,ua^4, u^2a^4, u^3a^4, u^4a^4	Fuel: 0.998, HC: 0.972 CO: 0.986, NO_x: 0.987
6	Log-transformed 2nd order polynomial	9	Exp(c, u, u^2, a, ua, u^2a, a^2, ua^2, u^2a^2)	Fuel: 0.945, HC: 0.764 CO: 0.696, NO_x: 0.654
7	Log-transformed 3rd order polynomial	16	Exp(c, u, u^2, u^3, a, ua, u^2a, u^3a, a^2, ua^2, u^2a^2, u^3a^2, a^3, ua^3, u^2a^3, u^3a^3)	Fuel: 0.995, HC: 0.689 CO: 0.717, NO_x: 0.960
8	Log-transformed 4th order polynomial	25	Exp(c, u, u^2, u^3, u^4, a, ua, u^2a, u^3a, u^4a, a^2, ua^2, u^2a^2, u^3a^2,u^4a^2, a^3,ua^3,u^2a^3,u^3a^3,u^4a^3,a^4,ua^4,u^2a^4,u^3a^4,u^4a^4)	Fuel: 0.996, HC: 0.969 CO: 0.957, NO_x: 0.975
9	Dual-regime 2nd order polynomial	18	c, u, u^2, a, ua, u^2a, a^2, ua^2, u^2a^2	Fuel: 0.998, HC: 0.959 CO: 0.987, NO_x: 0.974
10	Dual-regime 3rd order polynomial	32	c, u, u^2, u^3, a, ua, u^2a, u^3a, a^2, ua^2, u^2a^2, u^3a^2, a^3,ua^3, u^2a^3, u^3a^3,	Fuel: 0.999, HC: 0.959 CO: 0.991, NO_x: 0.989
11	Dual-regime 4th order polynomial	50	c, u, u^2, u^3, u^4, a, ua, u^2a, u^3a, u^4a, a^2,ua^2, u^2a^2, u^3a^2, u^4a^2, a^3,ua^3, u^2a^3, u^3a^3, u^4a^3, a^4,ua^4, u^2a^4, u^3a^4, u^4a^4	Fuel: 0.998, HC: 0.990 CO: 0.993, NO_x: 0.990
12	Log-transformed dual-regime 2nd order polynomial	18	Exp(c, u, u^2, a, ua, u^2a, a^2, ua^2, u^2a^2)	Fuel: 0.996, HC: 0.818 CO: 0.867, NO_x: 0.978
13	Log-transformed dual-regime 3rd order polynomial	32	Exp(c, u, u^2, u^3, a, ua, u^2a, u^3a, a^2, ua^2, u^2a^2, u^3a^2, a^3, ua^3, u^2a^3, u^3a^3)	Fuel: 0.998, HC: 0.981 CO: 0.929, NO_x: 0.982
14	Log-transformed dual-regime 4th order polynomial	50	Exp(c, u, u^2, u^3, u^4, a, ua, u^2a, u^3a, u^4a, a^2,ua^2, u^2a^2, u^3a^2, u^4a^2, a^3,ua^3,u^2a^3,u^3a^3,u^4a^3,a^4,ua^4, u^2a^4, u^3a^4, u^4a^4)	Fuel: 0.997, HC: 0.960 CO: 0.976, NO_x: 0.988

Table 5-2. EPA's New Facility-Specific Drive Cycle Characteristics

Seq.	Cycle	Avg. Spd (km/h)	Max. Spd (km/h)	Max. Accel (km/h/s)	Duration (s)	Length (km)
1	Freeway, High Speed	101.12	119.52	4.32	610	17.150
2	Freeway, LOS A-C	95.52	116.96	5.44	516	13.680
3	Freeway, LOS D	84.64	112.96	3.68	406	9.540
4	Freeway, LOS E	48.80	100.80	8.48	456	6.180
5	Freeway, LOS F	29.76	79.84	11.04	442	3.660
6	Freeway, LOS G	20.96	57.12	6.08	390	2.270
7	Freeway Ramps	55.36	96.32	9.12	266	4.100
8	Arterial/Collectors LOS A-B	39.68	94.24	8.00	737	8.110
9	Arterial/Collectors LOS C-D	30.72	79.20	9.12	629	5.380
10	Arterial/Collectors LOS E-F	18.56	63.84	9.28	504	2.590
11	Local Roadways	20.64	61.28	5.92	525	2.990
12	Non-Freeway Area-Wide Urban Travel	31.04	83.68	10.24	1348	11.600
13	LA04 (FTP Bag 2 and Bag 3)	31.36	90.72	5.28	1368	11.920
14	Running 505	40.96	90.72	5.28	505	5.744
15	LA 92	39.36	107.52	11.04	1435	15.696
16	ST01	32.32	65.60	8.16	248	2.224
17	New York Cycle	11.36	44.32	9.6	600	1.888

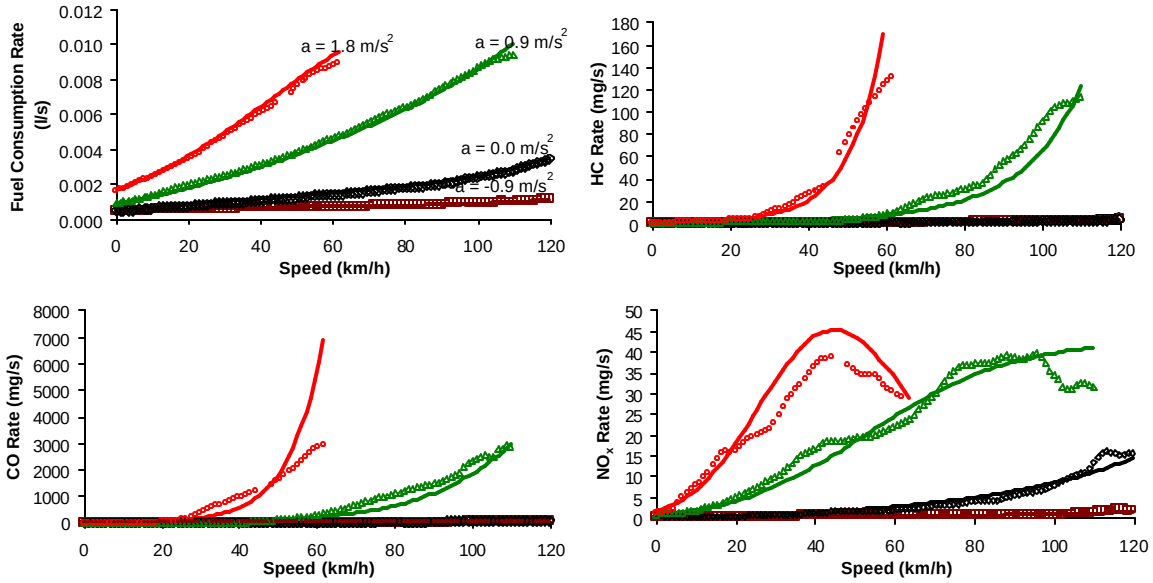

Figure 5-1. VT-Micro Model Predictions (Composite Vehicle – Log-Transformed Polynomial Model)

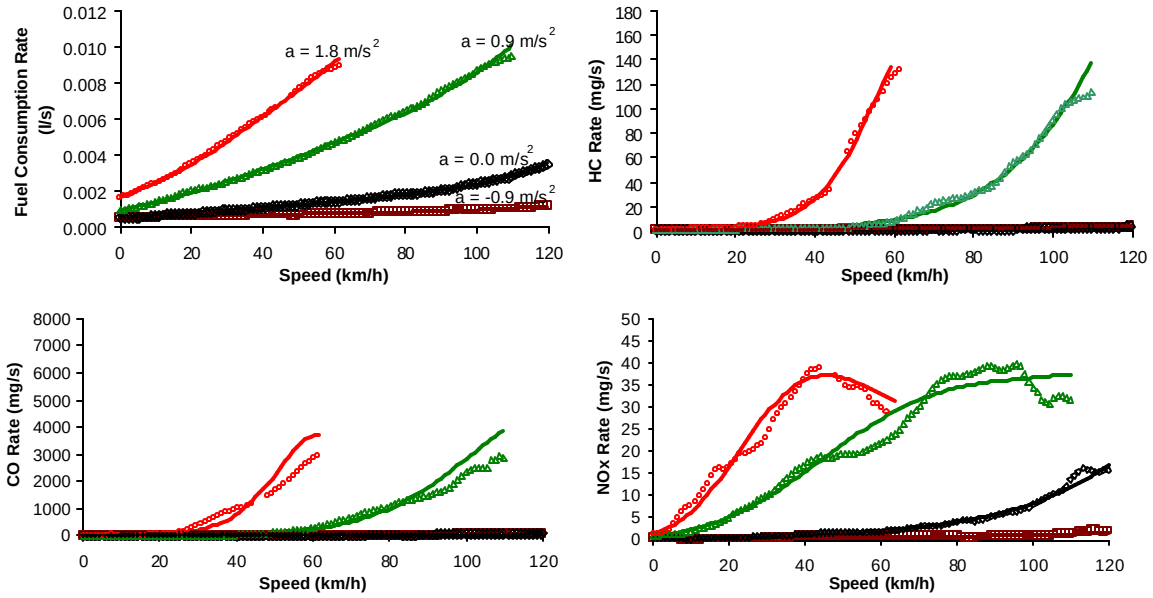

Figure 5-2. VT-Micro Model Predictions (Composite Vehicle – Log-Transformed Hybrid Polynomial Model)

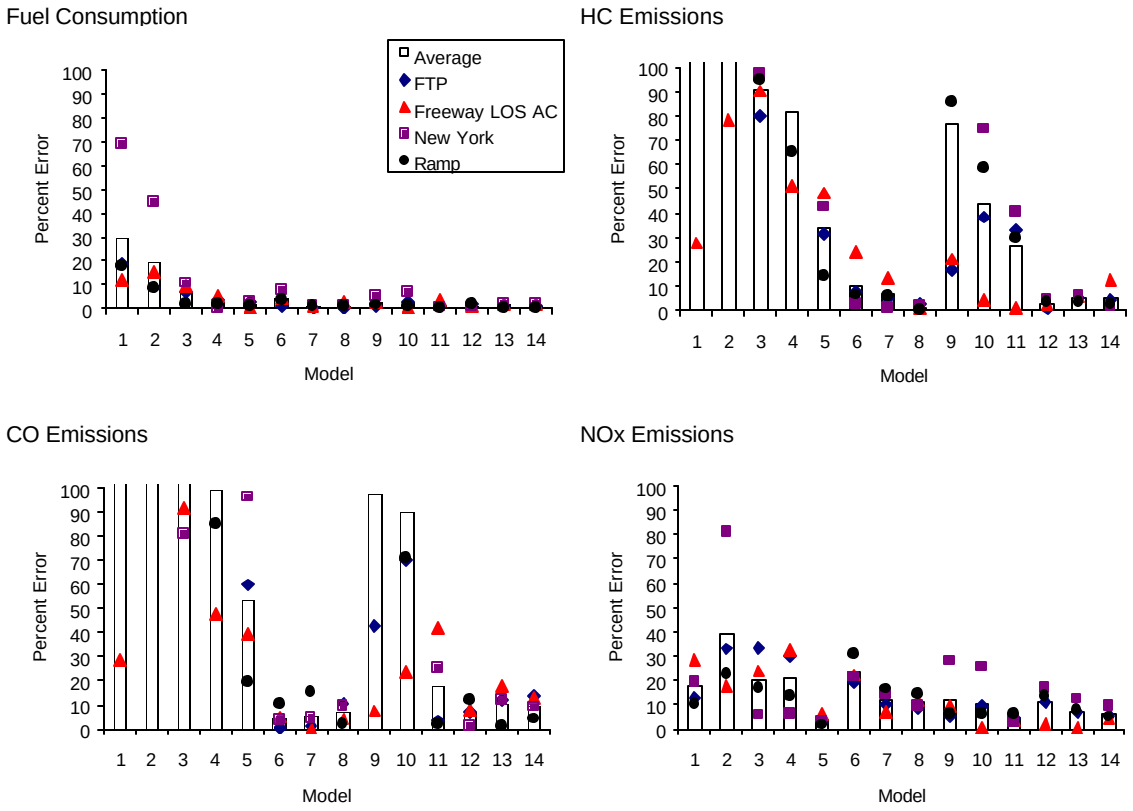

Figure 5-3. Variation in Trip MOE Error for the 14 Model Structures

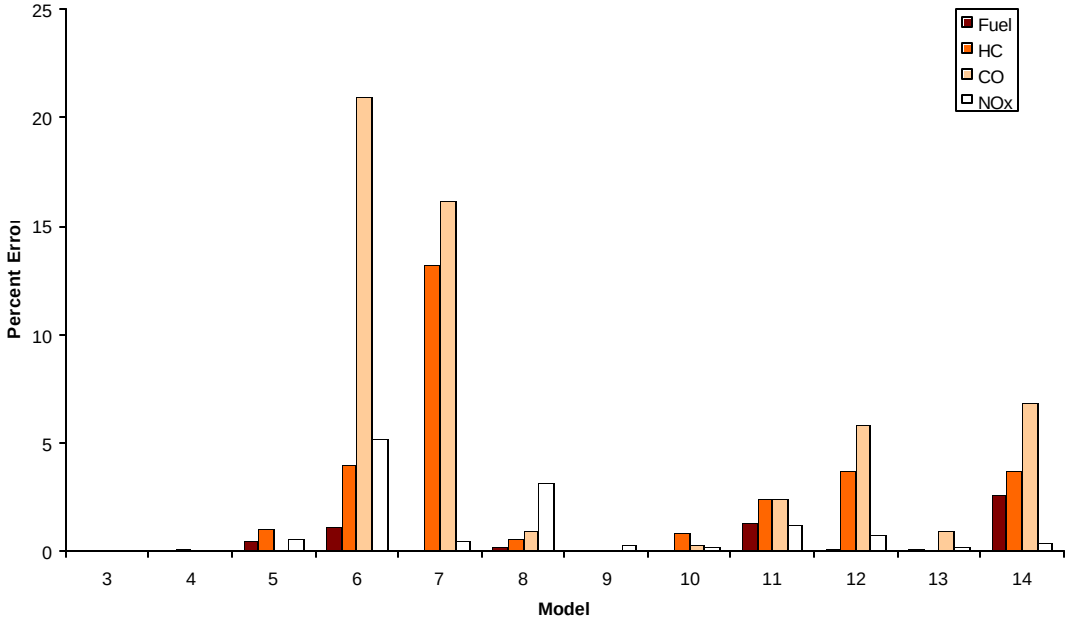

Figure 5-4. Model Comparison with ORNL Data Set (Total Error).

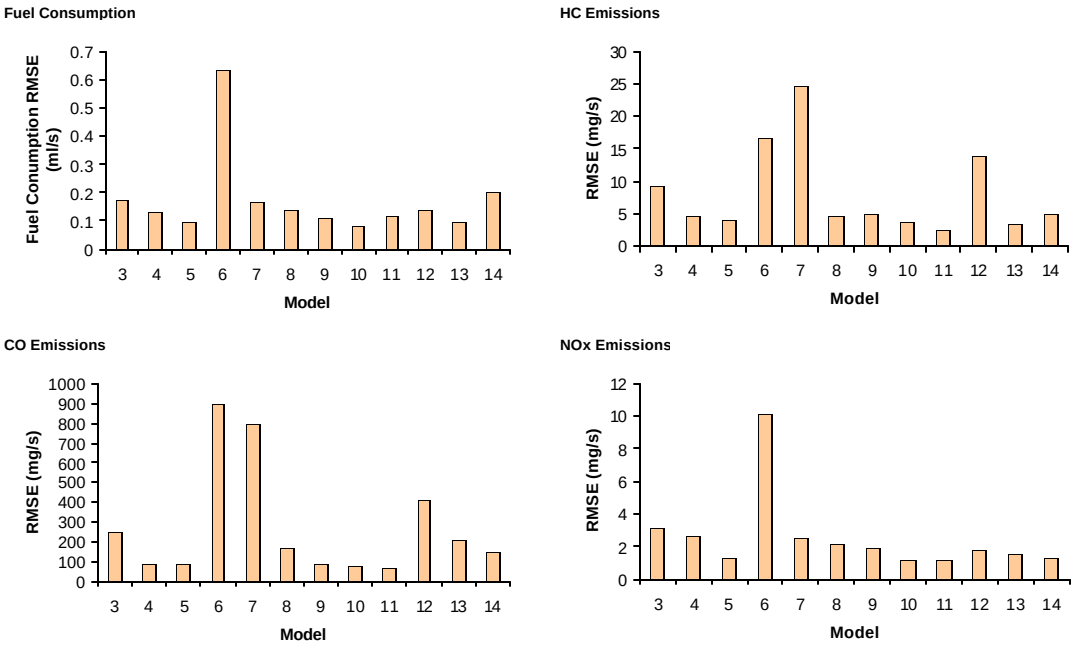

Figure 5-5. Model Comparison with ORNL Data Set (RMSE).

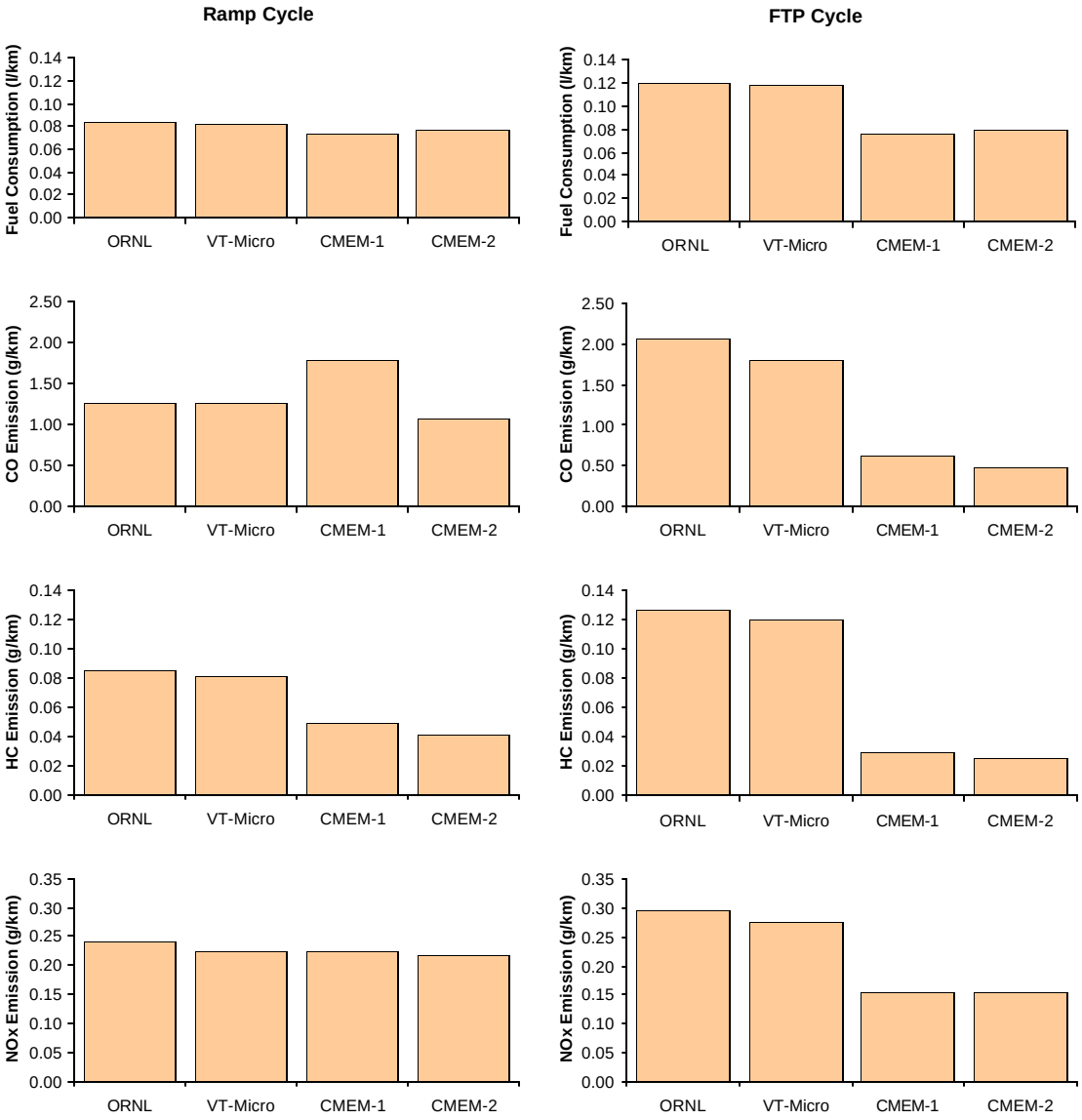

Figure 5-6. Comparison of VT-MICRO and CMEM Model using Driving Cycles

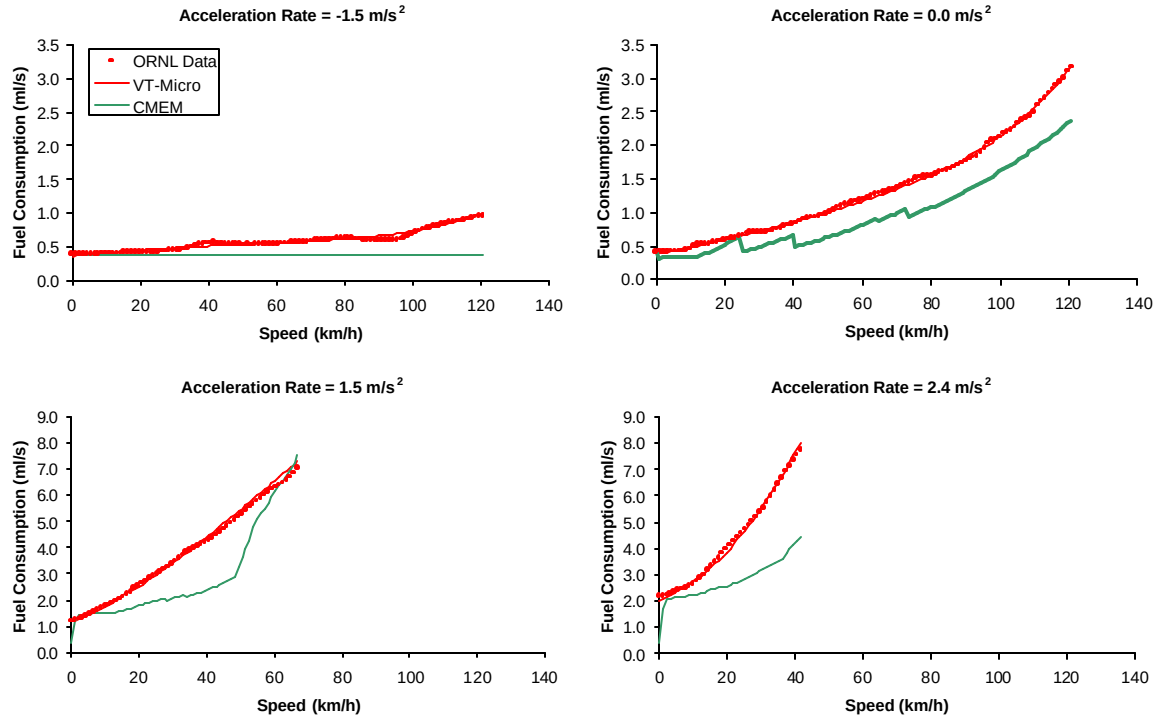

Conclusions:

1. VT-Micro fuel consmption is consistent with ORNL data
2. VT-Micro fuel consumption is generally higher than CMEM
3. CMEM fuel consumption is constant for deceleration
4. CMEM fuel consumption rate is constant for zero speed regardless of the degree of acceleration

Figure 5-7. Disaggregate Model Comparison of VT-Micro and CMEM Model Output (Fuel Consumption)

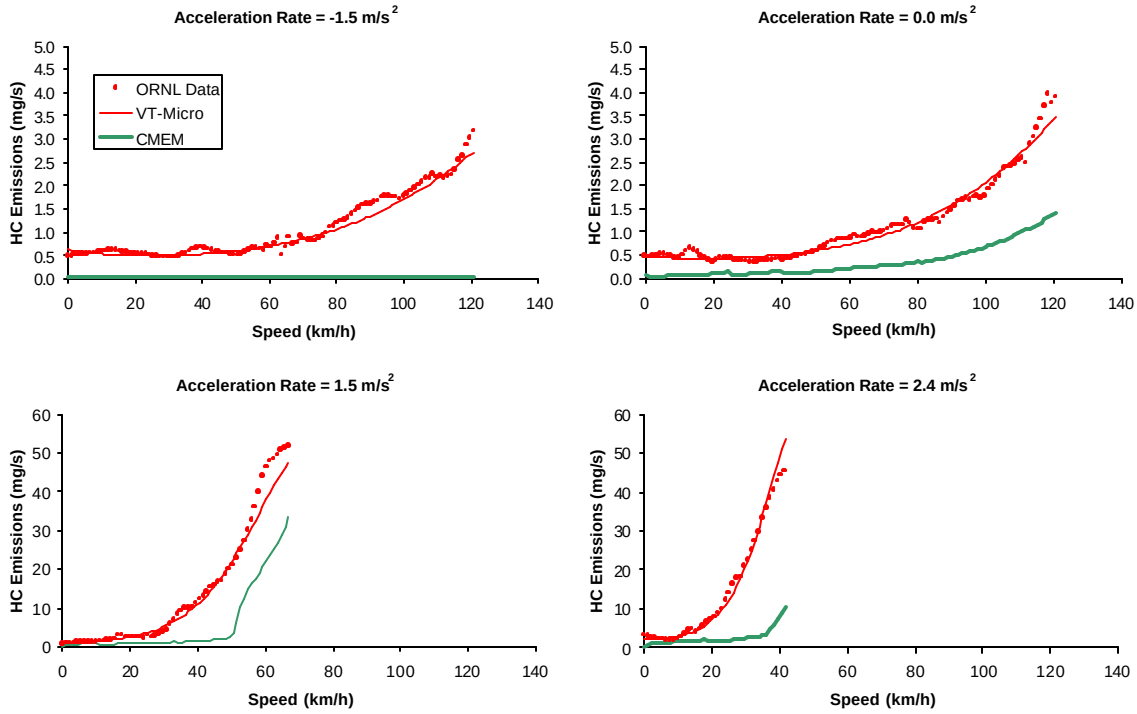

Conclusions:

1. VT-Micro HC emissions are consistent with ORNL data
2. VT-Micro HC emissions are higher than CMEM emissions
3. CMEM emissions are constant for deceleration
4. High HC emissions for accelerations
5. CMEM HC emission rate is identical at a speed of zero regardless of the acceleration level

Figure 5-8. Disaggregate Model Comparison of VT-Micro and CMEM Model (HC Emissions)

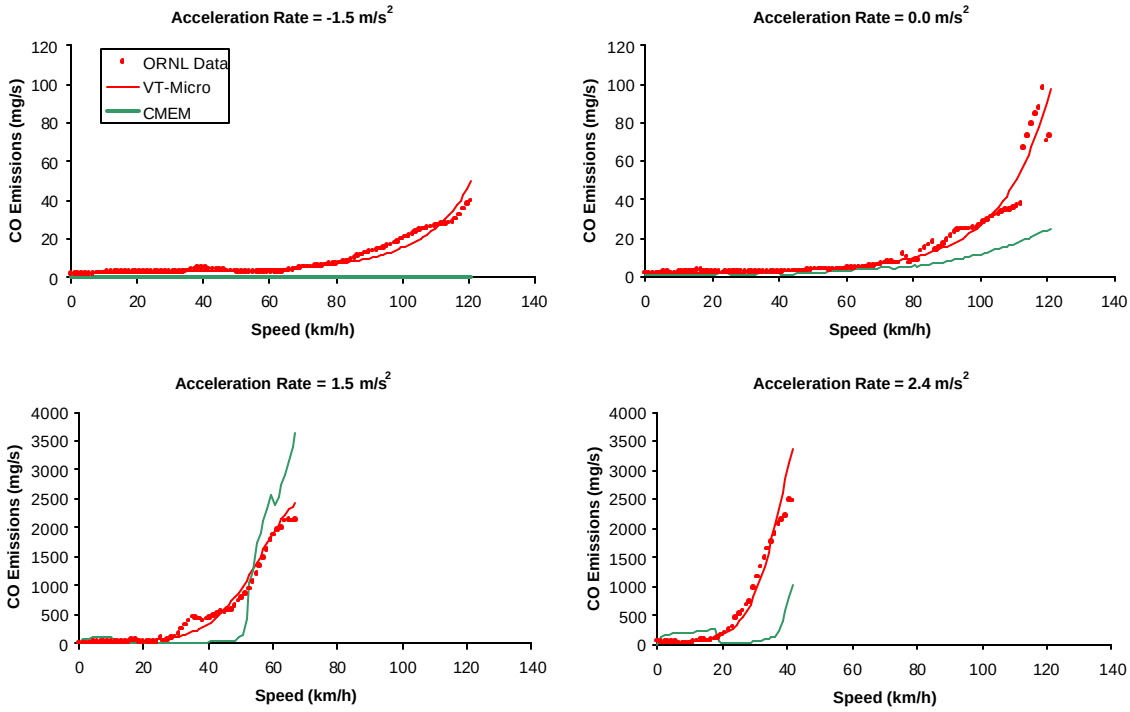

Conclusions:

1. VT-Micro CO emissions are consistent with ORNL data
2. VT-Micro CO emissions are generally higher than CMEM
3. CMEM emissions are constant for deceleration mode of operation
4. Field data and models estimate high CO emissions for high engine loads (high speeds and accelerations)
5. CMEM model produces higher CO emissions in the speed range from 0 to 20 km/h than in the speed range from 20 to 40 km/h for the same acceleration level
6. CMEM CO emission rate is identical at a speed of zero regardless of the acceleration level

Figure 5-9. Disaggregate Model Comparison of VT-Micro and CMEM Model (CO Emissions)

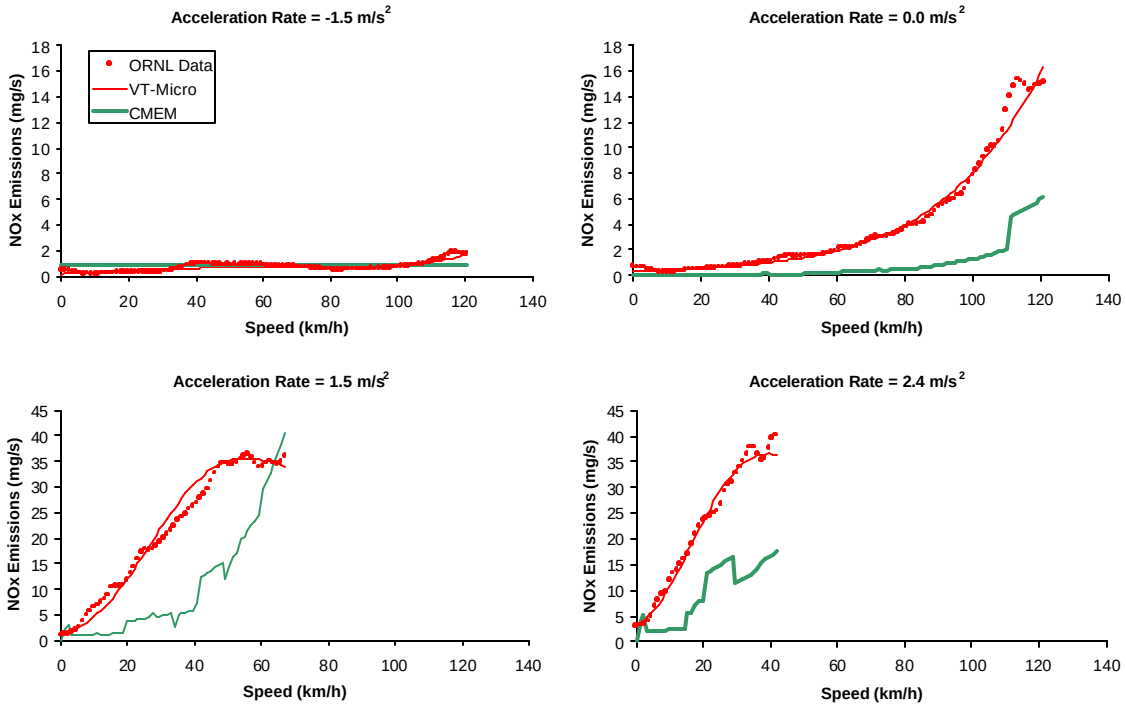

Conclusions:

1. VT-Micro NOx emissions are consistent with ORNL data
2. VT-Micro NOx emissions are generally higher than CMEM
3. CMEM NOx emissions are constant for deceleration mode of operation
4. ORNL data indicates that NOx Emissions decrease at high engine loads
5. CMEM NOx emissions for acceleration mode behaves strangely
6. CMEM assumes identical NOx emissions at zero speed regardless of the acceleration level

Figure 5-10. Disaggregate Model Comparison of VT-Micro and CMEM Model (NOx Emissions)

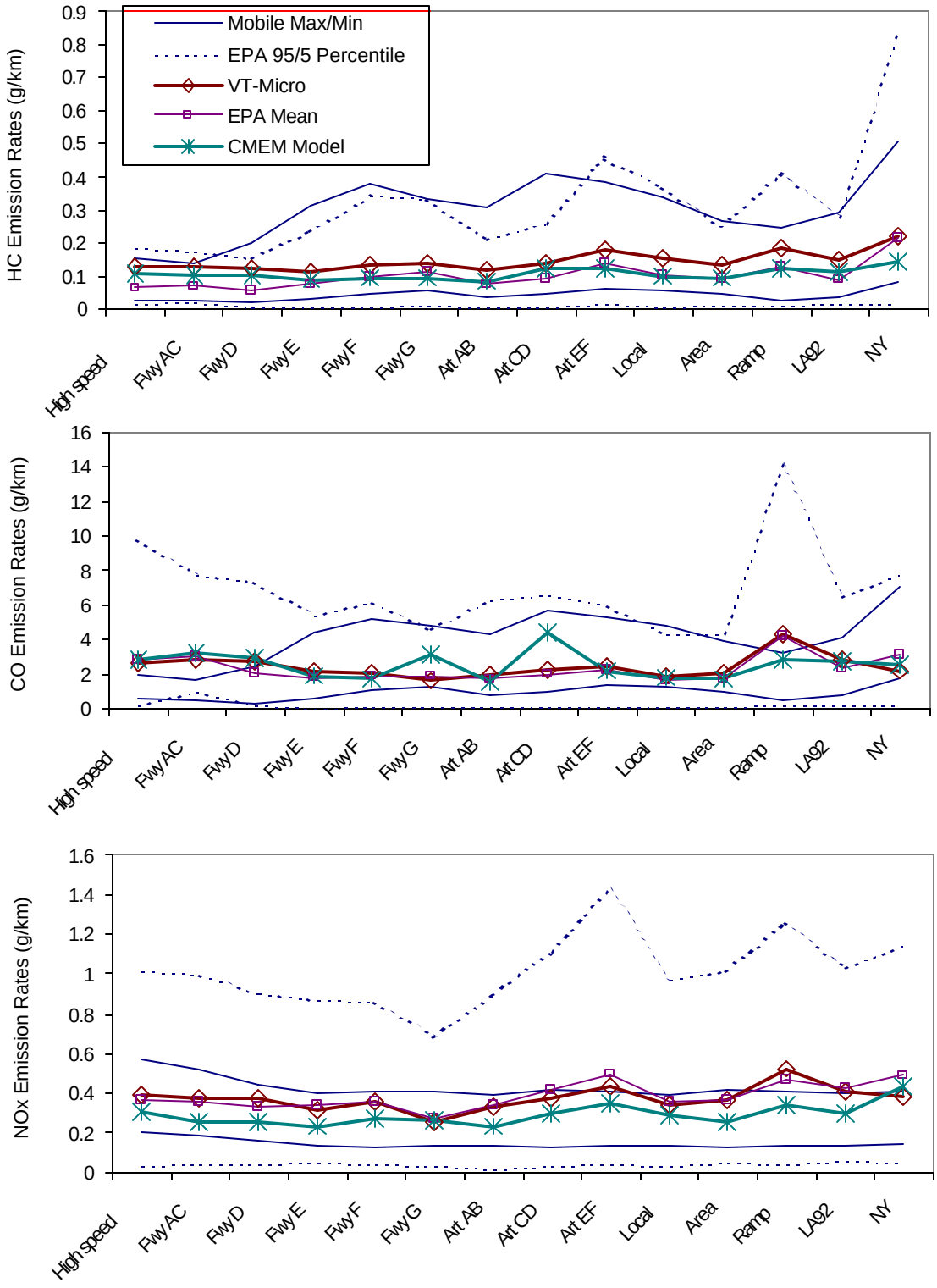

Figure 5-11. VT-Micro Comparison against MOBILE5a and EPA data

CHAPTER 6. VT-MICRO VERSION 2.0: MODELING HOT STABILIZED LIGHT DUTY VEHICLE AND TRUCK EMISSIONS

The chapter presents microscopic emission models that estimate second-by-second mobile source emissions in hot stabilized conditions using instantaneous vehicle speed and acceleration levels as input variables. The model is an extension to the original VT-Micro model that was developed using chassis dynamometer data on nine light duty vehicles. In this chapter, the VT-Micro model is expanded by including data from 67 light duty vehicles and trucks.

6.1 INTRODUCTION

Estimating accurate mobile source emissions is becoming more and more critical as a result of increasing environmental problems in large metropolitan urban areas. Current emission inventory models, such as MOBILE and EMPAC, are designed for developing large scale inventories, but are unable to estimate emissions from specific corridors and intersections. Alternatively, microscopic emission models are capable of assessing the impact of transportation scenarios and performing project-level analyses. This chapter presents an extension to the original VT-Micro model that was developed using chassis dynamometer data on nine light duty vehicles. In this chapter, the VT-Micro model is expanded by including data from 67 light duty vehicles and trucks.

6.1.1 Objectives of Research

The chapter presents a framework for developing microscopic emission models for assessing the environmental impacts of transportation projects. The framework develops emission models by aggregating data using vehicle and operational variables. Specifically, statistical techniques for aggregating vehicles into homogenous categories are utilized as part of the framework. In addition, the framework accounts for temporal lags between vehicle operational variables and vehicle emissions. Finally, the framework is utilized to develop the VT-Micro model version 2.0 utilizing second-by-second chassis dynamometer data for a total of 60 light duty vehicles and trucks.

6.1.2 Significance of Research

The research that is described in this chapter provides several significant contributions. First, the chapter presents a comprehensive framework for developing microscopic energy and emission models. This framework considers the use of statistical tools to categorize emission data based on vehicle-specific variables, develops procedures for operational variable binning, and develops techniques for adjusting for the temporal lag between operational variables and vehicle emissions. Secondly, the research develops a model that can be easily incorporated within microscopic traffic simulation software to evaluate the environmental impacts of alternative traffic management strategies, including the introduction of Intelligent Transportation System (ITS) technologies.

6.1.3 Chapter Layout

This chapter is organized into five sections. The next section describes the data sources that were utilized to develop the proposed models and the data collection procedures, driving cycles utilized for data collection, and test vehicle characterization. The third section describes the modeling framework and how this modeling framework was applied to the data. The fourth section describes how the model was validated both macroscopically and microscopically against field data. The final section provides the study conclusions.

6.2 EMISSION DATA DESCRIPTION

This section describes the data that were utilized in applying the VT-Micro framework for emission modeling. The data are described in terms of the data collection procedures, the vehicles tested, and the drive cycles that were utilized for data collection.

6.2.1 Data Collection Procedures

The data were gathered by EPA on a chassis dynamometer at the Automotive Testing Laboratories, Inc. (ATL), in Ohio and EPA's National Vehicle and Fuels Emission Laboratory (NVREL), in Ann Arbor, Michigan in the spring of 1997. All vehicles at ATL were drafted at Inspection and Maintenance lanes utilized by the State of Ohio and tested under as-received condition (without repairs). Of the total 101 vehicles, 62 vehicles were tested at ATL and 39 vehicles were tested at NVREL. Unfortunately, the 101 vehicle sample size was reduced to 96

vehicles because of insufficient data for 5 vehicles. All vehicles were tested at FTP under ambient conditions using the standard vehicle certification test fuel. Vehicle emission tests were performed in random order to offset any possible order bias that could result in different ambient conditions for the tested cycles. The HC, CO, NO_x, and CO_2 emissions were measured as composite "bags" and in grams on a second-by-second basis (Brzezinski *et al*., 1999a).

6.2.2 Test Vehicle Characterization

The 96 vehicles that were tested included model years that ranged from 1986 through 1996. These vehicles were initially screened in order to separate normal from high emitting vehicles using a threshold that was set at twice the manufacturer standards. Of the total sample size of 96 vehicles, 60 vehicles were classified as normal vehicles and 36 were classified as high emitting vehicles. Also, among the 60 normal vehicles, 43 vehicles were LDVs and the remaining 17 vehicles were LDTs, as illustrated in Figure 6-1. The 60 vehicles included 42 vehicles with automatic transmission and 18 vehicles with manual transmission. All 60 vehicles used fuel injection gasoline engines that ranged from 1.0 liter to 5.8 liters, with the majority of vehicles in the 2.0 to 4.0 liter range. The majority of vehicles had a mileage less than 160,000 kilometers (100,000 miles).

6.2.3 Drive Cycle Characterization

The EPA developed new facility-specific and area-wide drive cycles based on real-world driving studies. These drive cycles have been incorporated in the MOBILE6 model (Brzezinski *et al*., 1999a). In order to represent real-world driving conditions, the driving behavior in each drive cycle was developed using observed speed-acceleration profiles and specific power frequency distributions of chase car driving data from a range of roadway types during periods of various congestion levels. These drive cycles cover four roadway types that include: Freeways, Arterial/Collectors, Freeway Ramps, and Local Roadways. The roadways are further classified based on Level of Service (LOS) measures, similar to the transportation congestion index, from “A” to “G.” Table 4-4 provided a brief description of the new EPA cycles and some additional drive cycles used for emission testing. The additional cycles include the LA4 (urban dynamometer driving cycle), the California Air Resources Board (CARB) area-wide Unified Cycle (LA92), the New York City Cycle (a low speed cycle which has previously used for speed correction factors in the MOBILE model), and ST01 (the first 258 seconds of the vehicle

certification air conditioning cycle). Of the total 17 drive cycles, each vehicle was tested over 14 to 16 drive cycles. It should be noted that the ST01 drive cycle was not utilized for model validation because it includes cold start emissions. Figures A-1 to A-3 in Appendix A illustrate the speed profiles of the 16 drive cycles that were analyzed. The maximum speed of all cycles was 119.5 km/h on the Freeway High Speed Cycle, while the maximum acceleration rate was 11.04 km/h/s (3.07 m/s^2) on the Freeway, LOS F and LA92 cycles. It should be noted that the New York cycle had the lowest average speed of all drive cycles (11.4 km/h).

6.3 MODEL DEVELOPMENT

This section describes the framework that was utilized to develop the VT-Micro model. Specifically, the framework involves two major classification efforts, as illustrated in Figure 6-2. The first effort aggregates vehicles into categories that are similar in characteristics and technologies. The second aggregation effort aggregates data based on operation-based variables. The VT-Micro model approach described in this chapter is to utilize instantaneous vehicle speed and acceleration levels as operation-based variables. The use of speed and acceleration as operation-based variables allows the model to be utilized in conjunction with Global Positioning System (GPS) data for the field evaluation of environmental impacts of operational-level transportation projects (Rakha *et al*., 2000). Furthermore, such an emission model can easily be incorporated within microscopic traffic simulation software (Rakha and Ahn, 2002). The use of vehicle dynamics models within microscopic simulation software is critical in order to ensure that vehicle accelerations are accurate. These models can also account for grade effects on vehicle emissions by accounting for the additional acceleration in the direction of motion of the vehicle as a result of the grade.

The use of second-by-second emission data requires that data be temporally offset in order to ensure that there is no time lag between the speed/acceleration observations and the emission measurements. The proposed framework develops a procedure for offsetting the data and demonstrates how this procedure was applied to the EPA data. Finally, the section describes how the models were developed using the EPA data.

6.3.1 Vehicle Classification

Vehicle classification is a fundamental procedure required in developing mobile source emission models. For example, depending on vehicle characteristics, such as vehicle model year, engine technology, engine size, and vehicle mileage, the amount and pattern of vehicle emissions can vary significantly. Traditional emission models such as MOBILE and EMFAC categorize vehicles into common vehicle groups that include light-duty gasoline vehicles (LDGV), light-duty trucks (LDT), and heavy-duty trucks (HDT). While this classification is important, it only serves as a first step in categorizing vehicles, as illustrated in Figure 6-2. The proposed framework includes three levels of vehicle classifications. The first level involves categorizing vehicles based on whether a vehicle is a heavy duty truck, light duty truck, or light duty vehicle. The second level involves classifying vehicles based on whether the vehicle is diesel or gasoline powered. The final classification involves the use of statistical Classification and Regression Tree (CART) algorithms to further group vehicles into categories that are similar in their emission characteristics.

The CART algorithm is a data-mining technique that uses a regression tree method that automatically searches for important patterns and relationships and quickly finds hidden structures in highly complex data. Tree structured classifiers or binary tree structured classifiers are built by repeating splits at active nodes. An active node is divided into two sub-nodes based on a split criterion and a split value. The splitting process is generally continued until (a) the number of observations in a child node has met minimum population criteria or (b) minimum deviance criteria at a node are met, where the deviance criteria D is defined as the Sum of Squared Error (SSE), as computed in Equations 6-1 and 6-2.

The CART algorithm was utilized to classify the 60 normal test vehicles into a number of categories that were similar in emission behavior. The dependent variable (Y) was a 60-by-4 matrix that included 60 normal vehicles and 4 dependent variables. The dependent variables included HC, CO, CO_2, and NO_x emissions averaged over all 15 drive cycles. Similarly, the independent variable (X) was a 60-by-n matrix that included a number of vehicle attributes, including the vehicle model year, engine technology, engine size, and vehicle mileage. Alternatively, the X matrix can be thought of as a set of vectors $X_{k,}$ each composed of 60 elements, where k is the vehicle attribute index under consideration in the CART algorithm.

Within the CART algorithm, the observations in Y are divided on an independent variable X_k resulting in two children nodes, a_1 and a_2, each containing n_1 and n_2 observations of the original n observations ($n_1+n_2 = n$) using the deviance criterion that is presented in Equation 6-3. The SSE for all observations at node a is calculated using Equation 6-4, while the error at each of the sub-nodes is calculated using Equations 6-5 and 6-6. The problem is then formulated as an optimization problem in which the objective function is to maximize the deviance reduction function (Equation 6-3) by solving for the variable index k and the value of X_k for partitioning Y. Once this splitter is found, the original data at node a are separated into two children nodes a_1 and a_2 each having minimal combined deviance compared with all other possible nodes. Several numerical search procedures are used to maximize the deviance reduction. The most common splitting function is the "Gini" followed by the "Twoing" function (Roger *et al.*, 2000). While a detailed description of the CART algorithm is beyond the scope of this research, the reader is referred to a number of sources in the literature (Breiman *et al.*, 1984; Roger *et al.*, 2000; Wolf *et al.*, 1998; and S-Plus 6, 2001).

$$D = \sum_{i=1}^{n} (Y_i - m)^2 \qquad [6\text{-}1]$$

$$m = \frac{1}{n} \sum_{i=1}^{n} Y_i \qquad [6\text{-}2]$$

$$\Delta = D_a - (D_{a_1} + D_{a_2}) \qquad [6\text{-}3]$$

$$D_a = \sum_{i=1}^{n} [Y_i - m_a]^2 \quad \forall\, i \in a \qquad [6\text{-}4]$$

$$D_{a_1} = \sum_{i=1}^{n_1} [Y_i - m_{a_1}]^2 \quad \forall\, i \in a_1 \qquad [6\text{-}5]$$

$$D_{a_2} = \sum_{i=1}^{n_2} [Y_i - m_{a_2}]^2 \quad \forall\, i \in a_2 \qquad [6\text{-}6]$$

Where:

D = total deviance of Y, or the sum of squared errors (SSE),

Y_i = i^{th} observation in Y,

n = sample size over which D is calculated ($n = N$ for total sample),

m = arithmetic mean of Y, and

D = deviance reduction when parent node a is partitioned on X_1 to obtain children nodes a_1 and a_2,

The CART algorithm was applied on the data using the S-PLUS software, which allows the user to input a set of dependent variables, a set of independent variables, and a minimum number of observations within a category. In conducting the vehicle categorization, all test vehicles were initially divided into LDV and LDT vehicles because, as was discussed earlier, LDVs and LDTs have significantly different emitting characteristics. LDV vehicles were further categorized using the CART algorithm considering a number of independent variables that included the vehicle model year, engine size, vehicle mileage, vehicle power-to-weight ratio, and federal emission standard (tier0 and tier1). After running the S-PLUS software, it was found that only three vehicle characteristics were selected for vehicle aggregation, namely: vehicle model year, engine size, and vehicle mileage, as summarized in Table 6-1 and Figure 6-3. These three variables resulted in five vehicle categories. It should be noted that the minimum number of vehicles within a category was set at 5. As indicated in Table 6-1 two model year breakpoints were selected by the CART algorithm, namely 1990 and 1995. It is interesting to note that all post 1990 model year vehicles were equipped with fuel injection technology, which suggests, as would be expected, that fuel injection technology reduced vehicle emissions. Also, federal emission standard, tier1 was introduced in 1994 (60% tier0 and 40% tier1) and became more prevalent in 1995 (20% tier0 and 80% tier1, 100% tier1 in 1996). This again demonstrates that the model year that was selected by the CART algorithm corresponded to the introduction of tier1 vehicles into the vehicle fleet.

In the case of LDT categorization, the independent variables that were considered included the vehicle model year, engine size, vehicle mileage, vehicle gross weight, and federal emission standard (tier0 and tier1). The use of vehicle gross weight instead of power-to-weight ratio was considered in order to ensure consistency with the MOBILE and CMEM procedures. After running the software, it was found that only one vehicle characteristic, namely vehicle model year was chosen for LDT classification, generating two LDT vehicle groups, as summarized in Table 6-1 and Figure 6-4.

Table 6-2 summarizes the mean, standard deviation, and Coefficient of Variation (COV), computed as the ratio of standard deviation to mean, for all 15 drive cycles across all vehicle classes that were established by the CART algorithm. The results indicate that the variations within a class are reasonably small. Alternatively, Table 6-3 summarizes the mean, standard deviation, and COV based on the CMEM model categories for the same 60 vehicles. The CMEM classification includes 6 LDV categories (category 4, 5, 6, 7, 8, and 11) and 3 LDT categories (category 16, 17, and 18). Comparing Table 6-2 and Table 6-3 a number of conclusions can be drawn. First, the CMEM model categories can result in categories that vary considerably in sample size (ranging from 1 to 21 vehicles within a category), whereas as the CART algorithm ensures that the sample size is not less than a user specified minimum (in this case it was set at 5 vehicles). Second, it is noted that CMEM classification has slightly higher COVs in comparison with the CART algorithm classifications. For example, Category 5 (the largest dataset in the CMEM classification) has HC, CO, NO_x, and CO_2 COVs that are 0.949, 0.780, 0.947, and 0.161 while the CART algorithm LDV2 (the largest dataset in the CART classification) has COV values of 0.564, 0.401, 0.649, and 0.102, respectively.

6.3.2 Temporal Normalization of Data

The use of second-by-second emission data requires that data be temporally offset in order to ensure that there is no time lag between speed/acceleration observations and emission measurements. Analysis of second-by-second laboratory and on-board field data has revealed lags between operational variables and vehicle emissions in the range of 5 to 10 seconds. This section describes how the emission measurements were offset in order to remove any temporal lags between operation variables and emission measurements.

The EPA data were in the format of a database containing approximately 1,283,000 second-by-second records. Each record included the test site unique ID, the vehicle ID, the driving cycle, the time stamp since the start of the driving cycle, the instantaneous speed, and the instantaneous emission rate of HC, CO, CO_2, and NO_x, and other related data. As mentioned earlier, these data covered between 14 and 16 drive cycles.

The time lag is a very important factor in developing instantaneous emission models in order to accurately associate vehicle emissions with their corresponding operational variable values. In

identifying the temporal lag, the ORNL composite vehicle model was utilized in conjunction with the cycle second-by-second speed measurements to estimate instantaneous vehicle emission levels. It should be noted that the ORNL data did not include a time-lag, given that the operation variables were held constant for 5 seconds in order to capture steady-state behavior. A sum of squared error between the estimated second-by-second emissions and the measured emissions was utilized to identify the optimum temporal shift in the emission data in order to minimize the sum of squared error. The temporal shift ranged from 6 to 8 seconds for the NVREL data while the offset ranged from 0 to 1 second for the ATL data, which suggests that the ATL data had been temporally normalized as part of the data collection.

6.3.3 Model Construction

This section describes how the emission models were developed using regression procedures that are described in detail by Rakha *et al*., (2002). As was described earlier, a nonlinear multi-dimensional dual-regime polynomial model structure was utilized. This multiple regression model relates the dependent variable (instantaneous emission measurement) to a set of independent variables that include the vehicle's instantaneous speed and acceleration levels. In total 5 LDV and 2 LDT models were developed using the EPA data.

A first step in developing the VT-Micro model was to create a binning procedure in order to reduce the noise in the data and to reduce the number of raw data points. Specifically, emissions of all vehicles within a vehicle category and in a speed/acceleration bin were averaged to generate a single average emission estimate. The speed bins included vehicle speeds ranging from 0 to 120 km/h at increments of 1 km/h, while acceleration bins included accelerations that ranged from -6 to 10 km/h/s (-1.7 to 2.8 m/s^2) at increments of 1 km/h/s. Figure 6-5 illustrates a sample speed/acceleration frequency distribution for one of the 60 test vehicles over all 15 drive cycles. As illustrated in the figure, the majority of the speed and acceleration data occur at steady-state conditions (acceleration ranging between -1 and 1 km/h/s).

A sample data set for LDT1 is presented in Figure 6-6 for illustration purposes. The figure clearly demonstrates the large nonlinear behavior in all emissions as a function of the vehicle speed and acceleration. In addition, it is evident that, as vehicle acceleration and speed levels increase, the emissions generally tend to increase. Furthermore, it is noted that the gradient of the

emissions in the negative acceleration regime is generally smaller than that in the positive acceleration regime. Furthermore, the figure clearly demonstrates a high level of emission variability at high speed and high acceleration levels, which could be attributed to the small sample size of data points at these high engine loads or, alternatively, could be a result of variability in vehicles reaching fuel enrichment mode.

The regression model follows the same format that the VT-micro model does, which uses a combination of linear, quadratic, and cubic speed and acceleration terms, as expressed in Equation 5-6. The emission model utilizes a logarithmic transformation by second-by-second emission data in order to ensure that emission estimates are non-negative. Another reason for the use of a logarithmic transformation is to enhance the model accuracy in the low speed and low acceleration regime, which generally results in low emission rates. The logarithmic transformation allows the model to respond rapidly to changes in emissions as a function of speed/acceleration levels. It should also be noted that the emission model employs a hybrid model that separates positive acceleration and negative acceleration regimes. Sample model coefficients for estimating HC emission rates for LDT1 are summarized in Table 6-4.

The majority of microscopic emission models disregarded assume a constant emission rate when a vehicle is decelerating. However, as shown in Figure 6-7, emission rates increase as vehicle speeds increase, even in deceleration vehicle operations. The proposed dual-regime model enhances the accuracy of the emission model in deceleration mode, which is typically neglected and overlooked by other models. A detailed comparison of single-regime and dual-regime is described in the literature (Rakha *et al*., 2002). Since the dual-regime model introduces a discontinuity between the acceleration and deceleration modes of operation, an attempt was made to reduce this level of discontinuity by ensuring the regression model constant is identical in both regimes. It should be noted that the models were confined to speed and acceleration levels within the envelope of the EPA data. This limitation resulted from the inherent limitation of any model to extrapolate response values beyond the boundaries used in the model calibration procedure. While most vehicles can travel faster than 121 km/h (upper limit of the testing boundary), it is impossible to establish a reliable forecasting pattern for energy and emission rates at high speeds due to the heavy nonlinear nature of the response curves. The speed and acceleration boundary is consistent with the data boundary depicted in Figure 6-5. It should be

noted that all speed and acceleration profiles in EPA driving cycles used in the modeling were general enough for routine vehicle operations. However, in cases in which a vehicle exceeds the boundary, the authors recommend using boundary speed and acceleration levels in order to ensure realistic vehicle MOE estimates. Furthermore, it should be noted that these models have been successfully applied to Global Positioning System (GPS) speed measurements after applying robust smoothing techniques in order to ensure feasible speed measurements (Rakha *et al*., 2000a).

The EPA data did not include second-by-second fuel consumption data. However, it is possible to compute the fuel consumption data using carbon balance equations, as demonstrated in Equation 6-7. Given that ambient air does not include carbon, whatever carbon enters the engine as fuel will leave the engine as emissions such as HC, CO, and CO_2. Given that the molecular weight of carbon is 12 g/molecule and the molecular weight of oxygen is 16 g/molecule the molecular weight of CO_2 can be calculated to be 44 g/molecule (12+16x2). Therefore, CO_2 contains 27.3 percent (12/44) carbon. Similarly, the molecular weight of CO is 28 g/molecule (12+16) and there is 42.9 percent carbon in CO. Also, according to the Code of Federal Regulations Title 40 Part 86 (40 CFR 86), HC emissions contain 86.6 percent carbon by weight. Thus, the emissions of carbon, in grams per second can be computed using Equation 6-7. In addition, recognizing that typical gasoline contains 86.4 percent of carbon, and has a density of 738.8 g/liter (or 2800 g/gallon); there are 638.31 (0.864x738.79) grams of carbon in a liter of gasoline. Consequently, the fuel consumption rate can be computed using Equation 6-8.

$$C = 0.866\,HC + 0.429\,CO + 0.273\,CO_2 \qquad [6\text{-}7]$$

$$F = \frac{0.866\,HC + 0.429\,CO + 0.273\,CO_2}{638.31} \qquad [6\text{-}8]$$

Where:

C = instantaneous C emissions rate (g/s),
HC = instantaneous HC emission rate (g/s),
CO = instantaneous CO emission rate (g/s),
CO_2 = instantaneous CO_2 emission rate (g/s), and
F = instantaneous fuel consumption rate (l/s).

Figure 6-7 and Figure 6-8 illustrate sample model emission predictions superimposed on the raw data for Category LDT1 and LDV2. As illustrated in the figures, the variability in emission estimates typically increases at high speed and acceleration levels. Noteworthy is the fact that the LDT1 emission rates are higher than the LDV2 emission rates, as would be expected. Emission predictions for the other vehicle categories are provided in Appendix B (Figure B1 to B5). Figure 6-9 illustrates how the predicted fuel consumption compare to the field data for vehicle category LDT2. Noteworthy is the fact that the shape of the fuel consumption chart is extremely similar in the appearance to CO_2 chart.

6.4 MODEL VALIDATION

The next step in the analysis was to validate the newly developed emission models against bag trip measurements and against instantaneous second-by-second measurements. The details of the validation effort are described in this section.

6.4.1 Aggregate Model Validation

In an attempt to validate the model using aggregate emission data, the same EPA data that were utilized in developing the models were utilized for validation purposes because other independent data were not available. Research is currently underway to collect independent field data using an OEM2100 on-board emission measurement device for use in validation efforts. While the use of the EPA data for model validation is not ideal, it does offer a number of benefits. First, the database includes many off-cycle (non-FTP) emission results over different facility types and therefore provides a good assessment about the quality of data fits for different roadway types and different levels of congestion. Second, as was mentioned earlier, the EPA database was utilized for the development of EPA's MOBILE6 model. Consequently, such a comparison ensures that the VT-Micro model estimates are consistent with MOBILE6 emissions across the different facility types and different levels of congestion.

Figure 6-10 and Figure 6-11 compare the VT-Micro model emission predictions against the field measurements for all 15 drive cycles. The 5^{th} and 95^{th} percentile emission rates are computed based on differences in vehicle emissions within a vehicle category. For example, the LDT1 category includes 11 vehicles while the LDV2 category includes 15 vehicles. The bar plots represent the predicted emission estimates for composite vehicles LDT1 and LDV2, while the

vertical line and small horizontal bar stand for 95th percentile, 5th percentile, and mean value of field vehicle emission data, respectively. The predicted emissions are computed as the sum of instantaneous vehicle emissions along the entire trip. Figure 6-10 and Figure 6-11 clearly illustrate a good fit between the model estimates and the field measurements. Specifically, all predictions lie within the 95th percentile and the 5th percentile limits. Furthermore, the model estimates generally follow the mean category field measurements. Specifically, the error in trip emissions does not exceed 14 percent across all 15 drive cycles for all 4 emissions.

6.4.2 Instantaneous Emission Model Validation

Figures 6-13 and 6-14 illustrates an instantaneous model validation for the newly developed models. The model is compared to second-by-second field HC, CO, CO_2, and NO_x measurements against instantaneous model estimates. In order to ensure consistency in the comparison, two vehicle categories LDT1 and LDV2 were selected for comparison purposes. A new drive cycle ARTA was selected for validation because the cycle includes several full and partial stops in addition to travel at a fairly high speed (in the range of 100 km/h). Figure 6-12 clearly demonstrates that the ARTA drive cycle involves a more aggressive and realistic driving behavior compared to the old driving cycles.

Figures 6-13 and 6-14 illustrate the variation in the maximum, minimum, and mean value of the instantaneous vehicle emissions as measured on a dynamometer as it travels through the drive cycle. The maximum, minimum, and mean is computed based on all vehicles within a category (11 vehicles for LDT1 and 15 vehicles for LDV2) for all four pollutants. The dotted lines represent the mean values of vehicle emissions while the shaded grey region shows the max/min limits. The solid lines represent the model estimates of vehicle emissions based on instantaneous vehicle speed and acceleration levels.

The total vehicle emissions of HC, CO, CO_2, and NO_x for LDT1 as measured in the laboratory were 0.489, 10.805, 2.384, and 2162.7 grams. The estimated emissions based on the proposed hybrid model were 0.565, 11.188, 2.437, and 2155.4 grams, which correspond to a 16, 4, 2, and 0.3 percent difference in overall emissions for the entire cycle. Vehicle category LDV2 showed similar results, producing 17, 5, 7, and 0.4 percent errors in overall emissions. Figures 6-13 and 6-14 illustrate that, in general, the model prediction lines almost perfectly follow the dotted lines

(mean values) of the EPA vehicle emission measurements, and follow all the valleys and peaks in vehicle emissions. It should be noted that this feature demonstrates the uniqueness of the model for assessing the environmental impacts of traffic improvement projects, including ITS technology.

6.5 SUMMARY

The chapter presents a framework for developing microscopic emission models for assessing the environmental impacts of transportation projects. The framework develops emission models by aggregating data using vehicle and operational variables. Specifically, statistical CART algorithms for aggregating vehicles into homogenous categories are utilized as part of the framework. In addition, the framework accounts for temporal lags between vehicle operational variables and vehicle emissions. Finally, the framework is utilized to develop the VT-Micro model version 2.0 utilizing second-by-second chassis dynamometer data for a total of 60 light duty vehicles and trucks. A total of 5 LDV and 2 LDT categories are developed as part of this research effort.

The ultimate expansion of this model is its implementation within microscopic traffic simulation software. These models can then be utilized to evaluate the environmental impacts of microscopic vehicle behaviors, such as ramp metering, traffic signal coordination, and alternative ITS strategies. Also, the model can be applied to estimate vehicle emissions using instantaneous GPS speed measurements (Rakha *et al.*, 2000a). Currently, the VT-Micro model has been implemented in the INTEGRATION software for the environmental assessment of operational-level transportation projects.

Table 6-1. CART Based Vehicle Classification

Vehicle Category	Number of Vehicles in Category
Category for Light Duty Vehicles	
LDV1: Model Year < 1990	6
LDV2: 1990<=Model Year<1995, Engine Size < 3.2 liters, Mileage < 83653,	15
LDV3: Model Year >= 1995, Engine Size < 3.2 liters, Mileage < 83653,	8
LDV4: Model Year >=1990, Engine Size < 3.2 liters, Mileage >= 83653	8
LDV5: Model Year >=1990, Engine Size >= 3.2 liters	6
LDV High Emitters	24
Category for Light Duty Trucks	
LDT1: Model Year >= 1993	11
LDT2: Model Year < 1993	6
LDT High Emitters	12
Total Vehicles	96

Table 6-2. Variation of Vehicle Classification

Category	Measure	HC	CO	NOx	CO2
LDV1 (6 vehicles)	Standard Deviation	0.123	2.167	0.367	26.958
	Mean (g/km)	0.185	3.351	0.555	181.848
	Coefficient of Variation	0.663	0.647	0.661	0.148
LDV2 (15 vehicles)	Standard Deviation	0.029	0.529	0.190	19.521
	Mean (g/km)	0.051	1.319	0.293	190.844
	Coefficient of Variation	**0.564**	**0.401**	**0.649**	**0.102**
LDV3 (8 vehicles)	Standard Deviation	0.013	0.385	0.125	35.601
	Mean (g/km)	0.023	0.664	0.129	201.097
	Coefficient of Variation	0.556	0.580	0.966	0.177
LDV4 (8 vehicles)	Standard Deviation	0.209	1.466	0.317	41.181
	Mean (g/km)	0.154	3.203	0.341	188.847
	Coefficient of Variation	1.358	0.458	0.929	0.218
LDV5 (6 vehicles)	Standard Deviation	0.055	2.061	0.426	24.146
	Mean (g/km)	0.120	3.660	0.602	245.131
	Coefficient of Variation	0.457	0.563	0.707	0.099
LDT1 (11 vehicles)	Standard Deviation	0.039	1.529	0.284	49.146
	Mean (g/km)	0.077	2.117	0.362	269.938
	Coefficient of Variation	0.502	0.722	0.785	0.182
LDT2 (6 vehicles)	Standard Deviation	0.118	2.352	0.171	40.960
	Mean (g/km)	0.157	5.404	0.589	247.262
	Coefficient of Variation	0.750	0.435	0.290	0.166
Average Coefficient of Variation		0.526			

Table 6-3. CMEM Vehicle Classification

Category		HC	CO	NOx	CO2
Category 4 (7 vehicles)	Standard Deviation	0.077	1.578	0.212	34.593
	Mean (g/km)	0.122	2.919	0.439	179.109
	Coefficient of Variation	0.628	0.541	0.483	0.193
Category 5 (21 vehicles)	Standard Deviation	0.079	1.881	0.337	33.840
	Mean (g/km)	0.083	2.412	0.356	209.585
	Coefficient of Variation	**0.949**	**0.780**	**0.947**	**0.161**
Category 6 (3 vehicles)	Standard Deviation	0.340	1.223	0.458	27.855
	Mean (g/km)	0.268	2.606	0.563	179.199
	Coefficient of Variation	1.266	0.469	0.814	0.155
Category 7 (3 vehicles)	Standard Deviation	0.062	1.870	0.346	20.270
	Mean (g/km)	0.090	2.130	0.425	203.507
	Coefficient of Variation	0.693	0.878	0.814	0.100
Category 8 (1 vehicle)	Standard Deviation	N/A	N/A	N/A	N/A
	Mean (g/km)	0.043	1.246	0.362	159.877
	Coefficient of Variation	N/A	N/A	N/A	N/A
Category 11 (8 vehicles)	Standard Deviation	0.013	0.385	0.125	35.601
	Mean (g/km)	0.023	0.664	0.129	201.097
	Coefficient of Variation	0.556	0.580	0.966	0.177
Category 16 (12 vehicles)	Standard Deviation	0.090	2.532	0.271	41.963
	Mean (g/km)	0.125	3.651	0.527	260.195
	Coefficient of Variation	0.719	0.694	0.513	0.161
Category 17 (3 vehicles)	Standard Deviation	0.009	0.856	0.139	28.846
	Mean (g/km)	0.045	1.942	0.219	225.858
	Coefficient of Variation	0.192	0.441	0.636	0.128
Category 18 (2 vehicles)	Standard Deviation	0.057	3.721	0.100	35.080
	Mean (g/km)	0.076	3.036	0.265	326.485
	Coefficient of Variation	0.750	1.226	0.376	0.107
Average Coefficient of Variation		0.565			

Table 6-4. Sample Coefficients of LDT1 Model (HC Emissions)

Positive Acceleration Coefficients	Constant	Speed	$Speed^2$	$Speed^3$
Constant	-8.27978	0.06229	-0.00124	7.72E-06
Acceleration	0.36696	-0.02143	0.0005178	-2.33E-06
$Acceleration^2$	-0.04112	2.45E-03	0.00000677	-4.97E-07
$Acceleration^3$	1.39E-03	0.00000371	-0.00000739	1.05E-07
Negative Acceleration Coefficients	Constant	Speed	$Speed^2$	$Speed^3$
Constant	-8.27978	0.06496	-0.00131	8.23E-06
Acceleration	-0.27907	0.03282	-0.00065787	3.54E-06
$Acceleration^2$	-0.05888	7.05E-03	-0.00013252	6.48E-07
$Acceleration^3$	-4.77E-03	0.00043402	-0.00000758	3.98E-08

(Speed: km/h, Acceleration: km/h/s, HC Emission Rate: g/s)

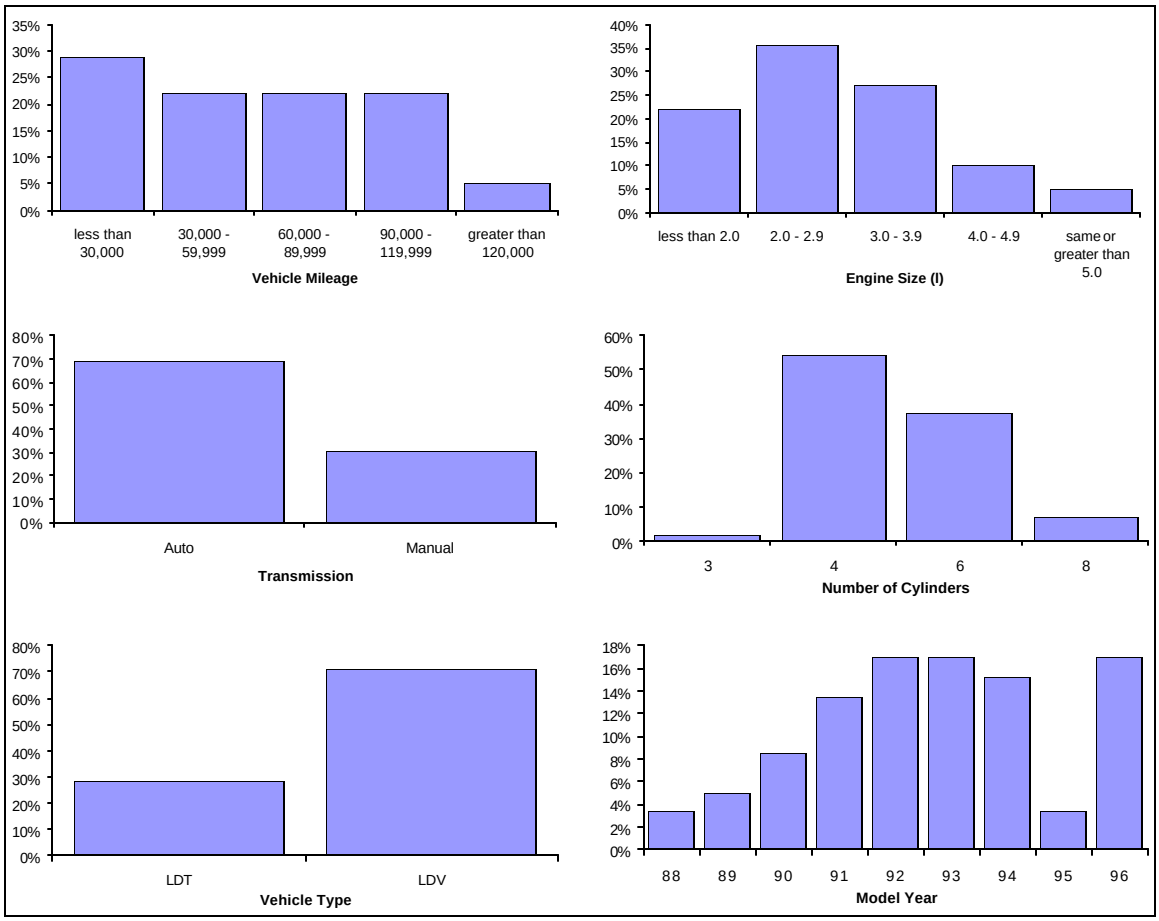

Figure 6-1. EPA Test Vehicle Characteristics

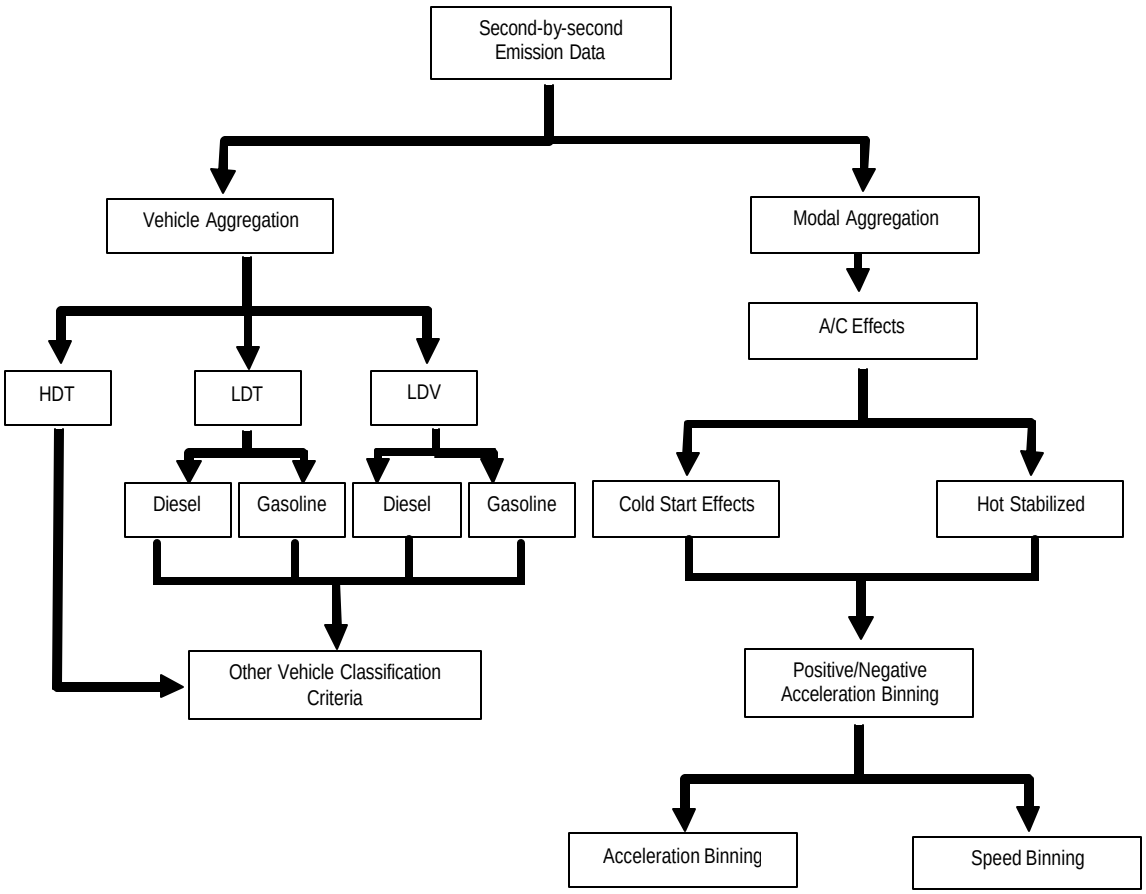

Figure 6-2. Second-by-second Emission Data Binning Framework

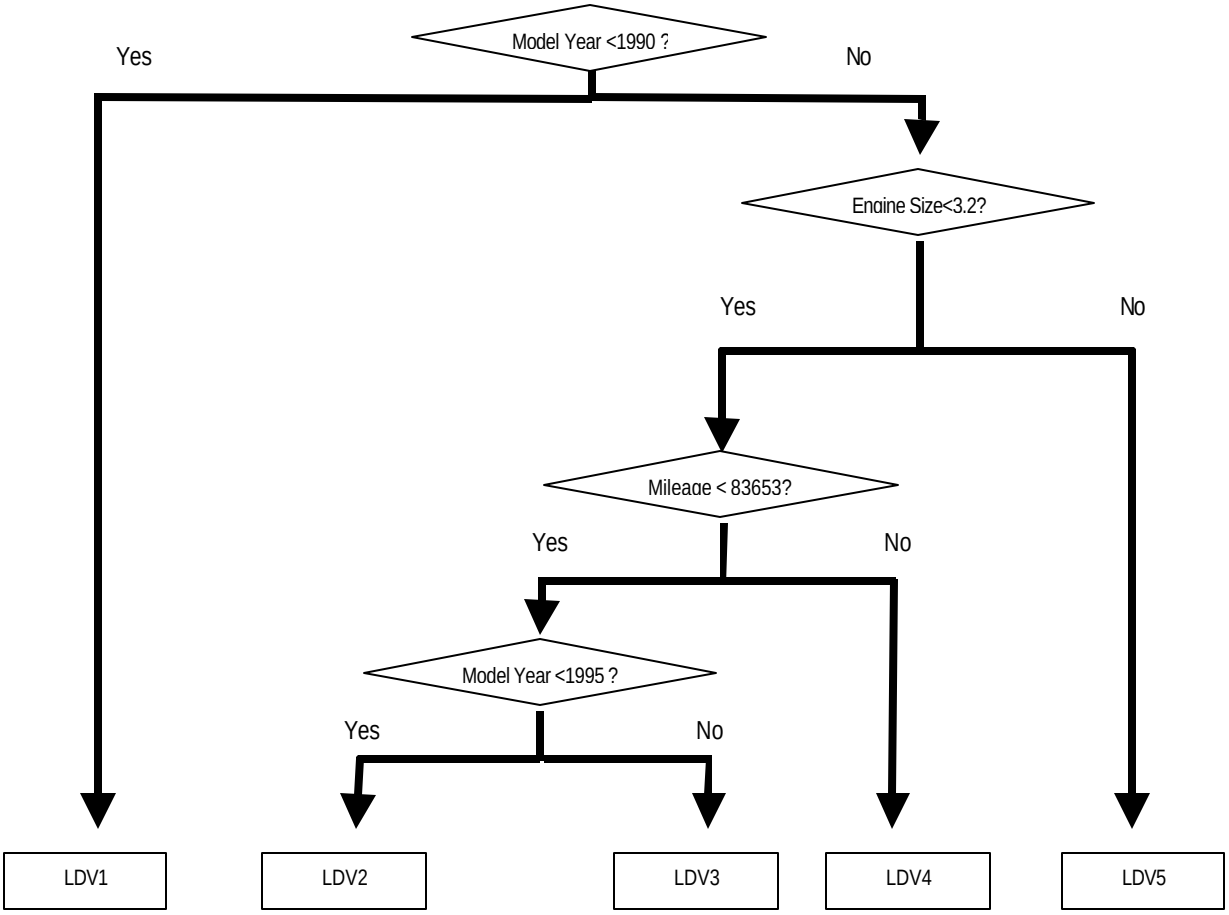

Figure 6-3. Light Duty Vehicle Classification using CART Algorithm

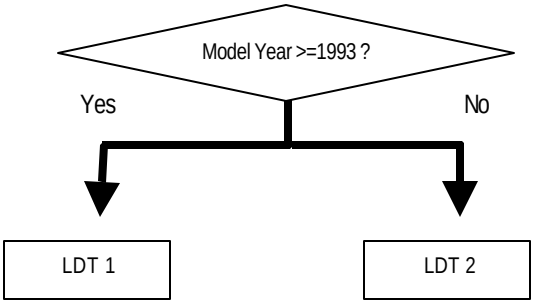

Figure 6-4. Light Duty Truck Classification using CART Algorithm

Speed (km/h)	Acceleration (m/s2)															
	-1.7	-1.4	-1.1	-0.8	-0.6	-0.3	0.0	0.3	0.6	0.8	1.1	1.4	1.7	1.9	2.2	
5			5	22	55	82	1322	59	55	32	31	12	21	8	3	1707
10	3	18	20	26	37	71	84	36	25	24	21	11	13	9	8	406
15	6	16	30	27	33	56	59	39	35	24	20	12	13	8	3	381
20	9	16	27	35	26	50	81	64	55	36	27	11	13	5		455
25	11	19	22	26	29	44	48	55	56	53	37	11	2	1		414
30	15	15	24	20	33	45	72	63	37	33	31	23	7	1		419
35	9	18	20	29	28	43	59	40	52	19	30	14	5	4		370
40	6	15	23	22	31	58	93	83	40	34	25	3	3		1	437
45	6	6	23	27	30	48	92	88	44	29	17		1			411
50	4	4	13	15	36	70	96	81	42	23	11	3				398
55	4	4	15	18	23	42	98	86	33	14	11	2				350
60	4	3	10	11	16	75	123	87	26	15	4	2				376
65	1	3	6	12	14	33	101	51	27	8	6	1				263
70			10	7	20	38	81	58	14	14	1					243
75			2	5	13	34	74	44	12	10						194
80	2		2	5	9	32	50	47	9	11						167
85		2	4	4	7	37	78	53	11	4						200
90	1		3	4	10	41	107	63	9	3						241
95				1	13	52	178	69	5	2	1					321
100		1		3	5	79	210	90	4		1					393
105			2	1	5	63	149	66	1							287
110			1		4	48	124	46	1							224
115				1	2	22	29	18								72
120						4	11	3								18
	81	140	262	321	479	1167	3419	1389	593	388	274	105	78	36	15	8747

Figure 6-5. Speed and Acceleration Distribution for Sample Vehicle (15 Drive Cycles)

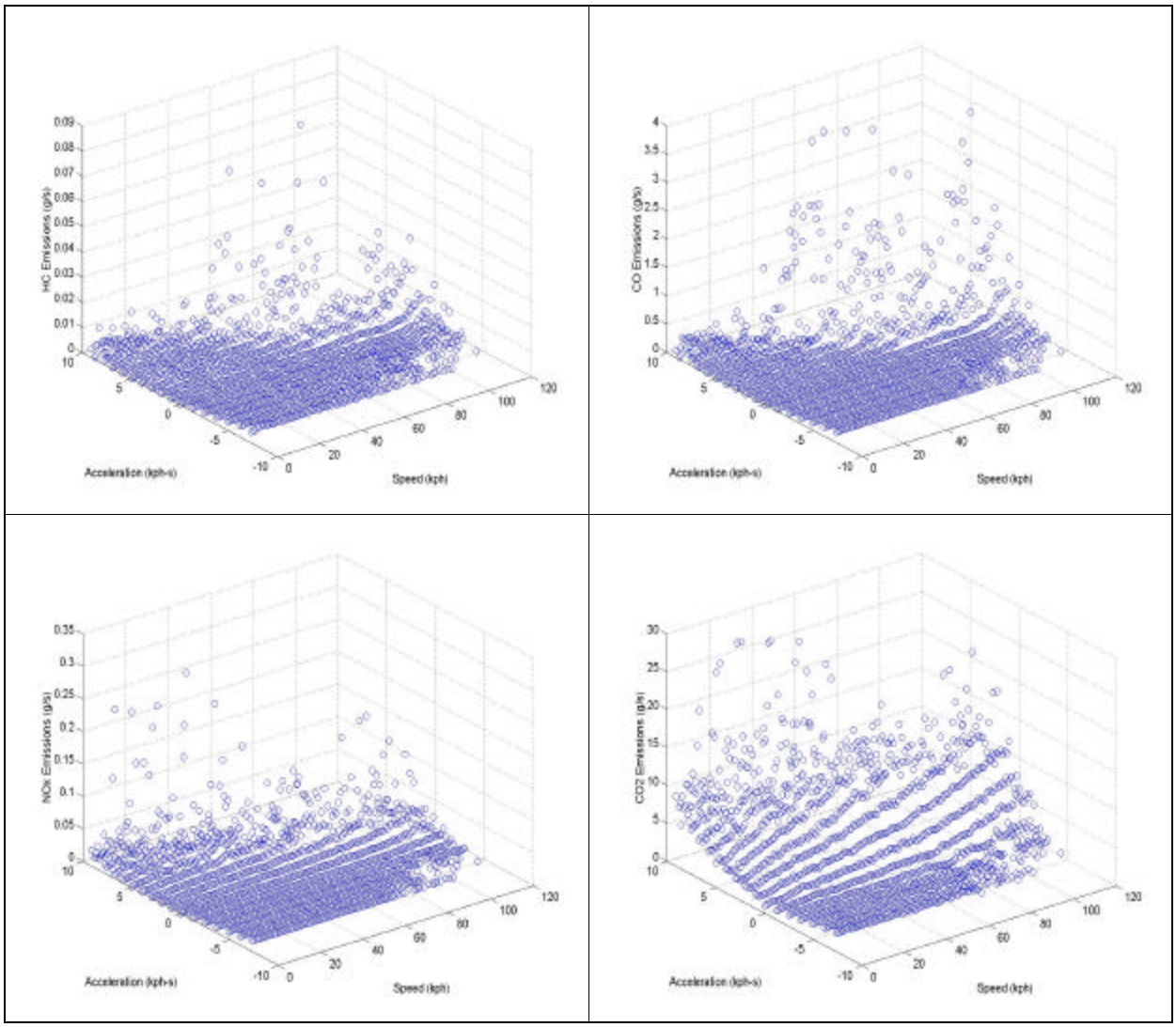

Figure 6-6. Sample Normalized Emission Data (LDT1)

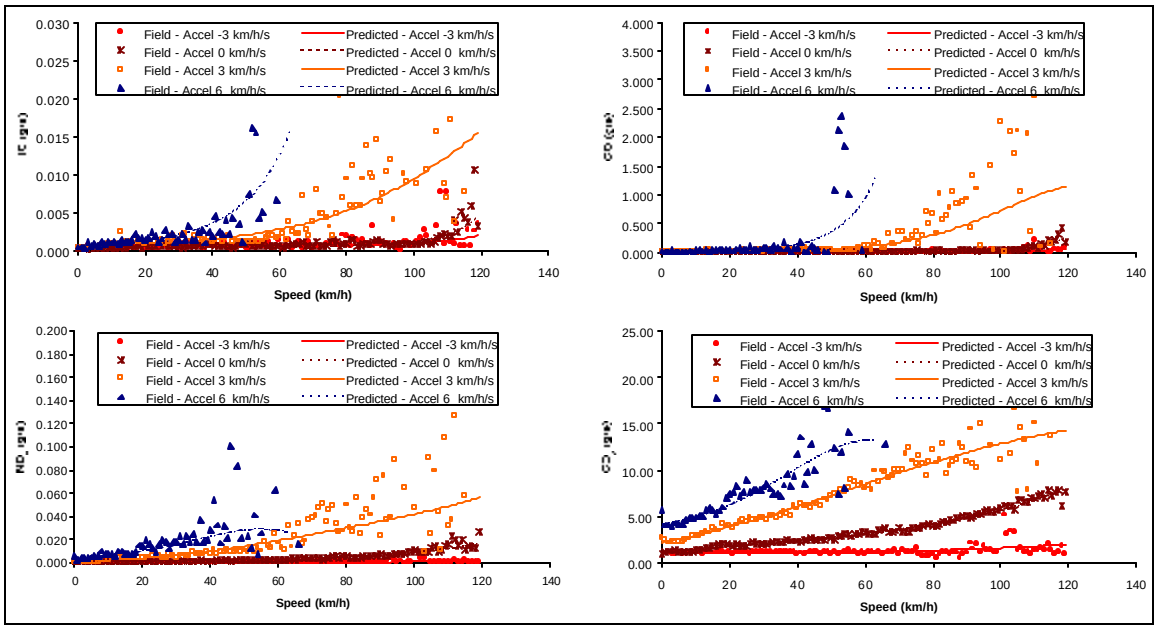

Figure 6-7. Model Prediction (LDT1)

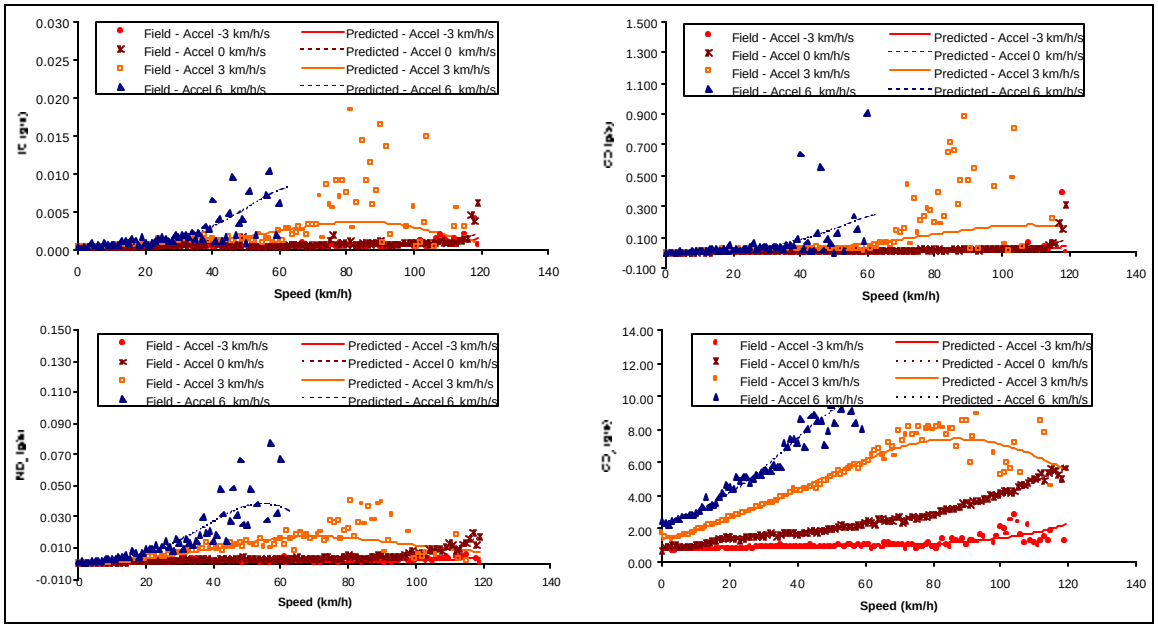

Figure 6-8. Model Prediction (LDV2)

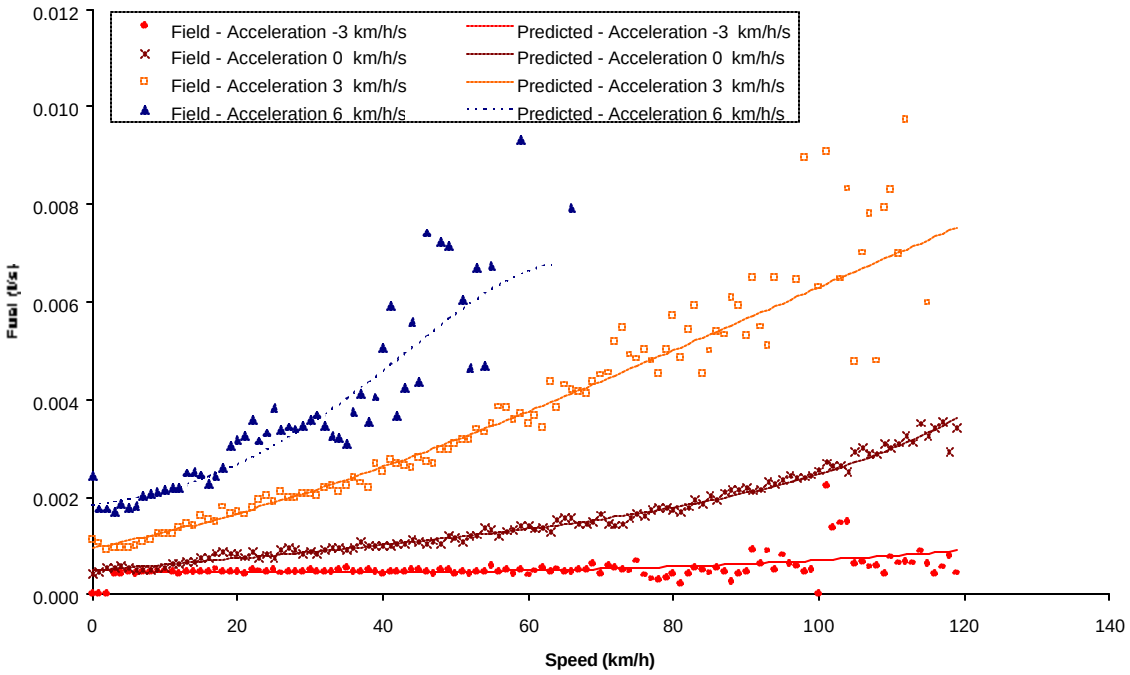

Figure 6-9. Fuel Consumption Prediction (LDT2)

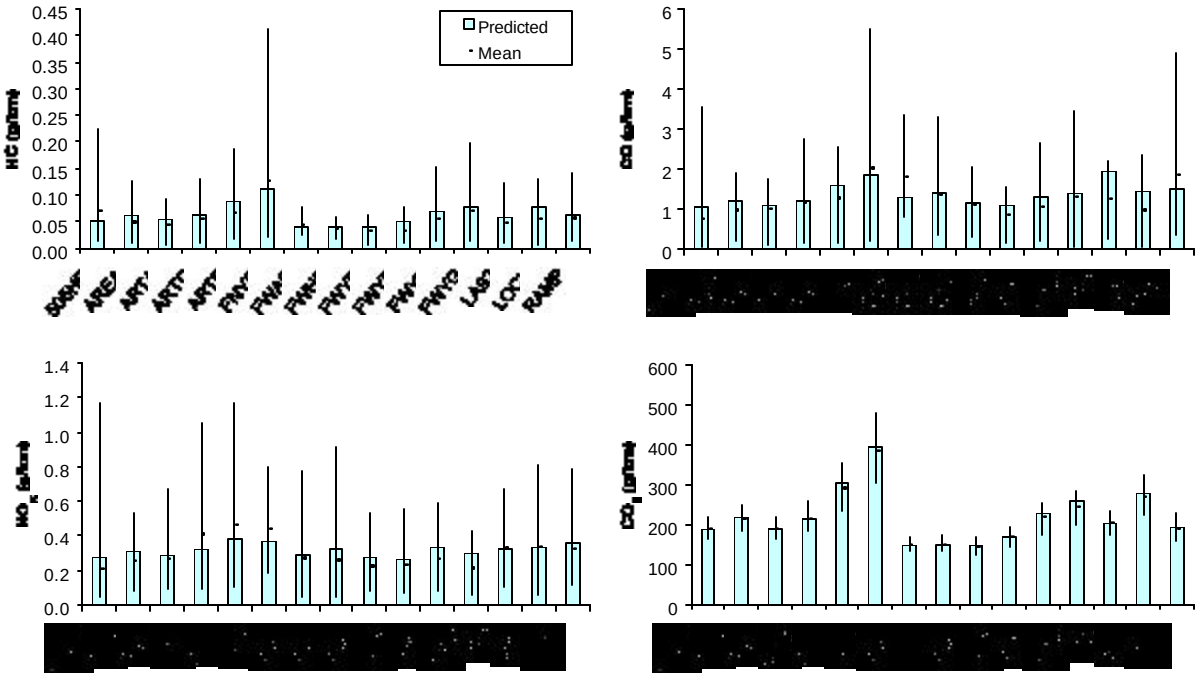

Figure 6-10. Model Validation for 15 Driving Cycles (LDT1)

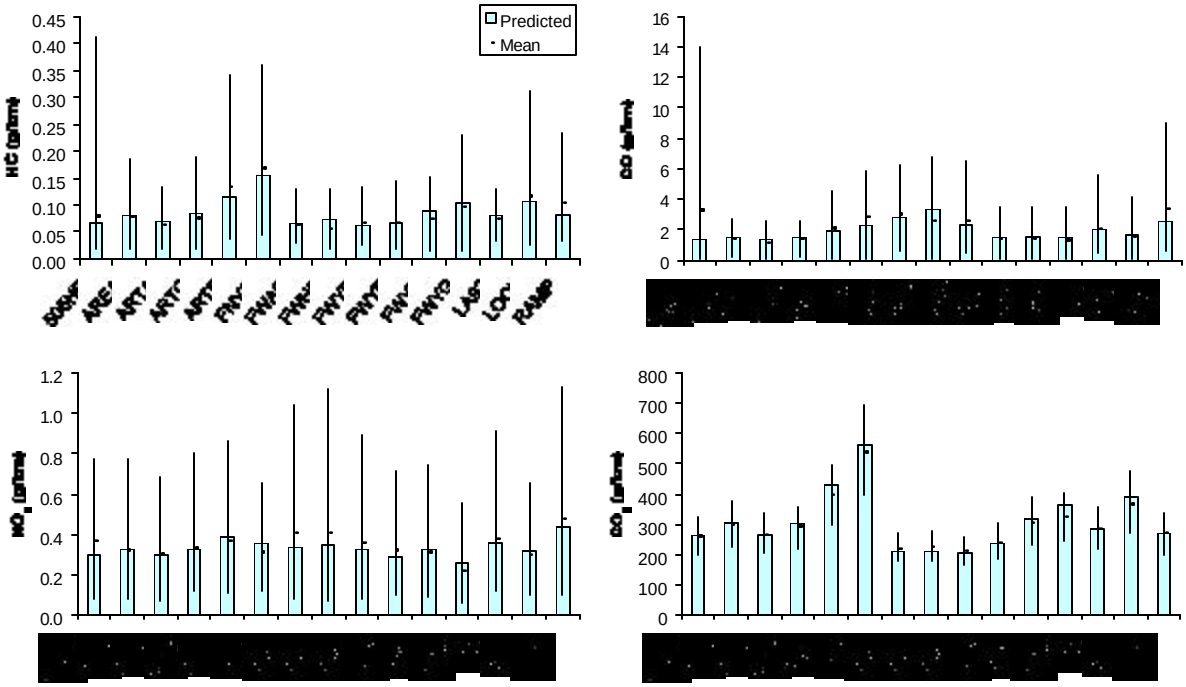

Figure 6-11. Model Prediction for 15 Driving Cycles (LDV2)

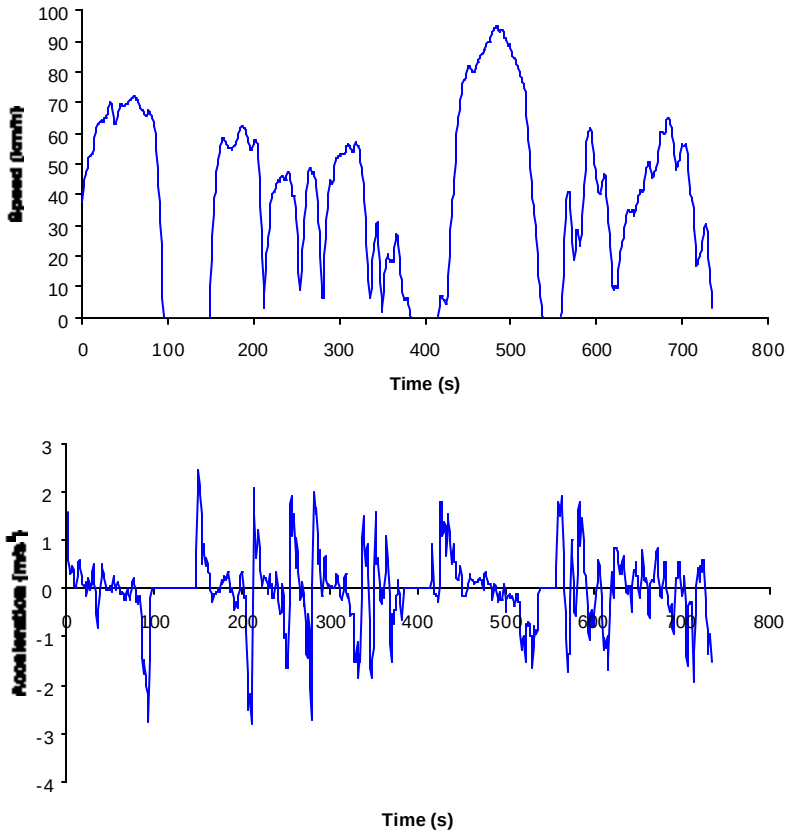

Figure 6-12. Speed and Acceleration Profiles for ARTA Driving Cycle

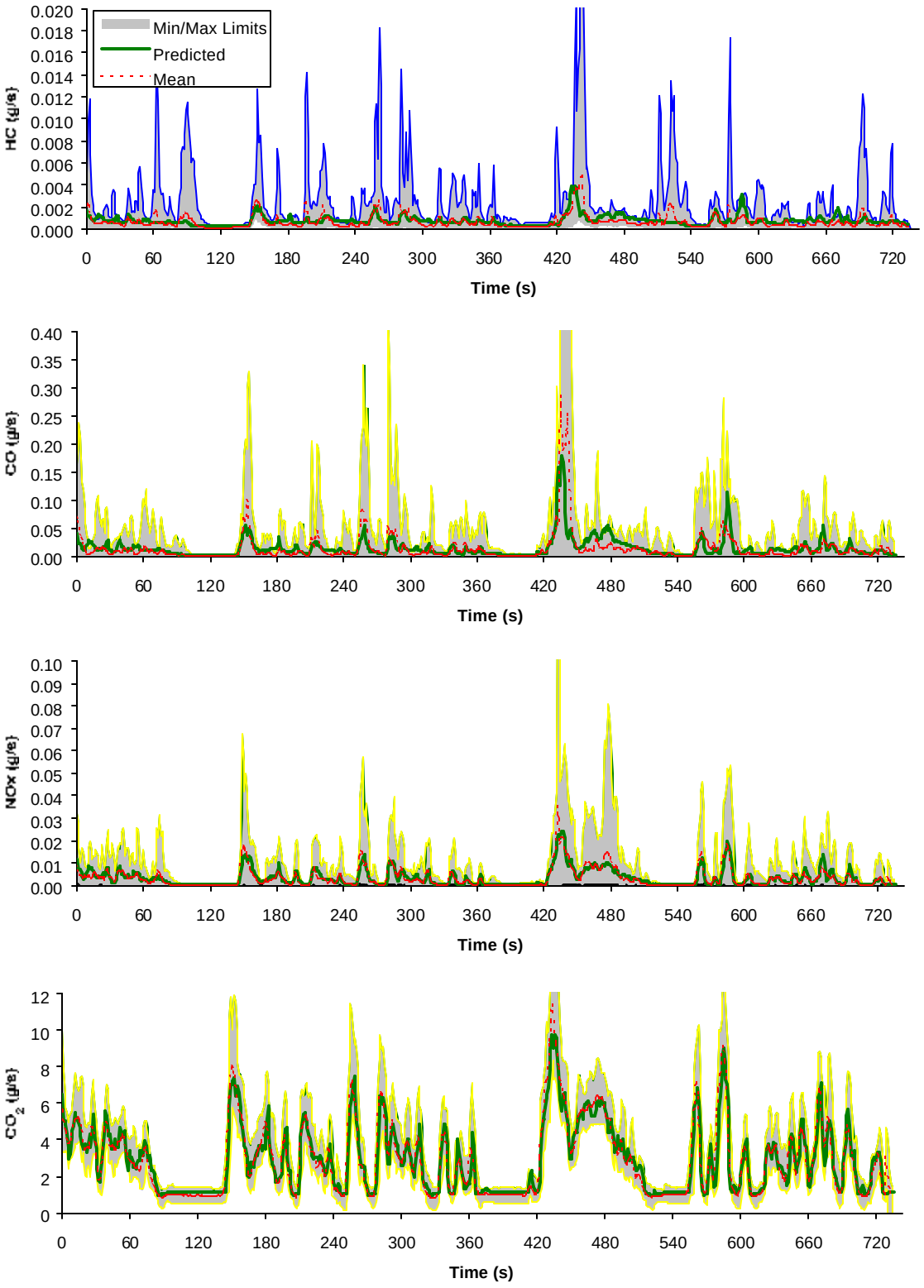

Figure 6-13. Instantaneous Model Validation for ARTA Cycle (LDT1)

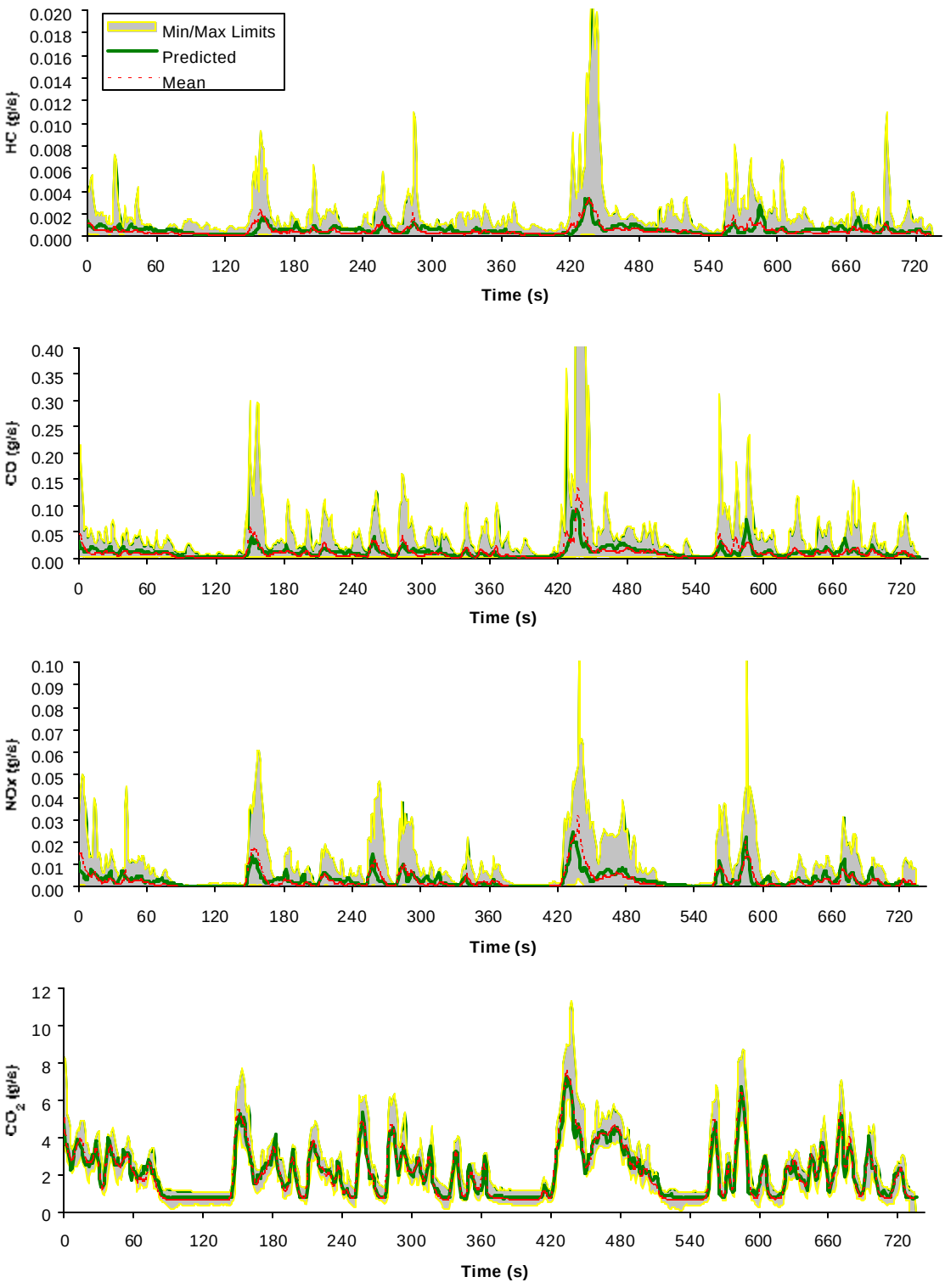

Figure 6-14. Instantaneous Model Validation for ARTA Cycle (LDV2)

CHAPTER 7. HIGH EMITTER EMISSIONS MODELING FOR VT-MICRO MODEL BASED ON SPEED AND ACCELERATION LEVELS

This chapter presents high emitter vehicle characteristics and standards and the development of microscopic high emitter vehicle emission models. High emitter standard is an important element to estimate accurate emissions. Depending on the criteria utilized, one vehicle can be a normal emitting vehicle or a high emitter. This research develops a multiplicative factor to make different emission cut-points for different driving cycles. Also, the chapter demonstrates microscopic emission models for high emitter vehicles that estimate second-by-second mobile source emissions in hot stabilized conditions using instantaneous vehicle speed and acceleration levels as input variables.

7.1 INTRODUCTION

High emitter or high emitting vehicles (HEVs) are motor vehicles that produce higher emissions than the average emitting vehicles under normal driving conditions. A small fraction of HEVs contributes significantly to the total of mobile source emissions (Wenzel and Ross, 1998, Wolf *et al.*, 1998). Consequently, identifying HEVs and estimating accurately their emissions are a critical processes to determine total vehicle emissions. This chapter introduces new high emitter identification methods and mathematical models to estimate high emitter emissions.

7.1.1 Objectives of Research

The objective of this chapter is estimating accurate emissions from HEVs. HEVs represent a small fraction of the vehicles using the road, yet they are responsible for a large portion of total mobile source emissions. According to previous research, twenty percent of the high emitters in the fleet are responsible for fifty percent of the total emissions. Even other researchers estimate that 5 percent of the vehicles emit 80 percent of the emissions (Wolf et al. 1998). These estimations differ due to the various definitions used in the literature for high emitters and due to a variety of procedures used to catalog high emitters. Establishing a clear definition for high emitters and estimating accurately high emitter emissions are relevant problems in mobile source emission studies. This research investigates high emitter emission standards, emission cut-points, and derives multiplicative factors for newly developed EPA driving cycles.

Although high emitters contribute a significant amount of total emissions, the modeling efforts related to these vehicles have been relatively little comparing to other vehicle emission studies. Most of research on high emitters focused on high emitter characterization and distribution. This research concentrates on mathematical modeling using a fleet of in-use vehicle emission data to estimate instantaneous emissions from HEVs.

7.1.2 Significance of Research

The most significant contribution of research is estimating instantaneous emissions from HEVs to be used in microscopic traffic modeling. The model utilizes speed and acceleration as independent variables. This approach allows the model to quantify emissions from various traffic and driver driving patterns caused by real-world urban driving conditions. This is very difficult to do using macroscopic emission models. This circumstance allows the model to access the environmental impact of HEVs for various driving conditions such as high-speed freeways, congested urban highways, and signalized local arterials. This model can be implemented to traffic simulators to understand the impact of Intelligent Transportation System (ITS) technologies, such as signal coordination, incident management, and electronic payment systems on the environment. In addition, this research develops a multiplicative factor to make different emission cut-points for different driving cycles. It is possible to utilize different emission test cycles depending on emission test site conditions to identify HEVs. For example, the low speed New York cycle may be tested in very contaminated urban areas while the Arterial LOS A cycle can be utilized for suburban or rural areas.

7.1.3 Chapter Layout

This chapter is organized into six sections. The first and current section introduces the problem statement. The second section describes state-of-the-art microscopic vehicle models and discusses relevant issues in high emitter modeling. The third section describes the data sources utilized to develop the proposed models. The fourth section describes high emitter criteria and provides estimates of a new scale factor applicable to various driving cycles to verify high emitters. The fifth section describes the model development process including data normalization, vehicle classification, and model construction. The sixth section describes the model validation using macroscopic and microscopic field data. The last section provides a summary of the study.

7.2 RESEARCH EFFORTS FOR HIGH EMITTERS

As stated before, a small fraction of vehicles on the road contribute about half of the on-road emissions (Wenzel and Ross, 1998, Wolf et al., 1998). However, the number of researches on HEV are relatively few compared to other sectors in emission modeling. This section briefly discusses the definition of high emitter modeling approaches adopted in two new emission models: MOBILE6 model and the Comprehensive Modal Emission Model (CMEM). MOBILE6 is the newest mobile source emission model using a macroscopic approach. The CMEM model is one of the most recently developed power-based microscopic emissions model.

7.2.1 High Emitter Definitions

In order to verify HEV on the road, EPA recommends the use of I/M program. In a I/M program, vehicles are tested on a dynamometer over a driving cycle called IM240. The cycle is designed to simulate a typical city driving cycle. To verify emission levels, second-by-second instantaneous emission measurements are taken and integrated by a computer. Failure rates for vehicles undergoing I/M tests are generally two to three times higher than manufacturer certification standards for new vehicles. However, because the IM 240 test does not include the cold start portions of the cycle, it is considered that these failure rates are higher than those occurring in normal vehicles. Therefore, using these failure rates, it is difficult to select the vehicles that are above a maximum allowable emission level. Defining the proper emission standards will provide a basis for improved emission compliance.

For modeling purposes, in order to decide whether a vehicle is a normal or a high emitter, standard emission criteria are used. Selecting standard emission criteria is influenced by the test cycle and the emission cut-points. Current practice uses the FTP test, LA4 cycle (also known as UDDS and city cycle), IM240 test, and FTP Bag2 to identify high emitters. The emission cut-points are considered to be: two times the new vehicle emission standard for HC and NOx and three times the standard for CO. Choosing the proper test type and cut-points is very important, because the emission rates vary substantially across test types. Georgia Tech researchers choose the FTP bag2 emission rate to classify vehicles as high emitters (Wolf et al., 1998). The FTP test is the baseline test performed on every vehicle within a given testing program. The Bag2 of the FTP contains no engine starts (hot-stabilized activities only) and little enrichment events

compared with other hot-stabilized test cycles. One EPA document utilizes the LA4 emission rates instead of the FTP bag2 to separate emitter status groups in their analysis while others use the FTP cycle for high emitter criteria (Brzezinski *et al.*, 1999a; Koupal and Glover, 1999; Glover and Koupal, 1999). The LA4 cycle includes bag1 and 2 of the FTP test but does not include any engine starts (Brzezinski *et al.* 1999a). According to both research groups, the emitter groups are defined according to the following pass/fail cut-points:

- 0.5 grams/km (0.8 grams/mi) Hydrocarbons (HC)
- 6.4 grams/km (10.2 grams/mi) Carbon Monoxide (CO)
- 1.3 grams/km (2.0 grams/mi) Oxides of Nitrogen (NOx)

These are also the final phase-in cut-points recommended by EPA for use in the I/M programs (i.e., using the IM240 test procedure) to identify vehicles in need of maintenance.

7.2.2 EPA's MOBILE6 Model

MOBILE6 is a new version of the MOBILE model, which was developed by the EPA's Office of Transportation and Air Quality (OTAQ). For high emitter vehicle modeling, MOBILE6 separates vehicle in two groups: a) 1981-1993 model year light-duty cars and trucks, and b) Tier 1 and Later light-duty vehicles and truck. For 1981 to 1993 vehicles, the emissions for high emitters are calculated from the basic emission rates (BERs) by applying high emitter correction factors derived using Ohio IM240 data. Different high emitter correction factors are utilized depending on the vehicle model year and technologies. High emitter correction factors are applied as a function of vehicle mileage. For Tier1 and later vehicles, high emitter BERs are estimated using average values of sample high emitter emissions. High emitter BERs are different by vehicle model year and technologies. The high emitter BERs are multiplied by high emitter correction factors which are function of mileage. High emitter correction factors were derived using Ohio IM240 data, but adjusted for newer vehicles. It should be noted that, for modeling purposes in MOBILE6, one vehicle can be a high emitter in HC and NOx and normal vehicle in CO. Thus, one vehicle data could be utilized for normal and high emitter modeling in MOBILE6. MOBILE6 added the effects of On-Board Diagnostic (OBD) systems which are available from manufacturers starting in 1996 model. They also include Inspection and

Maintenance (I/M) credits for different emission standards such as Tier1, LEV, and ULEV (Koupal and Glover, 1999; Glover and Koupal, 1999).

7.2.3 Comprehensive Modal Emission Model

The Comprehensive Modal Emissions Model (CMEM) is one of the most recently developed power demand-based emission models. CMEM was developed by researchers at the University of California, Riverside. The CMEM model estimates LDV and LDT emissions as a function of the vehicle's operating mode. For the test data, both engine-out and tailpipe emissions of over 300 vehicles, including more than 30 high emitters, have been measured second-by-second on three driving cycles: the Federal Test Procedure (FTP), the US06, and the Modal Emission cycle (MEC). CMEM predicts second-by-second tailpipe emissions and fuel consumption rates for a wide range of vehicle and technology categories (Barth *et al*., 2000).

In the CMEM model, the emissions in high emitters were calculated using the same approach as for the normal vehicle emission module. The CMEM model utilized four types of high emitters that were determined based on their emission characteristics. Each type of high emitter group is described as one of lean, rich, misfire, and catalyst related problems. The high emitter types were assigned by the Arizona IM240 data and its results were utilized in formulating the contribution of high emitters in the CMEM model.

The first type of high emitter is a vehicle in which the fuel-air ratio is chronically lean or goes lean at moderate power or transient operation. This type of vehicle shows typically low HC and CO and high NOx emissions. It is difficult to find out a physical failure mechanism exactly, but improper signal from the oxygen sensor or improperly functioning of the electronic engine control could be possibilities.

The second type of high emitter is a vehicle in which the fuel-air ratio is chronically rich or goes rich at moderate power. Under these conditions, the engine-out HC remains normal. However, these kind of vehicles have a high CO emission index and catalyst pass fraction, resulting in high tailpipe CO emissions. There are many possible reasons for this enrichment failure. One possibility is a leaking exhaust line which brings in oxygen before the oxygen sensor, resulting in the sensor calling for more fuel from the injectors.

In the third type of high emitter, the engine-out hydrocarbons are high and these vehicles have mild enrichment having high engine-out CO and high CO catalyst pass fraction. Also these vehicles have poor catalyst performance resulting in moderate to slightly high tailpipe CO, very high HC, and moderate to low NOx. The possible reasons of the problem are incomplete combustion in one or more cylinders (misfire) causing heavy engine-out HC and catalyst deterioration.

In the fourth type of high emitter, all emissions have high tailpipe emissions. These vehicles have chronically (burned-out or missing catalyst) or transiently (high catalyst pass fraction) poor catalyst performance. However, this type of high emitter is different from the third type since engine-out HC is normal or slightly high. This type of vehicles experience high emissions for HC, CO, and NOx. Eleven vehicles are categorized in this type category (Barth *et al*., 2000).

7.3 EMISSION DATA DESCRIPTION

This section describes the data that were utilized for high emitter vehicle modeling. The data used in this study is the same as was used in the MOBILE6 modeling and validation. The data utilized for this study were collected by EPA. In MOBILE6, facility specific drive cycles have been developed by Sierra Research. Sierra Research developed eleven facility-specific and one non-freeway area-wide driving cycles. These cycles are developed based on chase car and instrumented vehicle data tested at Baltimore, MD, Spokane, WA and Los Angeles CA. The information was collected during the FTP revision project for use in developing the supplemental certification cycles and new standards. A total of 101 vehicle data set were collected, including data for 3 heavy-duty trucks, 34 LDTs, and 64 LDVs. Since the data used in this study is the same one as used in previous chapter, more detailed descriptions regarding data collection procedures and drive cycle characterizations are found in Chapter 6.

7.4 HIGH EMITTER CRITERIA AND EMISSION CUT-POINTS FOR NEW CYCLES

MOBILE6, the standard EPA model to predict emissions in ground transportation systems, characterizes vehicle emission according to certification standard, technology, and emitter group (EPA 2001). However, this classification only depends on the Federal Test Procedure (FTP) certification level. It is desirable to verify if the FTP test is consistent with the other cycles to

classify high emitters. This study proposes a methodology to select high emitters using the microscopic emission behaviors of emitter groups for several different cycles using EPA emission data.

Among the 101 EPA vehicle data, 87 vehicle samples were selected for this study because the remaining 14 vehicles did not include FTP emission data, which is essential when comparing various driving cycles. The sample of 87 vehicles includes 24 light-duty trucks. The vehicle model years are distributed from 1983 through 1996. Most of the 87 vehicles use fuel injection engines, with 3 carbureted passenger cars and 4 carbureted light duty trucks. Also, among the 87 vehicles, 24 vehicles have manual transmission and the remaining 63 vehicles have automatic transmission. Table 7-1 through 7-4 show a sample vehicle description of the 87 vehicles that includes model years, make, model, emission standard, odometer reading, engine size, fuel injection type, and IM240 results (only for the ATL tested vehicles).

7.4.1 High Emitter Characteristics

Selecting the proper test type and cut-points to identify high emitters is a critical procedure, because the emission rates are significantly different across various test types. Table 7-5 illustrates the variability of HC emissions by various test cycles. The table shows the total HC emissions and the average HC emissions of the 87 test vehicles for 19 driving cycles. The difference between the FTP cycle and the LA4 emission rates are up to 43% according to Table 7-5. It should be noted that FTP, LA4, FTP bag2 cycles are commonly utilized for high emitter classification cycles. The difference can be explained due to the engine start portions of bag1 and 3 of the FTP cycle, which is not included in LA4, IM240, and the FTP bag2 cycle. The disparity of standards to classify high emitters is evident.

As shown in Table 7-5, the highest emission levels are associated with the ST01 and New York cycles. However, because the ST01 cycle includes cold start emissions, it is difficult to conclude that the ST01 cycle is the most aggressive cycle. It is noted that the relative difference between the Highway Level of Service (LOS) D cycle and the New York cycle is four fold. Table 7-5 shows which cycles produce more pollutants. As stated before, the HR505 is bag 1 of the FTP cycle measured under hot stabilized conditions. It is notable to compare the FTP, HR505, and LA4 cycles. Among these cycles, the FTP tests show the highest emission and the HR505 and

the LA4 cycles produce lower emissions. The LA4 cycle is bag1 and bag2 of the FTP cycle without cold start emission. The emissions in this cycle are calculated as follows using the HR505 and the FTP Bag2 (Brzezinski *et al.* 1999a):

LA4 Emissions = ((HR505*0.479)+(FTP Bag2*0.521)) [7-1]

In order to understand vehicle emission behaviors, it is necessary to investigate instantaneous emission from vehicles. Figure 7-1 shows second-by-second CO emissions for two vehicles along the complete ARTA cycle. The two vehicles are selected from the normal emitters complying with the vehicle manufacturer's standard (or the intermediate life certification standard emission using FTP test). As shown in the figure, emitting behaviors of each vehicle are significantly different along the cycle. It is also noted that the relative differences in emission values at some points are up to several hundreds times. The figure explains the importance in deciding an emission standard to classify normal and high emitters.

The IM240 test procedure is utilized to identify vehicles in need of maintenance. Even though the IM240 cycle was designed to resemble the LA4, the IM240 cycle is more aggressive than the LA4 cycle based on the average speed and aggressiveness of acceleration. As shown in Tables 7-6 and 7-7, IM240 includes high average speeds and more aggressive acceleration rates. Therefore, IM240 emission rates should be higher than the LA4 emission rates and the emission cut-points of LA4 should be lower than these IM240's cut-points (Pidgeon and Dobie 1991).

Table 7-8 shows the HC emitter group distribution for the 19 test cycles. This research employed the same cut-points that EPA used for conducting analyses with the FTP test cycle, mostly due to the fact that MOBILE6 utilizes the FTP test for the identification of high emitter (Koupal and Glover 1999, Glover and Koupal 1999). Temporally, clean vehicles are classified if the vehicle emission rates do not exceed the manufacturer's emission standard (or the intermediate life certification standard emission using FTP test). It is remarkable that 40 or more vehicles are classified as clean vehicles in some cycles such as the FTP test, HR505, and ARTA cycle. Other test cycles such as FNYC, FWAC, RAMP, and ST01 have less than 30 clean vehicles. It is noted that, when people test a high emitter, choosing a proper driving cycle is very important, as it is necessary to have different emission cut-points for different cycles. As shown in the Table 7-8, 40 vehicles are classified as clean in the FTP test, while no vehicle is found in

the ST01 cycle and only 22 vehicles are found in the New York cycle. It is noted that both the FTP and ST01 tests include cold engine start emissions. However the ST01 cycle (248 seconds) finishes earlier than the FTP test (1873 seconds). Consequently, the ST01 cycle is affected more comparing to the FTP test by cold start operations since the unit of the emission is grams/km. It is known that the impact of the cold engine contribution to emissions subsides after 200 seconds (Enns and Brzezinski 2001). The next section describes a proposed methodology to obtain new emission standards for all EPA new cycles.

7.4.2 Emission Cut-points for EPA New Cycles

In order to select whether a vehicle is a normal or high emitter, a vehicle is tested on a certain driving cycle using certain emission limits. If the emission rates of a vehicle along the cycle exceeds certain cut-point, the vehicle is categorized as a high emitter. If not, the vehicle is classified as a normal vehicle. Commonly, FTP tests or other similar tests such as LA4, FTP bag2, and IM240 are utilized to verify high emitters. However, because those driving cycles contain enrichment events compared with other hot-stabilized test cycles, more aggressive and high emitting driving cycles such as the low speed New York cycle may be required for high emitter testing at severely contaminated urban areas.

If the same cut-point is used for different cycles, a vehicle can be a normal emitter for some aggressive cycles and a high emitter for others. Therefore, we need different emission standards for different cycles. The purpose of the study is to obtain the emission cut-points for the new EPA driving cycles using EPA data. In order to obtain the emission cut-points for new EPA driving cycles, a scale factor method is applied.

Table 7-9 shows the HC emission statistics for clean vehicles when categorized according to the FTP test. In order to estimate a scale factor, clean vehicles were utilized instead of normal vehicles because clean vehicles have more reliable mechanical emission system than normal vehicles. Some normal vehicles emit significant pollution which is very close to the emission cut-point. In the group of test vehicles only 40 vehicles comply with the manufacturer's HC emission standard (or the intermediate life certification standard emission) when tested with the FTP cycle. Table 7-9 shows the HC emission rates statistics of 18 driving cycles for the same 40 vehicles. As shown in the table, the mean HC emission rates are distributed from 0.034

grams/km (0.055 grams/mi) to 0.279 grams/km (0.447 gram/mi) for the same vehicles. Also, it is noted that the maximum emission rate of the New York cycle is 4.9 grams/km (7.9 grams/mi) while the FTP bag2 has 0.16 grams/km (0.25 grams/mi) of maximum emission rate. The New York cycle has the highest value of standard deviation, too. These explain that, even when same vehicles are tested on different cycles, there are substantial variations in emission rates.

Table 7-10 shows the scale factors and other important statistics for the new EPA driving cycles. FTP HC emission rates are utilized as baseline emission rates to obtain the emission scale factors. The statistics shown in Table 7-10 are estimated from 40 vehicles in the database which emit less than the manufacturer emission standard. Scale factors are calculated based on the means of the emissions rate data. The mean of FTP HC emission rate is utilized as a baseline (denominator) of the means of new EPA driving cycles. Therefore, the scale factor is the relative difference between the mean of FTP HC emission rates and the other cycle's means. Table 7-10 shows that the New York , Ramp , and Arterial LOS E cycles have the highest scale factor values. The New York and Arterial LOS E cycles have very low average speeds which include frequent stop and go behaviors. The Ramp cycle has very steep acceleration behaviors which causes high engine enrichment conditions. Also, HR505, Freeway LOS D, FTP bag2, LA4 cycles have relatively low scale factor values. The scale factors developed can be utilized as multiplicative factors of the baseline emission cut-points (i.e., 0.5 grams/km or 0.8 grams/mi) to generate new emission cut-points for all new cycles. For example, if the scale factor of the HR505 cycle is 0.45, the HC emission cut-point for this cycle would be 0.22 grams/km (0.36 grams/mi). For the New York cycle, the HC emission cut-point would be 1.10 grams/km (1.74 gram/mi).

Table 7-11 shows the HC emission classification that results from using the scale factor method and the EPA single cut-point method. The new classification results are more consistent vehicle strata distributions comparing to the EPA's single cut-point method. In the New York cycle, it is noted that 38 vehicles are classified as clean using a single cut-point method while 50 vehicles are categorized as clean vehicles using the scaling factors suggested in this study. Tables 7-12 through 7-15 show the CO and NOx emission scale factors derived from the FTP cycle and show a comparison between the new scale factor and EPA cut-point methods. The same methods are applied to the CO and NOx emission scale factors as the HC emission scale factor method. The

results are also similar to HC emission scale factor method. For CO and NO_x, the New York, Ramp, and Arterial LOS E cycles have the highest scale factor values.

7.5 MODEL DEVELOPMENT

This section describes a high emitter model development process using EPA field data. The model development consists of high emitter vehicle categorization, normalization of data, and model building. The EPA data consist of second-by-second data for 101 LDVs and LDTs. However, only 36 high emitter vehicles were utilized in this analysis. High emitter vehicles were selected using twice the values for HC and NOx and three times values for CO of the intermediate life certification standard emission using the FTP test (Koupal and Glover 1999, Glover and Koupal 1999). Among the 36 vehicles, 24 vehicles were LDVs and the remaining 12 vehicles were LDTs. Twenty-four vehicles had an automatic transmission and 12 vehicles had manual transmission. Twenty-nine vehicles used fuel injection engines with gasoline while 7 vehicles are carbureted vehicles. Figure 7-2 shows the vehicle model year, engine size, and mileage distributions for test vehicles. The model year was distributed from 1983 to 1994. The engine sizes of the test vehicles were distributed from 1.5 liter to 5.8 liters, while most of vehicles fall in the less than 4.0 liter categories. In Figure 7-2, it is found that most of vehicles have driven more than 100,000 kilometers.

7.5.1 Vehicle Classification

This section describes a vehicle classification process that is a critical procedure to estimate accurate vehicle emissions. Depending on the vehicle characteristics, such as vehicle model year, engine technology, engine size, and vehicle mileage, the amounts and patterns of vehicle emission can vary significantly by vehicle groups. Traditional emission models categorize vehicle classification into common vehicle groups such as light-duty gasoline vehicles (LDGV) or passenger cars (PC). However, this methodology may not verify the significant differences in a vehicle group such as LDGV or PC due to the considerable variation of vehicle characteristics.

This model employed the same high emitter category as used in the CMEM model. Recall that the CMEM model classifies all high emitters into four categories. The first type of high emitter is a vehicle which the fuel-air ratio is chronically lean or goes lean at moderate power or transient operation. Four vehicles among 36 high emitters belong to this category. The second type of high

emitter is a vehicle in which the fuel-air ratio is chronically rich or goes rich at moderate power. Only one vehicle that fits in this category is found from 32 high emitters. In the third type of high emitting vehicle, the engine-out hydrocarbons are high and these vehicles have mild enrichment having high engine-out CO and high CO catalyst pass fraction. Twenty vehicles among 36 vehicles belong to this category. In the fourth type of high emitter, all emissions have high tailpipe emissions. These vehicles have chronically or transiently poor catalyst performance. Eleven vehicles are categorized in this type.

Table 7-16 shows the average emissions and variations for 15 driving cycles for vehicle classes without LA4 and ST01 cycles. From Table 7-16, it can be found that the results are reasonably consistent with the four types of high emitter vehicle characteristic. It should also be noted that there is only one vehicle in type 2, so the result can not represent the feature of high emitter type 2.

7.5.2 Temporal Normalization of Data

In order to use second-by-second emission data, it is required to ensure that there is no time lag between speed/acceleration observations and emission measurements. The EPA data were in the format of a database containing around 8900 to 9400 records per each vehicle. Each records included test site, vehicle ID, driving cycle, time ID for each driving cycle, instantaneous speed, second-by-second emissions (HC, CO, CO2, and NOx), and other related data. The EPA data consisted of the second-by-second speed and emission data for 101 LDVs and LDTs. Each vehicle data included the emission data from 14 to 16 driving cycles.

A time-lag is the offset in vehicle emissions between vehicle speed/acceleration and their corresponding emissions through the tailpipe. Note that the time-lags between vehicle accelerations and vehicle emissions typically range between 5 and 12 seconds depending on the data collection procedure. The time-lag is a very important factor in determining instantaneous emission modeling because if speed data are shifted a certain amount, the emission rates that correspond to the speed data are totally different. In order to check the time-lag, the VT-micro model based on the ORNL data was utilized. The sum of second-by-second emissions calculated by the VT-micro model through each driving cycle was compared with each total emission of EPA emission data. The minimum differences between the calculated emissions and the EPA

data were selected for the time-lag. Experimentally, it was found that most of the Eastliberty (NVREL) test site data had 0 to 1 second time-lags while nearly all of Ann Arbor (ATL) data had 6 to 8 second time-lags.

7.5.3 Model Construction

This section provides a description of the model construction procedure. Overall, the emission model utilized in this study is the same mathematical model as used in the VT-Micro model. The model is a nonlinear regression model based on a multi-dimensional polynomial model structure. This multiple regression model that relates a dependent variable "second-by-second emission measurements" to a set of quantitative independent variables is a direct extension of a polynomial regression model in several possible terms of independent variables. The model utilizes instantaneous vehicle speed and acceleration as independent variables. The choice of independent variables and an appropriate regression format was dependent on the experimental exercise.

In order to develop the high emitter model, the second-by-second EPA data has been transformed to a table format to reduce the noise in a bin at the same speed and acceleration. Speed and acceleration data of EPA data were changed to integer values by rounding off. The emission data of all vehicle in a vehicle category at a speed/acceleration bin were averaged to create a single average emission estimate in the bin. In the table, the x-axle value represents acceleration and the y-axle stands for speed. The EPA data were transformed to table format using standard Pivot functions in the Microsoft Excel program. Vehicle speeds ranged from 0 to 121 kph at increments of 1 kph, while acceleration values varied from –6 to 10 kph/s at increments of 1 kph/s (0.278 m/s^2). Figure 6-5 shows a sample HC table that explains the frequency of the cell showing the speed and acceleration distribution of the sample vehicle data. As shown in the figure, most of the speed and acceleration data were found in the low speed range and the -1 to 1 kph/s acceleration range. Each table then was generated for four high emitter categories and four pollutants. A sample data set for one high emitter (1992 Eagle Summit, 1.5 Liters, Mileage 129,457, Manual Transmission, High Emitter type 4) and one normal emitter (1993 Eagle Summit, 1.5 Liters, Mileage 52447, Manual Transmission) for HC and CO emissions is presented in Figure 7-3. The figure clearly demonstrates significant emission differences between the high emitter and the normal vehicle. The emission discrepancy

is discovered not only at high engine load but also at low speed and low acceleration regime. It is also found that the emission rates form a large nonlinear behavior as a function of the vehicle speed and acceleration in the high emitter as well as the normal vehicle.

As mentioned, the regression model developed here follows the same format used in the VT-Micro model. The second-by-second emission data were transformed to logarithms in the emission model to eliminate negative estimates and improve model accuracy in the low speed and low acceleration regime, which generally produces relatively small amounts of emission rates. The most frequent speed and acceleration combinations during routine vehicle operations exist in the low speed and low acceleration regime. It should be noted that the emission model employs the hybrid models separating the positive and negative acceleration regions. This dual-regime modeling approach significantly reduces errors when compared to the single-regime model, especially in the negative acceleration regime, which takes up approximately 40 percent of vehicle operation. Since a dual-regime model divides the dataset into deceleration and acceleration regimes including constant speed (when acceleration is 0), there are possible discontinuity or significant distinctions between the constant speeds and the adjacent deceleration values when estimating emissions. In an attempt to overcome this problem, the emission data for the negative acceleration regime was shifted by a constant of the regression model for the positive acceleration regime. This approach allowed for the use of the same intercept values for both acceleration and deceleration models.

It should be noted that the models should be utilized within the envelope of the EPA data (0 to 121 kph and –6 to 10 kph/s). While most vehicles can travel faster than the upper limit of the testing boundary, it is impossible to establish a reliable forecasting pattern for energy and emission rates at high speeds due to the heavy nonlinear nature of the response curves. However, in cases in which a vehicle exceeds the boundary, it is recommended to use boundary speed and acceleration levels in order to ensure realistic vehicle MOE estimates. It should be noted that all speed and acceleration profiles in the EPA driving cycles were associated with routine vehicle operations. The speed and acceleration boundary is consistent with the data boundary depicted in Figure 6-5.

Since the model adopts the same framework that was utilized to develop the VT-Micro model, more detailed descriptions regarding the model construction procedures are found in Chapter 6 including fuel consumption estimation procedures.

Since the primary goal of the modeling was the prediction of emissions of high emitter vehicles within each of the vehicle categories tested, the model parameters of four pollutants for each vehicle classes are determined through the regression modeling process. While the model itself does not focus on modeling specific makes and models of vehicles, it is possible to develop the model for specific makes or models of vehicles or even single vehicles applying the regression process.

Figure 7-4 shows the raw data lines and prediction lines for emissions from High Emitter Group 4 (type 4) vehicles, which have high emissions in all MOEs. As shown in the figure, the prediction lines fit relatively well with the original data in all four emissions. The prediction lines accurately follow the solid lines for –3 and 0 kph-s (-0.83 and 0 m/s^2) data and cross the middle area of the oscillated data of 3 and 6 kph-s (0.83 and 1.67 m/s^2) data at high speed and acceleration region. Emission predictions for the other vehicle categories are provided in Appendix C (Figures C1 to C3).

Since the EPA data did not include second-by-second fuel consumption information, the fuel consumption of vehicles could be estimated using a same method utilized in Chapter 6. Equations 6-7 and 6-8 illustrates fuel consumption estimation using carbon balance equations.

Using the equations, the fuel consumption data were calculated from EPA emission data and a fuel consumption regression model was built. Figure 7-5 shows estimated fuel consumption data and predicted values for High Emitter Group 4. It was found that the shape of the fuel consumption chart looks extremely similar to the appearance of CO_2. Figure 7-5 illustrates the prediction lines fit well with the fuel consumption data.

7.6 MODEL VALIDATION

The next step in the analysis was to validate the newly developed emissions model. Model validation is a fundamental step in the model development process as it examines the model uncertainty and model performance. In order to confirm the model performance, this study

investigated macroscopic and microscopic validation technique using aggregate emission data and instantaneous emission data.

7.6.1 Aggregate Model Validation

The newly developed model is validated with the aggregate EPA emission data that utilized for model developments since other independent data were not available.

Figure 7-6 demonstrates the close correspondence between the emission model and the field data by illustrating the variation in the 95^{th} percentile, 5^{th} percentile, and mean EPA field measurements for 15 drive cycles. The 95^{th} percentile, 5^{th} percentile, and mean values are estimated from the eleven vehicles that is total number of vehicles in High Emitter Group 4 group. The bar plots represent the proposed model emission estimates using a composite vehicle high emitter type 4. Each vertical line and small horizontal bar stand for the 95^{th} percentile, 5^{th} percentile, and mean value of vehicle emission data. The predicted emissions are computed as the sum of instantaneous vehicle emissions for each of the 15 drive cycles. Figure 7-6 clearly illustrates a good fit between the model estimates and the field measurements. Specifically, all predictions lie within the 95^{th} percentile and the 5^{th} percentile limits. Furthermore, the model estimates generally follow the average field emission values of the vehicle fleets. The average relative differences for 15 driving cycles between model prediction and mean value of data show excellent performance of the model (3 % for HC, 4 % for CO, 10 % for NO_x, and 1 % for CO_2).

7.6.2 Instantaneous Emission Model Validation

This section validates the model comparing instantaneous field emission data against the model estimates. The speed/acceleration profile of the ARTA drive cycle is utilized to simulate the emission model. The ARTA cycle includes a more aggressive and realistic driving behavior compared to the old driving cycles as depicted in Figure 6-12. The vehicle category High Emitter Group 4 is selected for comparison purposes. Figure 7-7 illustrates the variation in the maximum, minimum, and mean value of the instantaneous vehicle emissions as measured on a dynamometer as it travels through the drive cycle. Each maximum, minimum, and mean value is calculated from the eleven vehicles contained in the vehicle category High Emitter Group 4 for four pollutants. The dotted lines represent the mean values of vehicle emissions while the upper/lower thin line shows the max/min limits. The solid lines are the model estimates of

vehicle emissions based on instantaneous vehicle speed and acceleration levels. Figure 7-7 shows that, in general, the model prediction lines almost perfectly follow the data lines (mean values) of the EPA vehicle emission measurements. It should be noted that this figure demonstrates the uniqueness of the model to assess traffic improvement projects, including ITS technology, on the environment. The total vehicle emissions of HC, CO, NOx, and CO2 as measured in the laboratory were 13.503, 157.487, 16.836, and 1545.33 grams. The estimated HC emissions based on the proposed hybrid model were 14.271, 164.943, 16.411, and 1532.27 grams, which correspond to 3, 5, 3, and 1 percent differences in overall emissions for the entire cycle.

Figure 7-8 illustrates another validation result by showing measured data and the corresponding prediction values in the Cartesian Coordination System. The slope of the MOEs, except for NOx (0.77), is very close to 1.0, which means perfect fit with prediction and raw data. It should be noted that the y intercept was set to 0 when created each graph to reduce the possible skewness of the chart.

7.7 SUMMARY

This study discussed the development of new high emitter cut-points and microscopic high emitter vehicle emission models. IM240 and MOBILE model emission standards have been mostly utilized for classifying high emitters. The procedure to differentiate high emitters from the normal vehicles is a critical step in emission modeling. Without a consistent high emitter criteria standard , it is impossible to estimate accurate mobile source emissions. The results of this study support the following conclusions:

- When similar vehicles are tested, the emission rates are very different depending on the test cycle when the test conditions such as temperature, test fuel, etc are same.
- Depending on the test cycle and emission cut-point standards, a vehicle can be a high emitter or a normal vehicle.
- Each test cycle needs its own emission cut-point to classify emitter statues. A scale factor method was applied to EPA's new driving cycles in order to obtain the emission cut-point for each cycle.

- Using the scale factor method, it is possible to utilize different emission test cycles depending on a emission test site condition. For example, the low speed New York cycle may be tested in very contaminated urban areas while the Arterial LOS A cycle can be utilized in suburban or rural areas.

The study also presents a microscopic high emitter emission models that estimate second-by-second mobile source emissions in hot stabilized conditions using instantaneous vehicle speed and acceleration levels as input variables. The models overcome one of the major drawbacks of traditional mobile source emission models: the insensitivity of the environmental impact of operational-level projects in which changes in traffic behavior between a before-and-after scenario are critical. Capturing emission impacts from individual vehicle behaviors caused by drivers, traffic signals, and traffic flows are very important. The emission models were developed using the EPA second-by-second emission data, which include off-cycle emissions and aggressive driving behaviors. The high emitters in the database are categorized by vehicle characteristics and technologies using the same method used by the CMEM model, thus creating four high emitter groups. In the model validation, the models are found to produce vehicle emissions consistent with EPA data in aggregate and instantaneous model validations. In the aggregate model validation, the average relative differences for 15 driving cycles between model prediction and mean value of data show excellent performance of the model showing less than 10 % of errors for all MOEs. Also, model predictions almost perfectly follow the data lines (mean values) of the EPA vehicle emission measurements in instantaneous emission validations generating less than 5 % overall errors through the entire ARTA drive cycle.

Table 7-1. EPA's Sample Vehicle-Light Duty Vehicles Tested at Eastliberty

Site	Veh. No.	Veh. Class	Model Yr.	MAKE	MODEL	Standard	Miles	Eng. Size	Fuel Inj.	IM240
EASTLIBERTY	5001	LDV	88	Buick	Centery	Tier0	129,698	2.5	TBI	PASS
EASTLIBERTY	5002	LDV	89	Oldsmobile	Cutlass	Tier0	61,956	2.5	TBI	FAIL
EASTLIBERTY	5003	LDV	91	Ford	Crown	Tier0	53,003	5	PFI	PASS
EASTLIBERTY	5005	LDV	91	Chevrolet	Cavalier	Tier0	54,658	2.2	TBI	PASS
EASTLIBERTY	5006	LDV	89	Chevrolet	Cavalier	Tier0	107,611	2	TBI	PASS
EASTLIBERTY	5007	LDV	88	Oldsmobile	Delta	Tier0	101,534	3.8	PFI	PASS
EASTLIBERTY	5008	LDV	92	Ford	Taurus	Tier0	74,078	3	PFI	PASS
EASTLIBERTY	5009	LDV	89	Pontiac	Grand	Tier0	155,181	3.1	PFI	FAIL
EASTLIBERTY	5010	LDV	93	Toyota	Camry	Tier0	29,392	2.2	TBI	PASS
EASTLIBERTY	5011	LDV	93	Geo	Metro	Tier0	105,445	1	TBI	PASS
EASTLIBERTY	5012	LDV	88	Pontiac	Grand	Tier0	89,764	2.3	TBI	PASS
EASTLIBERTY	5013	LDV	93	Pontiac	Grand	Tier0	72,348	2.3	PFI	PASS
EASTLIBERTY	5014	LDV	91	Cadillac	Deville	Tier0	51,707	4.9	TBI	FAIL
EASTLIBERTY	5015	LDV	93	Pontiac	Grand	Tier0	58,538	2.3	PFI	PASS
EASTLIBERTY	5016	LDV	89	Buick	Lesabre	Tier0	65,212	3.8	TBI	FAIL
EASTLIBERTY	5017	LDV	91	Vw	Cabriolet	Tier0	67,496	1.8	TBI	PASS
EASTLIBERTY	5018	LDV	95	Dodge	Neon	Tier1	20,855	2	TBI	PASS
EASTLIBERTY	5019	LDV	90	Chevrolet	Camaro	Tier0	71,258	3.1	PFI	FAIL
EASTLIBERTY	5020	LDV	92	Ford	Taurus	Tier0	84,148	3.8	TBI	PASS
EASTLIBERTY	5021	LDV	95	Dodge	Neon	Tier1	28,525	2	PFI	PASS
EASTLIBERTY	5022	LDV	89	Chevrolet	Cavalier	Tier0	110,929	2	TBI	PASS
EASTLIBERTY	5023	LDV	88	Ford	Tempo	Tier0	107,979	2.3	PFI	PASS
EASTLIBERTY	5024	LDV	91	Ford	Tempo	Tier0	97,522	2.3	PFI	FAIL
EASTLIBERTY	5026	LDV	89	Mercury	Sable	Tier0	107,075	3	PFI	FAIL
EASTLIBERTY	5027	LDV	92	Eagle	Summit	Tier0	129,457	1.5	PFI	FAIL
EASTLIBERTY	5028	LDV	93	Mazda	626	Tier0	103,171	2	PFI	FAIL
EASTLIBERTY	5030	LDV	86	Ford	Taurus	Tier0	50,755	2.5	TBI	FAIL
EASTLIBERTY	5031	LDV	88	Toyota	Camry	Tier0	197,090	2	PFI	FAIL
EASTLIBERTY	5032	LDV	85	Mercury	Cougar	Tier0	113,584	3.8	TBI	FAIL
EASTLIBERTY	5035	LDV	87	Ford	Tempo	Tier0	118,148	2.5	TBI	FAIL
EASTLIBERTY	5036	LDV	87	Nissan	Stanza	Tier0	58,173	2	PFI	PASS
EASTLIBERTY	5037	LDV	83	Plymouth	Reliant	Tier0	94,399	2.2	NO	FAIL
EASTLIBERTY	5038	LDV	96	Chevrolet	Lumina	Tier1	16,557	3.1	PFI	PASS
EASTLIBERTY	5039	LDV	88	Honda	Civic	Tier0	184,457	1.5	TBI	FAIL
EASTLIBERTY	5040	LDV	89	Honda	Civic	Tier0	161,598	1.5	TBI	PASS
EASTLIBERTY	5041	LDV	87	Toyota	Tercel	Tier0	136,654	1.5	NO	PASS
EASTLIBERTY	5043	LDV	89	Honda	Civic	Tier0	122,821	1.5	TBI	PASS
EASTLIBERTY	5045	LDV	93	Pontiac	Grand	Tier0	85,789	3.4	PFI	FAIL
EASTLIBERTY	5049	LDV	86	Chevrolet	Celebrity	Tier0	131,601	2.8	NO	PASS
EASTLIBERTY	5051	LDV	89	Chevrolet	Cavalier	Tier0	123,581	3.1	PFI	PASS
EASTLIBERTY	5052	LDV	91	Chevrolet	Cavalier	Tier0	90,945	2.2	TBI	PASS
EASTLIBERTY	5054	LDV	91	Ford	Escort	Tier0	105,861	1.8	PFI	FAIL
EASTLIBERTY	5057	LDV	93	Chevrolet	Corsica	Tier0	41,766	3.4	PFI	PASS
EASTLIBERTY	5059	LDV	93	Toyota	Camry	Tier0	67,344	2.2	PFI	PASS
EASTLIBERTY	5060	LDV	93	Honda	Accord	Tier0	61,163	2.2	PFI	PASS
EASTLIBERTY	5061	LDV	90	Nissan	Maxima	Tier0	120,786	3	PFI	PASS
EASTLIBERTY	5062	LDV	93	Eagle	Summit	Tier0	52,447	1.5	PFI	PASS
EASTLIBERTY	5063	LDV	96	Pontiac	Grand	Tier1	20,451	3.1	PFI	PASS

Table 7-2. EPA's Sample Vehicle-Light Duty Trucks Tested at Eastliberty

Site	Veh. No.	Veh. Class	Model Yr.	MAKE	MODEL	Standard	Miles	Eng. Size	Fuel Inj.	IM240
EASTLIBERTY	5025	LDT1	91	Nissan	Pickup	Tier0	103,346	2.4	PFI	PASS
EASTLIBERTY	5029	LDT1	89	Plymouth	Voyager	Tier0	118,586	3	PFI	PASS
EASTLIBERTY	5033	LDT1	87	Chevrolet	S10	Tier0	128,681	2.5	TBI	PASS
EASTLIBERTY	5034	LDT1	85	Chevrolet	S10	Tier0	89,435	1.9	NO	PASS
EASTLIBERTY	5042	LDT1	85	Chevrolet	Astro	Tier0	179,855	4.3	NO	FAIL
EASTLIBERTY	5044	LDT1	88	Chevrolet	S15	Tier0	115,693	2.5	TBI	FAIL
EASTLIBERTY	5046	LDT1	85	Ford	Ranger	Tier0	56,488	2.8	NO	FAIL
EASTLIBERTY	5047	LDT1	91	Ford	Econoline	Tier0	79,573	5.8	PFI	FAIL
EASTLIBERTY	5048	LDT1	89	Ford	Ranger	Tier0	123,419	2.3	TBI	PASS
EASTLIBERTY	5050	LDT1	85	Ford	Econoline	Tier0	86,203	5.8	NO	PASS
EASTLIBERTY	5053	LDT2	91	Ford	E150	Tier0	97,531	5.8	PFI	FAIL
EASTLIBERTY	5055	LDT1	91	Plymouth	Voyager	Tier0	72,032	2.5	TBI	PASS
EASTLIBERTY	5056	LDT1	91	Chevrolet	Astro	Tier0	90,880	4.3	TBI	PASS
EASTLIBERTY	5058	LDT1	93	Chevrolet	S10	Tier0	48,578	4.3	TBI	PASS

Table 7-3. EPA's Sample Vehicle-Light Duty Vehicles Tested at Ann Arbor

Site	Veh. No.	Veh. Class	Model Yr.	MAKE	MODEL	Standard	Miles	Eng. Size	Fuel Inj.	IM240
ANNARBOR	5213	LDV	92	Toyota	Corolla	Tier0	77,310	1.6	PFI	NULL
ANNARBOR	5217	LDV	96	Honda	Accord	Tier1	7,573	2.2	PFI	NULL
ANNARBOR	5218	LDV	92	Saturn	Sl	Tier0	89,995	1.9	TBI	NULL
ANNARBOR	5219	LDV	92	Chevrolet	Beretta	Tier0	94,316	3.1	PFI	NULL
ANNARBOR	5222	LDV	92	Mazda	Protege	Tier0	10,727	1.8	PFI	NULL
ANNARBOR	5223	LDV	96	Chevrolet	Lumina	Tier1	17,233	3.1	PFI	NULL
ANNARBOR	5224	LDV	92	Chevrolet	Cavalier	Tier0	90,196	2.2	PFI	NULL
ANNARBOR	5228	LDV	94	Chrysler	Lhs	Tier0	59,937	3.5	PFI	NULL
ANNARBOR	5229	LDV	96	Honda	Civic	Tier1	9,433	1.6	PFI	NULL
ANNARBOR	5231	LDV	94	Saturn	Sl	Tier0	25,930	1.9	PFI	NULL
ANNARBOR	5232	LDV	94	Hyundai	Elantra	Tier0	57,960	1.8	PFI	NULL
ANNARBOR	5234	LDV	94	Ford	Escort	Tier1	51,168	1.9	PFI	NULL
ANNARBOR	5237	LDV	92	Chevrolet	Lumina	Tier0	16,133	3.4	PFI	NULL
ANNARBOR	5240	LDV	96	Toyota	Camry	Tier1	18,992	3.0	PFI	NULL
ANNARBOR	5241	LDV	90	Dodge	Daytona	Tier0	6,813	3.3	PFI	NULL

Table 7-4. EPA's Sample Vehicle-Light Duty Trucks Tested at Ann Arbor

Site	Veh. No.	Veh. Class	Model Yr.	MAKE	MODEL	Standard	Miles	Eng. Size	Fuel Inj.	IM240
ANNARBOR	5225	LDT1	96	Ford	Ranger	Tier1	10,064	2.3	PFI	NULL
ANNARBOR	5230	LDT1	94	Chevrolet	Astro	Tier0	77,178	4.3	PFI	NULL
ANNARBOR	5233	LDT1	92	Chevrolet	Lumina	Tier0	33,872	3.1	PFI	NULL
ANNARBOR	5235	LDT1	90	Plymouth	Voyager	Tier0	98,530	3.0	PFI	NULL
ANNARBOR	5238	LDT1	96	Ford	Explorer	Tier1	N/A	4.0	PFI	NULL
ANNARBOR	5239	LDT1	94	Pontiac	Tran	Tier1	68,305	3.8	PFI	NULL
ANNARBOR	5220	LDT2	94	Ford	F150	Tier0	97,629	5.8	PFI	NULL
ANNARBOR	5221	LDT2	96	Ford	F150	Tier1	12,877	4.9	PFI	NULL
ANNARBOR	5226	LDT2	90	Jeep	Cherokee	Tier1	N/A	4.0	PFI	NULL
ANNARBOR	5227	LDT2	90	Chevrolet	Suburban	Tier0	97,658	5.7	TBI	NULL

Table 7-5. Total HC Emissions and Average HC Emissions for Sample Vehicles (87 vehicles)

Cycles	Total HC Emissions (grams)	Average HC Emission (grams/vehicle)
LA4	18.35	0.73
FWYD	50.97	0.59
FWAC	53.76	0.62
FWHS	54.01	0.62
HR505	73.10	0.84
FWYE	74.89	0.86
ARTA	87.74	1.01
LA92	91.99	1.06
RAMP	95.41	1.10
FTP Bag2	101.47	1.20
AREA	103.73	1.19
FWYF	105.57	1.21
FTP	110.97	1.28
ARTC	113.52	1.30
FWYG	117.72	1.35
LOCL	127.02	1.46
ARTE	154.45	1.78
New York	217.03	2.49
ST01	306.91	3.53
IM240	Not Available	

Table 7-6. IM240 Test and LA4 Cycle Speeds Comparison (Source:Pidgeon, W. M. and Dobie, N. 1991)

	Average Speed (kph)	Average Speed w/o Idle Modes (Kph)	Max. Speed (Kph)
IM240	48	49.28	90.72
LA4	31.36	38.56	90.72

Table 7-7. IM240 test and LA4 cycle Driving Behaviour Comparison (Source: Pidgeon, W. M. and Dobie, N. 1991)

	Percentage of Driving Schedule in each 16kph Range (without idle modes)					
	0-16 kph	16-32 kph	32-48 kph	48-64 kph	64-80 kph	80-96 kph
IM240	5.2	18.3	34.3	13.9	8.7	19.1
LA4	13.8	19.2	45.9	11	3.4	6.6
	Average Rate of Acceleration (kph/sec)					
IM240	4.96	2.56	1.33	1.38	1.36	0.69
LA4	3.68	2.88	1.15	1.07	1.28	0.61
	Average Rate of Deceleration (kph/sec)					
IM240	5.60	3.68	1.76	1.92	3.20	1.26
LA4	3.84	3.36	1.30	0.86	0.98	0.67

Table 7-8. Emitter Group Distribution Using FPT Driving Cycle Criteria for HC

	Clean (<=0.26g/km)	Normal (>0.26 g/km)	High (>0.50 g/km)	Sum (Vehicles)
FTP	40	15	32	87
FTP Bag 2	55	6	26	87
LA4	53	9	25	87
HR505	46	24	16	86
AREA	35	25	26	86
ARTA	41	20	26	87
ARTC	33	26	28	87
ARTE	28	29	30	87
New York	22	31	34	87
FWAC	27	32	28	87
FWHS	33	23	30	86
FWYD	37	23	27	87
FWYE	37	26	24	87
FWYF	34	25	28	87
FWYG	38	24	25	87
LA92	32	27	27	86
LOCL	39	25	23	87
RAMP	24	24	39	87
ST01	0	7	79	86

Table 7-9. HC Emission Statistics for EPA New Driving Cycles (40 FTP Criteria Clean Vehicles)

	Mean (grams/km)	Standard Deviation (grams/km)	Maximum (grams/km)	Minimum (grams/km)
FTP	0.128	0.044	0.238	0.050
FTP Bag2	0.034	0.034	0.156	0.006
LA4	0.046	0.066	0.413	0.006
HR505	0.058	0.132	0.856	0.006
AREA	0.095	0.149	0.750	0.006
ARTA	0.079	0.130	0.663	0.006
ARTC	0.099	0.169	1.006	0.006
ARTE	0.207	0.598	3.719	0.013
New York	0.279	0.774	4.938	0.013
FWAC	0.073	0.100	0.538	0.006
FWHS	0.061	0.095	0.600	0.000
FWYD	0.049	0.071	0.444	0.006
FWYE	0.074	0.137	0.756	0.006
FWYF	0.069	0.079	0.338	0.006
FWYG	0.078	0.091	0.381	0.006
LA92	0.085	0.122	0.725	0.006
LOCL	0.076	0.096	0.519	0.006
RAMP	0.154	0.293	1.700	0.006

Table 7-10. HC Scale Factors Derived from FTP Cycle

	mean (grams/km)	Std. Dev. (grams/km)	maximum (grams/km)	minimum (grams/km)	scale factor
FTP	0.128	0.044	0.238	0.050	1.000
FTP BAG2	0.034	0.034	0.156	0.006	0.266
LA4	0.045	0.066	0.413	0.006	0.354
HR505	0.058	0.132	0.856	0.006	0.450
AREA	0.095	0.150	0.750	0.006	0.740
ARTA	0.079	0.130	0.663	0.006	0.613
ARTC	0.099	0.170	1.006	0.006	0.776
ARTE	0.207	0.598	3.719	0.013	1.615
New York	0.279	0.774	4.938	0.013	2.180
FWAC	0.073	0.100	0.538	0.006	0.571
FWHS	0.061	0.095	0.600	0.000	0.473
FWYD	0.049	0.071	0.444	0.006	0.379
FWYE	0.073	0.137	0.756	0.006	0.573
FWYF	0.069	0.079	0.338	0.006	0.535
FWYG	0.078	0.091	0.381	0.006	0.611
LA92	0.085	0.122	0.725	0.006	0.664
LOCL	0.076	0.096	0.519	0.006	0.596
RAMP	0.154	0.293	1.700	0.006	1.204

Table 7-11. Comparison Between Multiple Cut-Points and Single Cut-point Methods (HC)

	New Classification Applying Scale Factor (Vehicles)			Old Classification applying the EPA Cut-point (Vehicles)		
	Clean	Normal	High	Clean	Normal	High
FTP	40	15	32	40	15	32
FTP Bag2	36	10	41	55	6	26
LA4	41	8	38	53	9	25
HR505	48	5	34	57	8	22
AREA	46	6	35	51	7	29
ARTA	48	5	34	52	7	28
ARTC	45	9	33	51	7	29
ARTE	50	9	28	45	7	35
New York	50	12	25	38	12	37
FWAC	50	9	28	56	14	17
FWHS	49	7	31	56	14	17
FWYD	44	11	32	56	14	17
FWYE	45	8	34	51	12	24
FWYF	38	13	36	49	9	29
FWYG	39	14	34	51	5	31
LA92	47	7	33	51	9	27
LOCL	42	9	36	49	7	31
RAMP	48	11	28	46	10	31
Mean	44.778	9.333	32.889	50.389	9.556	27.056
Standard Deviation	4.466	2.910	3.909	5.337	3.166	5.886

Table 7-12. CO Scale Factors Derived from FTP

	mean (grams/km)	Std. Dev. (grams/km)	maximum (grams/km)	minimum (grams/km)	scale factor
FTP	0.801	0.261	1.316	0.176	1.000
FTP BAG2	0.263	0.249	0.820	0.000	0.329
LA4	0.603	1.691	10.068	0.007	0.752
HR505	0.972	3.556	21.020	0.016	1.213
AREA	0.836	1.927	11.332	0.035	1.043
ARTA	0.874	2.208	13.176	0.020	1.090
ARTC	1.240	3.399	20.180	0.043	1.547
ARTE	2.886	12.400	72.941	0.008	3.601
FNYC	3.713	14.858	87.586	0.016	4.633
FWAC	1.638	1.992	11.949	0.184	2.044
FWHS	0.977	0.809	3.531	0.000	1.219
FWYD	0.852	0.856	3.898	0.078	1.063
FWYE	0.970	2.974	17.645	0.004	1.211
FWYF	0.570	0.522	1.945	0.004	0.712
FWYG	0.637	0.701	2.895	0.004	0.795
LA92	0.930	1.138	6.523	0.008	1.160
LOCL	0.574	0.638	2.742	0.004	0.716
RAMP	2.480	6.571	38.879	0.012	3.095

Table 7-13. Comparison Between Multiple Cut-Points and Single Cut-point Methods (CO)

	New Classification Applying Scale Factor (Vehicles)			Old Classification applying the EPA Cut-point (Vehicles)		
	Clean	Normal	High	Clean	Normal	High
FTP	34	30	23	34	30	23
FTP Bag2	28	21	38	51	16	20
LA4	74	13	0	81	6	0
HR505	54	17	16	46	24	17
AREA	36	25	26	36	25	26
ARTA	42	23	22	41	20	26
ARTC	45	24	18	33	26	28
ARTE	60	14	13	28	29	30
FNYC	61	12	14	22	31	34
FWAC	46	26	15	27	32	28
FWHS	36	23	28	33	23	31
FWYD	37	25	25	37	23	27
FWYE	40	28	19	37	26	24
FWYF	29	28	30	34	25	28
FWYG	30	28	29	38	24	25
LA92	35	27	25	33	27	27
LOCL	30	29	28	39	25	23
RAMP	48	24	15	24	24	39
Mean	41.950	23.500	21.550	36.150	25.250	25.600
Standard Deviation	12.416	5.414	8.513	14.390	7.144	8.300

Table 7-14. NOx Scale Factors Derived from FTP

	mean (grams/km)	Std. Dev. (grams/km)	maximum (grams/km)	minimum (grams/km)	scale factor
FTP	0.298	0.161	0.619	0.063	1.000
FTP BAG2	0.188	0.140	0.606	0.006	0.633
LA4	0.214	0.144	0.553	0.003	0.718
HR505	0.241	0.158	0.638	0.000	0.811
AREA	0.311	0.216	1.069	0.000	1.045
ARTA	0.285	0.208	1.075	0.000	0.958
ARTC	0.357	0.296	1.388	0.000	1.201
ARTE	0.449	0.391	1.931	0.000	1.510
FNYC	0.440	0.306	1.463	0.006	1.477
FWAC	0.311	0.224	1.138	0.000	1.045
FWHS	0.324	0.266	1.244	0.000	1.088
FWYD	0.303	0.223	1.181	0.000	1.017
FWYE	0.278	0.205	1.119	0.000	0.934
FWYF	0.327	0.262	1.456	0.000	1.099
FWYG	0.242	0.184	0.881	0.000	0.814
LA92	0.362	0.251	1.363	0.000	1.215
LOCL	0.335	0.319	1.781	0.006	1.125
RAMP	0.418	0.316	1.369	0.000	1.404

Table 7-15. Comparison Between Multiple Cut-Points and Single Cut-point Methods (NOx)

	New Classification Applying Scale Factor (Vehicles)			Old Classification applying the EPA Cut-point (Vehicles)		
	Clean	Normal	High	Clean	Normal	High
FTP	58	14	15	58	14	15
FTP Bag2	54	15	18	65	12	10
LA4	53	17	17	63	11	13
HR505	55	15	17	59	12	16
AREA	56	14	17	55	14	18
ARTA	54	15	18	55	16	16
ARTC	58	16	13	53	14	20
ARTE	57	18	12	47	17	23
FNYC	60	15	12	43	22	22
FWAC	57	14	16	56	15	16
FWHS	54	17	16	52	18	17
FWYD	57	14	16	57	14	16
FWYE	55	14	18	58	13	16
FWYF	59	13	15	55	15	17
FWYG	58	16	13	65	11	11
LA92	56	14	17	55	12	20
LOCL	58	13	16	57	11	19
RAMP	55	17	15	46	16	25
Mean	56.333	15.056	15.611	55.500	14.278	17.222
Standard Deviation	1.970	1.474	1.975	5.963	2.845	3.889

Table 7-16. Variation of High Emitter Classification

Category (total 36 vehicles)		HC	CO	NOx	CO2
High Emitter Type 1 (4 vehicles)	Mean (g/km)	0.460	3.688	2.307	239.150
	Standard Deviation	0.246	1.517	1.044	20.046
High Emitter Type 2 (1 vehicle)	Mean (g/km)	0.357	11.898	2.555	305.468
	Standard Deviation	N/A	N/A	N/A	N/A
High Emitter Type 3 (20 vehicles)	Mean (g/km)	2.261	44.574	0.871	258.857
	Standard Deviation	3.518	71.760	0.756	71.432
High Emitter Type 4 (11 vehicles)	Mean (g/km)	2.053	26.466	2.278	211.194
	Standard Deviation	1.167	25.729	0.860	41.201

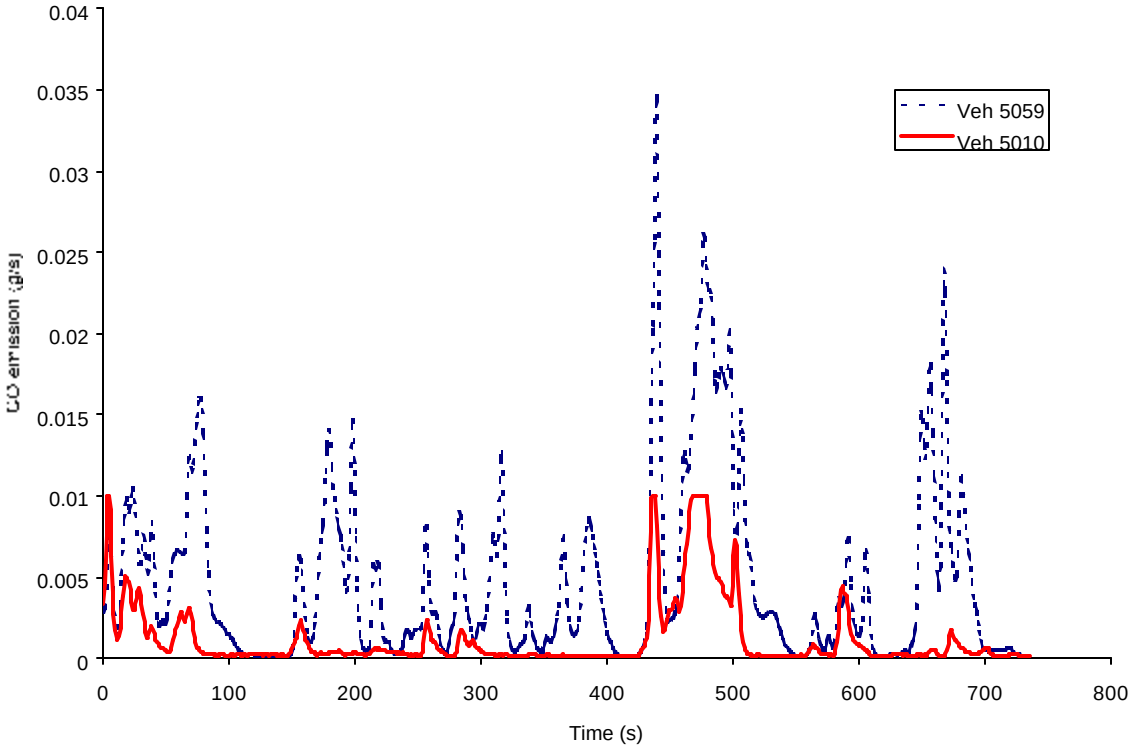

Figure 7-1. ARTA Driving Cycle HC Emissions of Different Test Vehicles

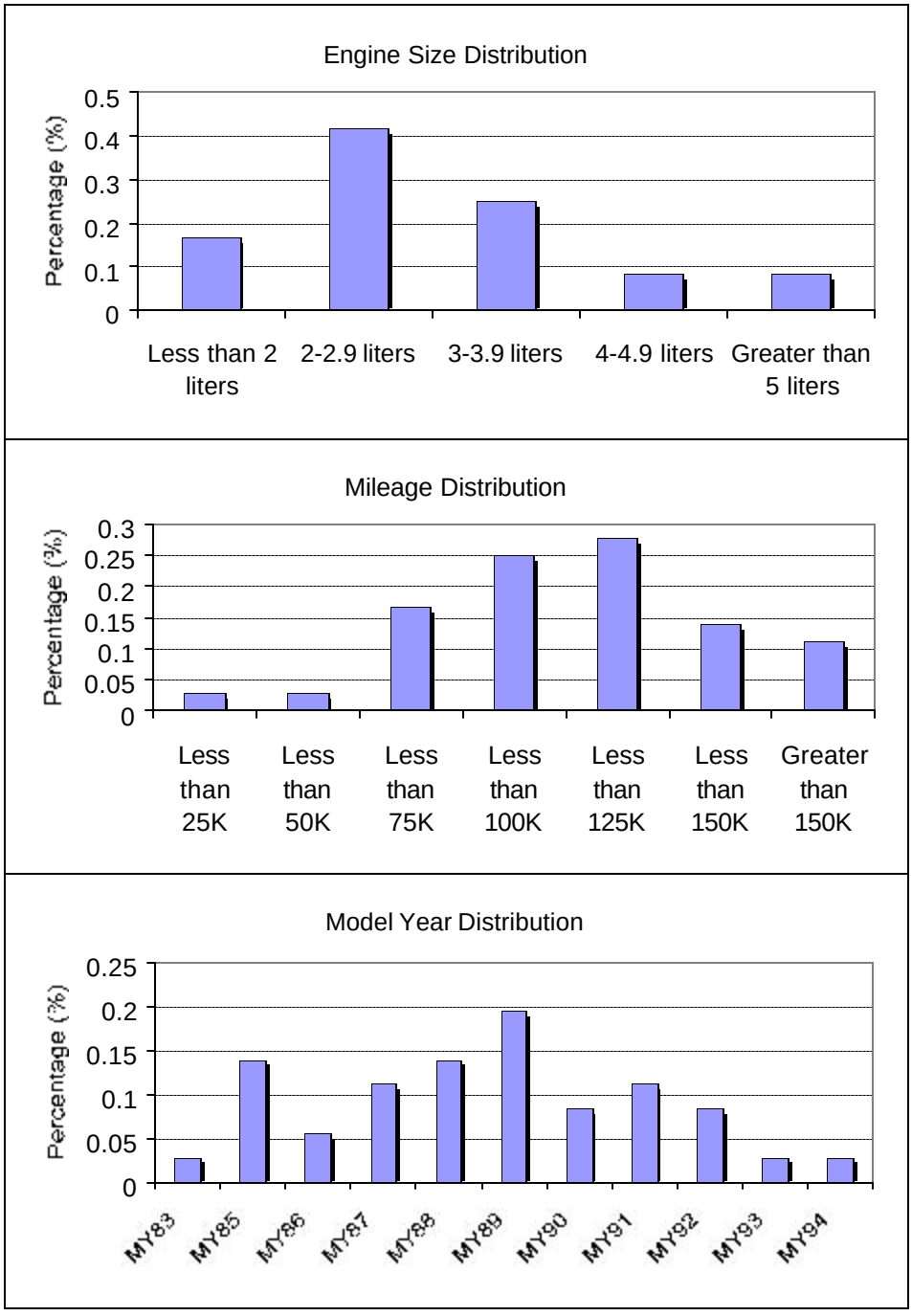

Figure 7-2. High Emitter Modelling Test Vehicle Characteristics

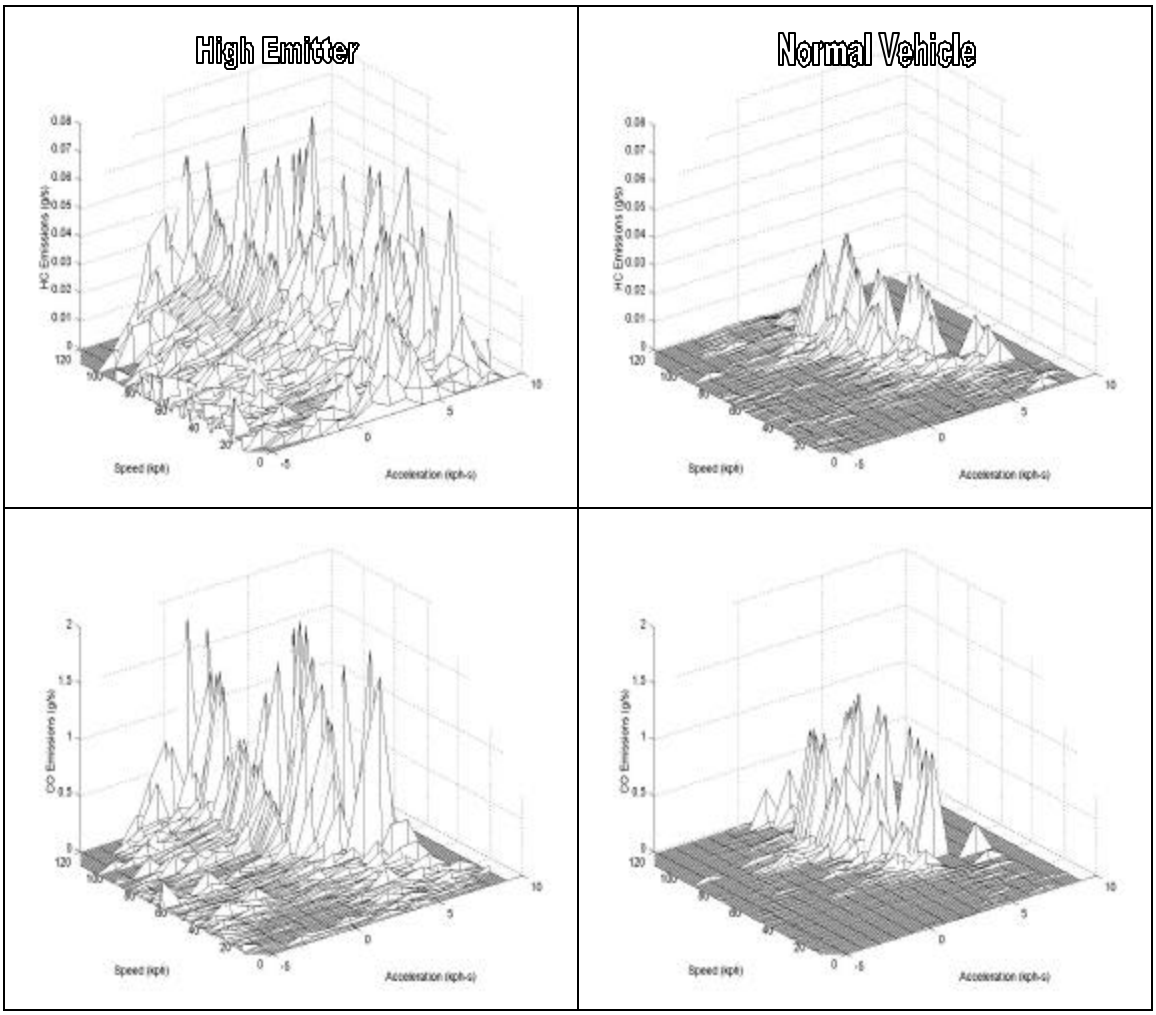

Figure 7-3. Sample Normalized Emission Data

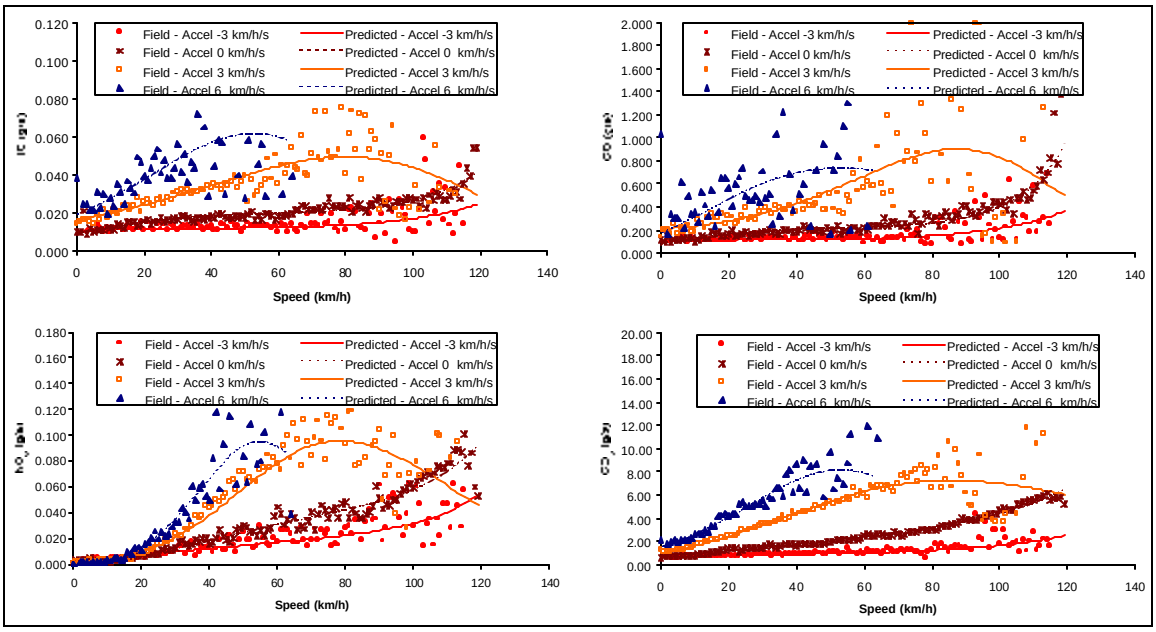

Figure 7-4. Model Prediction (Vehicle Category High Emitter Group 4)

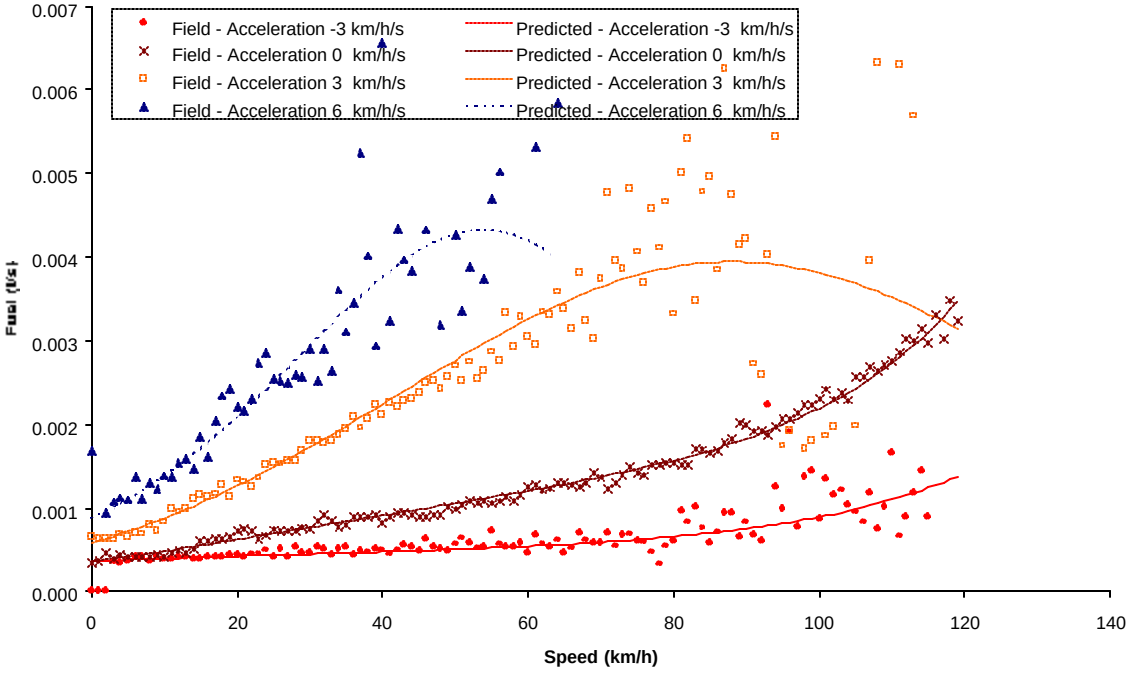

Figure 7-5. Fuel Consumption Prediction (Vehicle Category High Emitter Group 4)

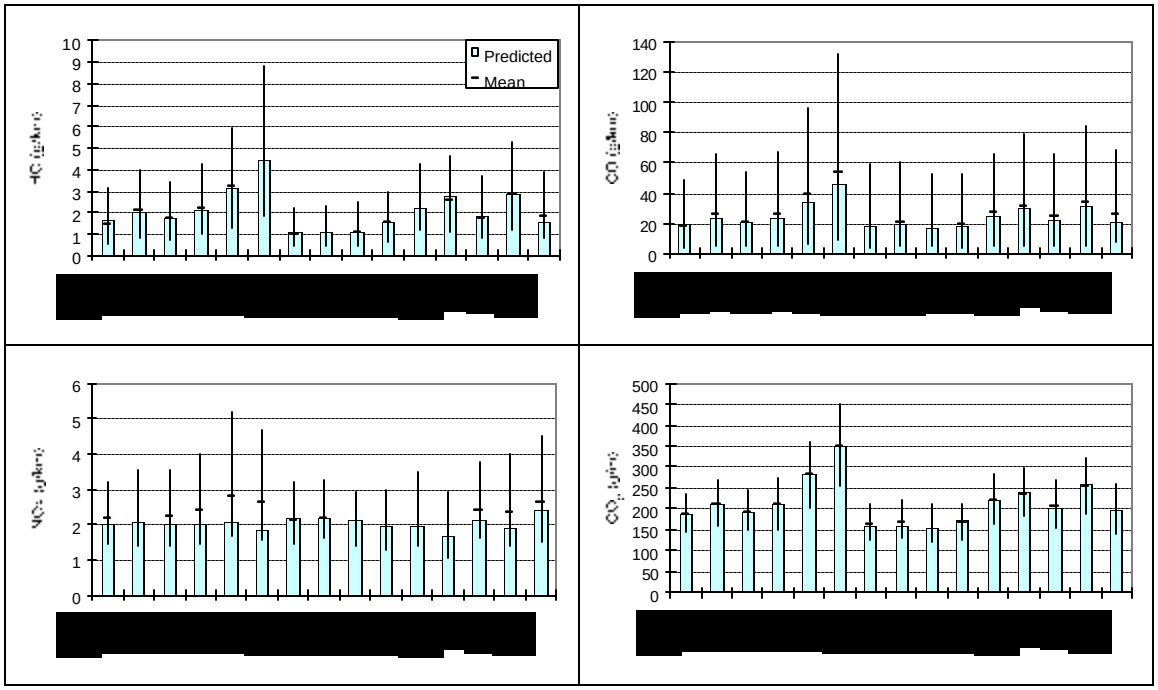

Figure 7-6. Aggregate Model Validation for Vehicle Category High Emitter Group 4

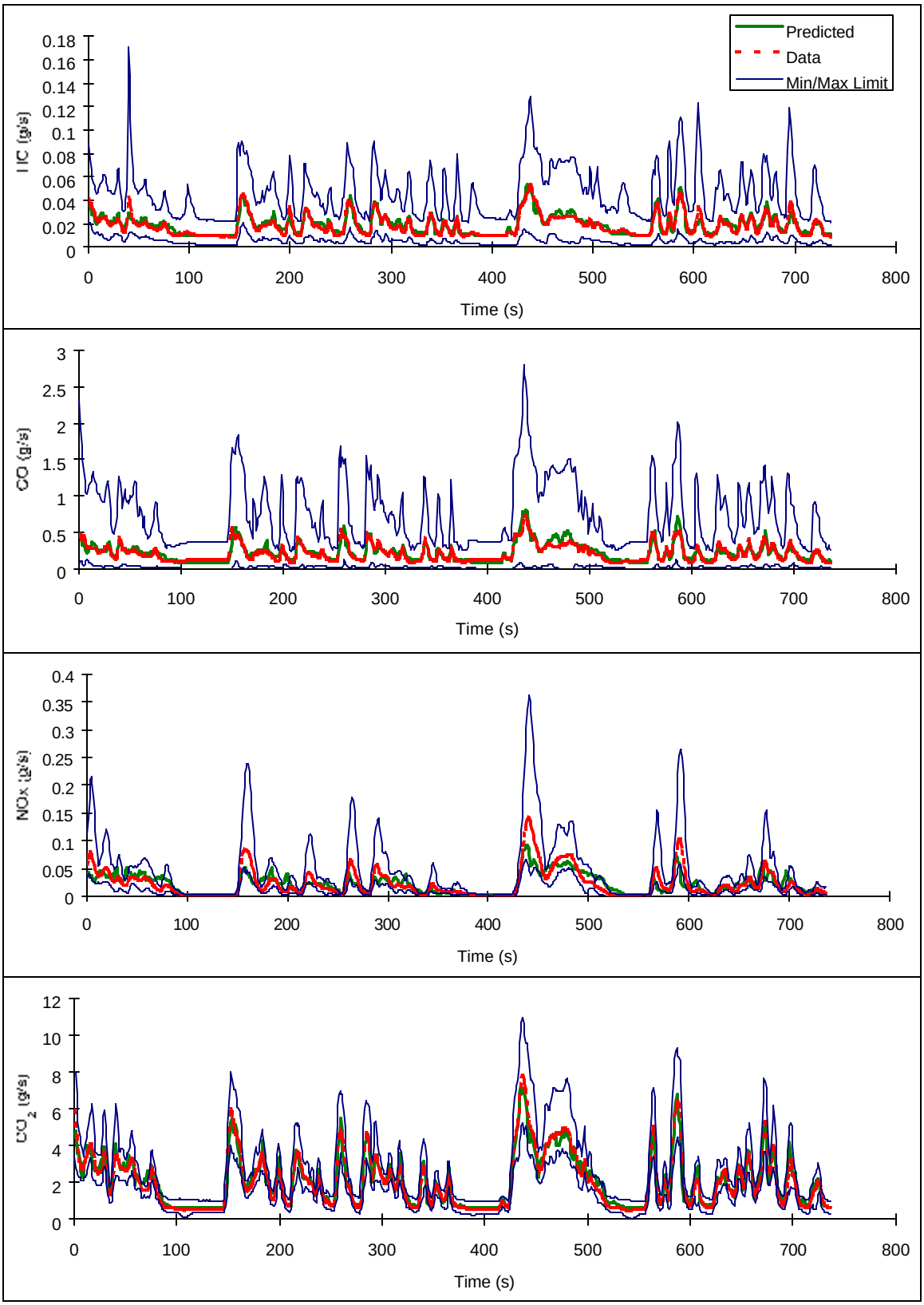

Figure 7-7. Instantaneous Model Validation for Vehicle Category High Emitter Group 4

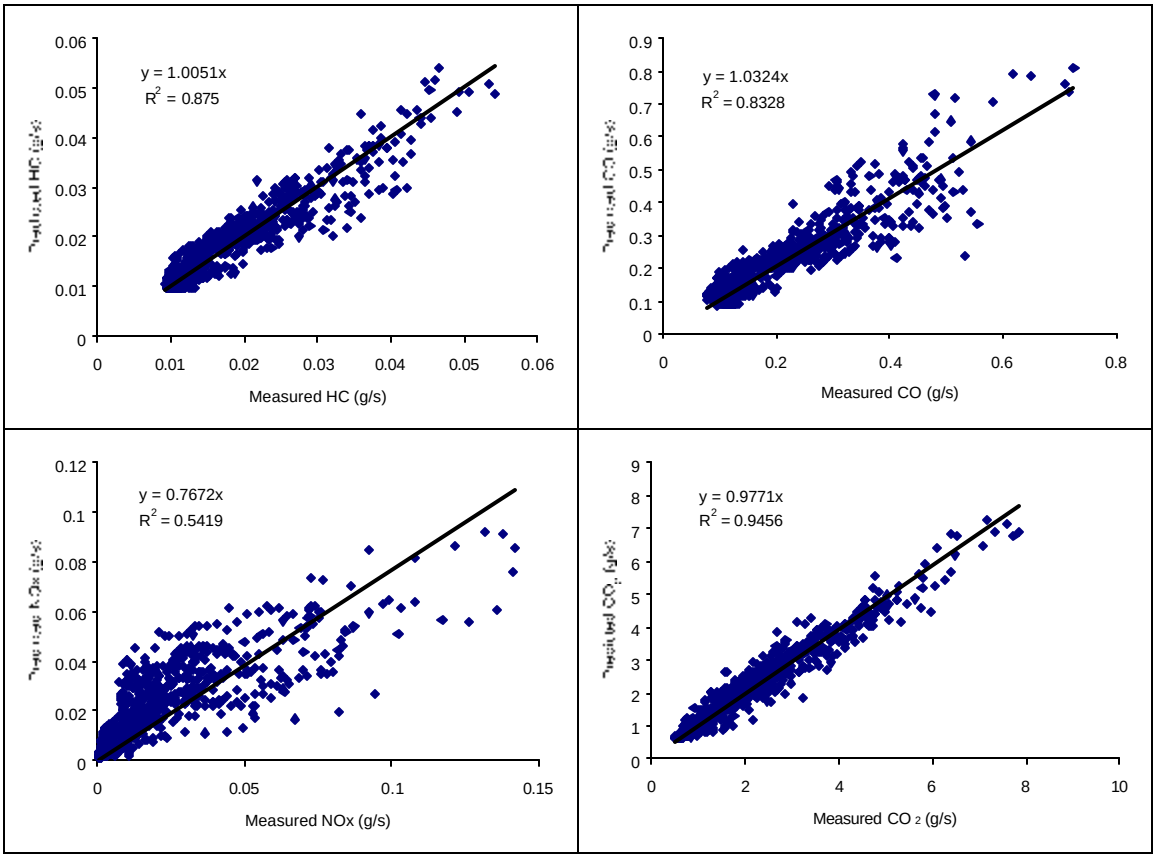

Figure 7-8. Instantaneous Prediction Verification using X-Y Coordination for Vehicle Category High Emitter Group 4

CHAPTER 8. MICROSCOPIC MODELING OF VEHICLE START EMISSIONS

The research described in this chapter develops a microscopic framework for estimating instantaneous vehicle start emissions for Light Duty Vehicles (LDVs) and Light Duty Trucks (LDTs). The framework assumes a linear decay in instantaneous start emissions over a 200-second time horizon.

8.1 INTRODUCTION

The engine operation of a vehicle is classified into two modes, namely: transient and hot stabilized. The transient mode of operation is further divided into cold start and hot start modes. Typically, vehicles emit a higher number of pollutants in the transient modes of operation when compared to the hot stabilized mode. The Environmental Protection Agency's (EPA's) MOBILE model, which is commonly utilized to estimate mobile source emissions, models cold start operation following a 12-hour soak period, while hot start operation is defined as any transient behavior that involves a soak period of less than 12 hour. The soak period is defined as the duration of time between engine turn-off and engine re-start. The duration of each transient mode is assumed to be less than 505 seconds in the Federal Test Procedure (FTP), which is used to test new vehicles for compliance with EPA emission standards.

The engine operation modes of a vehicle, which primarily refer to the operating temperature of the combustion chamber and catalytic converter, have a significant effect on vehicle fuel consumption and emission rates. During the period of operation prior to reaching the optimum operating temperature of the engine, incomplete combustion occurs in the engine and very little oxidation occurs in the catalyst (Wayson *et al.,* 1998, Venigalla *et al*, 1995). Hydrocarbons (HC) and carbon monoxide (CO) emissions are significantly higher during the cold start engine operation due to the low air-to-fuel ratios and poor performance of cold catalytic converters. Alternatively, the cold starts result in relatively fewer extra emission for oxides of nitrogen (NO_x) when compared to HC and CO emissions. The cold start emissions are typically high initially and decrease with time to a stabilized level as the engine reaches its normal operating temperature.

8.1.1 Objectives of Research

The objective of this study is to develop vehicle fuel consumption and emission models representing engine transient operations. The final goal of these models is to enhance microscopic traffic models and predict environmental impacts of various transportation alternatives.

Hot start emission modeling and soak time functions are not developed in this study due to the limited availability of data. Instead, the proposed model uses start state-of-practice procedures for accounting for soak time on vehicle start emissions.

8.1.2 Significance of Research

While research has been conducted on vehicle start emissions, the focus of previous research efforts have been primarily on estimating the percentage of vehicles in different modes of operation. Furthermore, previous fuel and emissions modeling approaches have been focused on the characterization of macroscopic trip-based models. This dissertation presents a proposed framework for estimating vehicle start emissions to be incorporated in microscopic emission models that can be utilized to assess the energy and environmental impacts of operational-level transportation projects.

8.1.3 Chapter Layout

This chapter is organized in five sections. The following section describes how engine start emissions are modeled in MOBILE6 and includes a description of fundamental driving cycles that are utilized for cold start modeling. The third section describes the proposed framework for modeling vehicle start emissions microscopically. Subsequently, the fourth section describes the data sources that were utilized to develop the proposed modeling approach. The same section also describes the model development procedures, the analysis of second-by-second cold start emission data, and how the model can be implemented within a microscopic emission model. Subsequently, the model is validated for a number of composite vehicle categories. Finally, the conclusions of the research and recommendations for future work are presented in section 6.

8.2 STATE-OF-PRACTICE MODELING OF VEHICLE START EMISSIONS

This section describes the fundamental concepts of engine start emission modeling employed in the EPA's MOBILE6 model. In particular, the drive cycles that are utilized for cold start modeling and the basic modules for modeling engine start emissions are described.

8.2.1 Overview of the FTP and HR505 Drive Cycles

The FTP drive cycle is utilized as a test cycle for certifying vehicle emission performance standards for new vehicles. The FTP cycle consists of three parts: a cold start segment, a hot stabilized segment, and a hot start segment. The first part, which is also called Bag1, lasts for 505 seconds and extends over a length of 5.74 km (3.59 miles). Before the test, the vehicle is stored for a minimum of 12 hours to simulate a 12-hour overnight soak period and allow the measurement of cold start emissions. The second segment of the FTP cycle, which is termed Bag2, lasts 867 seconds and extends over a length of 6.26 km (3.91 miles) under hot stabilized engine conditions. Bag2 emissions are collected immediately after the Bag1. After a 10-minute soak time, the 505 seconds of the start segment (Bag1), is re-run in the last part of the cycle, which is termed Bag3. Total emissions for the cycle are the obtained by adding the measurements of all three bags.

In order to compute the additional emissions that result from a cold start the speed profile of Bag1 should be run under hot stabilized engine conditions. To perform this measurement, the Hot Running 505 (HR505) drive cycle is utilized. The HR505 drive cycle involves a speed profile that is identical to Bags 1 and 3 of the FTP drive cycle, with the exception that the engine is in a hot stabilized mode of operation. Using the HR505 cycle emissions and emissions from both Bags 1 and 3 of the FTP cycle, it is then possible to compute the additional emissions that are associated with engine starts (Glover *et al*. 1998).

8.2.2 Modeling Vehicle Start Emissions in MOBILE6

MOBILE6 estimates vehicle start emissions using a soak time function that accounts for a full range of vehicle soak times. Specifically, using the cold start emission rate (soak time of 720 minutes or 12 hours) calculated using Equation 8-1, and the 10-minute soak time emission rate, computed in Equation 8-2, a soak time dependent emission rate is computed using Equation 8-3.

Both the 720-minute and 10-minute soak time emission rates are pollutant and vehicle dependent. Specifically, the MOBILE6 model modifies the basic emission rate using a deterioration function that is based on a simple linear regression model using vehicle mileage as the independent variable. These deterioration rates are vehicle specific (function of vehicle type and technology) and emission specific (HC, CO, and NO_x).

$$E_1 = (Bag1 - HR505) \times 5.74 \quad [8\text{-}1]$$

$$E_2 = (Bag3 - HR505) \times 5.74 \quad [8\text{-}2]$$

$$E(t) = E_1 \times SF(t) \quad [8\text{-}3]$$

Where:

E_1	= Vehicle start emissions after a 12-hour soak period (g),
E_2	= Vehicle start emissions after a 10-minute soak period (g),
$E(t)$	= Vehicle start emissions after a soak period of "t" minutes (g),
Bag1	= Bag 1 emission rate (g/km),
Bag3	= Bag 3 emission rate (g/km),
HR505	= HR505 emission rate (g/km),

As was mentioned earlier, the MOBILE6 model utilizes a soak time function to account for the entire distribution of soak times observed in the field ranging from a minimum of zero minutes to a maximum of 720 minutes. Using field data, engine start emissions for a 10-minute and a 720-minute soak time are measured and utilized to derive a soak time dependent vehicle start emission rate. Specifically, the 720-minute soak time vehicle emission rate is adjusted to account for different soak times using a multiplicative dual-regime Soak Function (SF) that is less than or equal to 1.0, where the breakpoint between the two regimes is vehicle and emission specific. The dual-regime SF is computed using the California Soak Function (CSF) or California interpolation curves, using Equation 8-4. The CSF is computed using vehicle and emission specific regression parameters using Equations 8-5 and 8-6. For illustrative purposes, Figure 8-1 demonstrates how the HC CSF for a catalyst-equipped vehicle varies as a function of the soak time duration. The figure clearly demonstrates a breakpoint in the CSF function at a soak time of 89 minutes (t_d = 89 minutes).

$$SF(t) = \begin{cases} CSF(t) \times \left[R + (1-R)\frac{(t-10)}{(X-10)} \right] & t \le t_d \\ CSF(t) & t > t_d \end{cases} \quad [8\text{-}4]$$

$$CSF(t) = a + bt + ct^2 \quad [8\text{-}5]$$

$$R = \frac{E_1}{E_2 \times CSF(10)} \quad [8\text{-}6]$$

Where:

SF(t) = Soak Function for a soak time of "t" minutes (unitless),

CSF(t) = California Soak Function for a soak time of "t" minutes (unitless),

a, b, c = California Soak Function coefficients,

X = Variable set to zero for soak times from 0–10 minutes. For the range from 10 minutes to 720 minutes, it is equivalent to the highest minute in the domain of the California Soak Function. For example, for HC emissions for a catalyst equipped vehicle two domains exist (0-89 minutes) and (90-720 minutes), then X=0 for times of 10 minutes or less, X=89 for times from 11 minutes through 89 minutes. For the remaining soak period of 90 minutes through 720 minutes, no soak adjustment is applied and only the California Soak Function is employed (Glover *et al*. 1998), and

t_d = Boundary of first domain.

8.3 PROPOSED MODELING FRAMEWORK

The proposed modeling framework utilizes the MOBILE6 procedures to estimate total vehicle start emissions as a function of the vehicle soak time, as illustrated in Figure 8-2. The total vehicle start emission rate is then disaggregated into instantaneous emission rates assuming a linear decay function over 200 seconds. The linear decay function and the 200-second temporal time span were derived using sample second-by-second emission data, as will be described later in the study. The base emission rate at time zero that corresponds to a soak time of "t" seconds is computed using Equation 8-7 by solving for the height of the triangle knowing the triangle's area (*E(t)*) and the length of the triangle base (200s). Subsequently, the instantaneous emission rate associated with a vehicle start at any instant "T" during the trip is computed using Equation 8-8.

Noteworthy is the fact that Equation 8-8 ensures that the additional vehicle emissions that are associated with a vehicle start tend to zero after the vehicle has traveled 200 or more seconds.

Finally, the cumulative emissions that result from a vehicle start at any instant "T" during the trip are computed using Equation 8-9. It should be noted that Equation 8-9 estimates vehicle start emissions over an entire trip identical to the MOBILE6 procedures only when the trip duration equals or exceeds 200 seconds ($E^t_T = E(t)$).

$$e(t) = \frac{E(t)}{100} \quad [8\text{-}7]$$

$$e^t_T = \left(e(t) - \frac{e(t)}{200} \times \min(T, 200) \right) \quad [8\text{-}8]$$

$$E^t_T = \left(\frac{e(t) + e^t_T}{2} \right) \times \min(T, 200) \quad [8\text{-}9]$$

Where:

$E(t)$	= Vehicle start emissions after a soak period of "t" minutes (g),
$e(t)$	= Vehicle start emission rate at start of trip (g/s),
e^t_T	= Vehicle start emission rate after "T" seconds of trip (g/s),
E^t_T	= Total vehicle start emissions over initial "T" seconds of trip (g), and
T	= Time traveled within trip (s).

8.4 DEVELOPMENT OF VEHICLE START EMISSION MODEL

This section describes how the proposed framework was utilized in the development of a microscopic vehicle start emission model. Initially, the data that were utilized for the model development are described. Subsequently, the model development approach is overviewed followed by a detailed description of the model development specifics.

8.4.1 Data Description

This section describes the data that were utilized for the modeling of engine start emissions. These data were provided by EPA as two sets of data. The first dataset included second-by-second emission data during cold start operations for five test vehicles for two drive cycles,

namely: ST01 and LA92. Vehicle emissions of HC, CO, and NO_x were measured in grams on a second-by-second basis by testing vehicles on a chassis dynamometer. Table 8-1 summarizes the characteristics of the five test vehicles that were employed in the study. The two drive cycles were developed recently to supplement old driving cycles. Specifically, the LA92 cycle, which is also called the Unified cycle, was created by the California Air Resources Board to simulate a typical driving behavior, which replaces the Federal Test Procedure (FTP) cycle. While the full LA92 drive cycle spans over 1,436 seconds, only the first 298 seconds are considered in this study to model second-by-second engine start emissions. The 258-second ST01 cycle, which was developed by EPA's revised FTP project, was designed to simulate typical driving during the beginning of a trip. As illustrated in Figure 8-3, the speed traces for the first 300 seconds of both drive cycles appear to be very similar.

The second dataset included emissions for bags 1 and 3 of the FTP cycle and bag emissions for the HR505 drive cycle. These data were collected for a total to 96 vehicles (Brzezinski, 1999a). The 96 vehicles tested included model years that ranged from 1986 through 1996. These vehicles were initially screened in order to separate normal from high emitting vehicles using a threshold that was set at twice the manufacturer standards. Of the total sample size of 96 vehicles, 60 vehicles were classified as normal vehicles and 36 were classified as high emitting vehicles. Also, among the 60 normal vehicles, 43 vehicles were Light-Duty Vehicles (LDVs) and the remaining 17 vehicles were Light-Duty Trucks (LDTs), as illustrated in Figure 8-4. The 60 vehicles included 42 vehicles with automatic transmission and 18 vehicles with manual transmission. All 60 vehicles used fuel injection gasoline engines that ranged from 1.0 liter to 5.8 liters, with the majority of vehicles in the 2.0 to 4.0 liter range. The majority of vehicles had a mileage less than 160,000 kilometers (100,000 miles). Since the EPA data don't include second-by-second fuel consumption information, the fuel consumption data could be estimated using other emissions. The detailed method is described in Chapter 6.

8.4.2 Vehicle Start Effects on Vehicle Emissions

Prior to developing vehicle start emissions, Figure 8-5 illustrates the comparison of hot stabilized emission, cold start emission, and hot start emission for a sample vehicle (vehicle 5174) over the first 298 seconds of the LA92 drive cycle. The figure clearly demonstrates the higher emission rates associated with a cold start versus a hot stabilized mode of operation; however this is not

necessarily the case for a hot start emission. Furthermore, the figure clearly demonstrates that longer soak times result in higher transient mode emissions. Finally, the figure clearly demonstrates that the effect of soak time diminishes with time. Table 8-2 further demonstrates numerically the higher vehicle emissions for transient versus stabilized mode of operations for the five test vehicles. Table 8-2 also demonstrates that vehicle start effects are higher for HC and CO emissions when compared to NO_x emissions.

Figure 8-6 illustrates the temporal variation in emissions caused by a vehicle start (difference between cold start and hot stabilized emissions). The figure demonstrates that vehicle start effects diminish with time when the vehicle attains hot stabilized conditions. Consequently, the estimation of instantaneous vehicle start emissions requires the calibration of two parameters, namely the time required for a vehicle to achieve hot stabilized conditions (x-axis intercept) and the maximum vehicle start emission rate (y-axis intercept). The calibration of these two parameters can be achieved by fitting a regression line to the data, as illustrated in Figure 8-7. In order to ensure that only data points that incur emission start effects are utilized in fitting a linear decay function, observations are considered until 10 consecutive zero or negative emission differences are observed. The results of the calibration effort demonstrate that the time required for the test vehicles to achieve hot stabilized conditions range from 96 to 309 seconds with an average value of 195 seconds and a standard deviation of 52 seconds, as summarized in Table 8-3. Consequently, a 200 second decay time was assumed, which is consistent with the times proposed by Singer *et al*. (1999). To simplify the analysis, a linear decay relationship with time was assumed. Figure 8-8 illustrates the linear decay in HC emissions as a result of a vehicle start. The y-axis intercept in Figure 8-8 corresponds to an area under the regression line of 1.563, which is the difference between the cold start and hot stabilized emissions for the LA92 drive cycle.

8.4.3 Development of a Vehicle Start Emission Model

Having identified the time required for a vehicle to achieve hot stabilized conditions (200 seconds), the calibration of vehicle start emissions is reduced to the calibration of a single parameter, namely the maximum base vehicle start emission rate (y-axis intercept). This rate can be estimated using Equation 8-8, as was discussed earlier. The procedure assumes that the additional emissions caused by an engine start is independent of the underlying drive cycle.

While this assumption is consistent with what is proposed in the literature (Enns and Brzezinski, 2001), further research is required to establish its validity. In summary, the proposed model assumes that the vehicle start emissions decay over a 200-second time interval regardless of the drive cycle, the ambient temperature, the fuel composition, and the road conditions.

Utilizing the 60 normal and 37 high emitter vehicles that were described earlier, the excess fuel consumption and emissions associated with a cold start (soak time of 720 minutes) were computed for each of the vehicle categories of the VT-Micro model (Ahn *et al*., 2002). Utilizing the proposed framework the y-axis intercept was computed for each of the vehicle categories, as summarized in Table 8-4. The values in Table 8-5 represent average additional MOE estimates for each vehicle category. For example, for the LDV2 vehicle class, the vehicle start emissions are averaged over the 15 vehicles that constitute the vehicle class. The results clearly demonstrate that over the 505 seconds of the FTP bag 1 drive cycle, vehicle start effects resulted in increases in HC and CO emissions in the range of 30 to 90 percent depending on the vehicle category. These increases in vehicle emissions only resulted in relatively minor increases in fuel consumption (ranging from 6 to 17 percent). Finally, in most instances NO_x emissions increased as a result of cold start effects, however in some rare instances the emissions actually decreased (HE4 category).

8.5 MODEL VALIDATION

This section presents some validation efforts of the proposed framework against aggregate bag measurements and against instantaneous second-by-second measurements.

8.5.1 Macroscopic Engine Start Emission Validation

In order to validate the model using aggregate emission data, the same FTP cycle bags that were utilized in developing the models were utilized with the objective of identifying any shortcomings in the proposed models. Table 8-6 summarizes the differences in model predictions versus field bag measurements. The predicted emissions are computed as the sum of the instantaneous vehicle emissions as a result of hot stabilized operation and the additional emissions caused by cold start effects along the entire trip (e.g., the first 505 seconds of FTP cycle). The hot stabilized emissions are estimated using the VT-Micro model described by Ahn *et al.* (2002). The bag1 field measurements represent the average emission rates across all

vehicles that constitute a vehicle class. For example, the LDT1 category emission rates are averaged over 11 vehicles while the LDV2 category results are averaged over 15 vehicles. A comparison of the aggregate field measurements and model predictions demonstrates that the error in model estimates range from 2 to 14 percent.

Having demonstrated the validity of the model for estimating cold start emission impacts, the next step was to validate the proposed model for hot start conditions (soak time of 10 minutes). Table 8-7 summarizes the model estimation error relative to field measurements as a result of a vehicle start (in this case a hot start). It should be noted that in a number of instances the field measurements (e.g., 22 among 91 vehicles for CO) indicated that trips that involved a hot start incurred less emissions than trips that did not involve any vehicle start. In these cases, it was assumed that the hot start emission rate was equal to the hot stabilized emission rate. The results that are presented in Table 8-7 demonstrate higher model prediction errors, in the range of 6.6 to 42.3 percent. It should be noted that since the contribution of hot starts on vehicle emissions is minor in comparison to cold start effects, these errors are of less concern.

8.5.2 Microscopic Cold Start Emission Model Validation

In an attempt to validate the proposed model microscopically, instantaneous field HC, CO, CO_2, and NO_x measurements were compared against instantaneous model predictions. The emission data were collected by the EPA on a chassis dynamometer at the Automotive Testing Laboratories, Inc. (ATL), in Ohio and EPA's National Vehicle and Fuels Emission Laboratory (NVREL), in Ann Arbor, Michigan in the spring of 1997. Emissions were compared using the ST01 drive cycle because it was the only drive cycle that included vehicle start effects. The emissions were gathered under standard ambient conditions (same with the FTP test condition) using the standard vehicle certification test fuel. The HC, CO, NO_x, and CO_2 emissions were measured as composite "bags" and instantaneously on a second-by-second basis (Brzezinski *et al.*, 1999a).

The Vehicle class LDV2 was selected for comparison purposes since this class is the largest vehicle group among the normal emitting vehicle classes. The speed profile of the ST01 drive cycle, which is illustrated in Figure 8-3, involves several sharp vehicle accelerations and decelerations. Figure 8-9 illustrates how the mean instantaneous vehicle emissions, as measured

on a dynamometer, vary along the entire drive cycle. The mean emission rate is computed as the arithmetic average across all 15 vehicles in the LDV2 category. The figure also illustrates how predicted hot stabilized emissions, without considering cold start effects, vary along the entire trip. A comparison of the model predicted and field measured emissions clearly demonstrates the need to capture the cold start effects on vehicle emission behavior.

A comparison of Figures 8-9 and 8-10 clearly demonstrates the enhancement in the VT-Micro emission predictions by accounting for cold start emission effects. However, it can be noted from Figure 8-10 that the model predictions appear to over-estimate vehicle emissions during the initial 10 seconds of the trip. The use of exponential smoothing of vehicle emissions, which illustrated in Equation 8-10, allows the model to increase gradually, as illustrated in Figure 8-11 using a smoothing factor of 0.3.

The total vehicle emissions of HC, CO, NO_x, and CO_2 for LDV2 as measured in the laboratory were 2.46, 25.93, 2.20, and 587.46 grams. The estimated emissions based on the proposed engine start emission model were 2.24, 21.35, 2.35, and 635.29 grams, which correspond to 8.9, 17.6, 7.0 and 8.1 percent difference in overall emissions for the entire cycle. Figure 8-11 illustrates that the model prediction lines generally follow the dotted lines (mean values) of the EPA vehicle emission measurements. The figure displays that the prediction lines of HC and CO emissions generally follow the peaks and valleys in field emission data, demonstrating the linear decay function of cold start emission models. Figure 8-11 demonstrates that NO_x, and CO_2 emissions are less sensitive to cold start effects when compared to HC and CO emissions. Finally, the figure clearly illustrates that the vehicle attains hot stabilized conditions over approximately 200 seconds.

$$\hat{e}_T^t = a e_T^t + (1-a)\hat{e}_{T-1}^t \qquad [8\text{-}10]$$

Where:

a = Smoothing factor,

e^t_T = Vehicle instantaneous emission rate after "T" seconds of trip (g/s), and

$\hat{e}^t_T$ = Smoothed vehicle instantaneous emission rate after "T" seconds of trip (g/s).

8.6 SUMMARY

Engine start emissions are a critical element to model accurately environmental impacts of transportation projects. Specifically, studies have shown that almost 20 percent of all vehicle trips involve cold starts. Furthermore, this study has demonstrated that over the 505 seconds of the Bag1 of the FTP cycle between 30 to 90 percent of the total HC emissions can be attributed to cold start effects. Unfortunately, the modeling of vehicle start effects on vehicle emissions has not been fully developed, particularly in the case of microscopic emission modeling. The deficiency in modeling vehicle start effects could be attributed to the lack of second-by-second data that reflect engine start effects.

This study utilized second-by-second emission data to develop a framework that captures the impact of engine starts on vehicle emissions using a microscopic type of approach. The framework ensures that aggregate emission estimates are consistent with MOBILE6 estimates. Specifically, the framework uses the MOBILE6 procedures to estimate the total vehicle start emissions. Subsequently, instantaneous vehicle emissions are estimated by considering a linear decay function in vehicle start emissions assuming that a vehicle attains hot stabilized conditions after 200 seconds of travel.

The proposed model estimates were validated by comparing them against aggregate and instantaneous field data. The results indicated that aggregate emission estimates were within 14 percent of field measurements for all four emissions considered (HC, CO, NO_x, and CO_2). Furthermore, instantaneous emission predictions were found to generally follow field measurements.

Based on the findings of the study it is recommended that further research be conducted in a number of areas including the following:

a. Further data collection and procedures need to be developed to account for the effect of soak time on vehicle start emissions.

b. Further research is required to characterize the effect of ambient temperature, relative humidity, vehicle type, and driving behavior on vehicle start emissions including the

impact of these variables on the time required for an engine to attain hot stabilized conditions.

c. Further research is required to characterize the effect of vehicle starts on diesel engine emissions.

Table 8-1. EPA Sample Test Vehicles Characteristics

Vehicle ID	Model Year	Make	Model	Engine Size (Cylinder)	Transmission
5174	91	Chevrolet	Corsica	2.2 (4)	Automatic
5177	94	Ford	Thunderbird	3.8 (6)	Automatic
5181	94	Oldsmobile	Achieva	2.3 (6)	Automatic
5182	94	Buick	Roadstar	5.7 (8)	Automatic
5183	94	Saturn	Saturn	1.9 (4)	Manual

Table 8-2. EPA Sample Test Vehicle Engine Start Emissions for LA92 Drive Cycle

	HC (g)			CO (g)			NO_x (g)		
	Cold Start	Hot Start	No Start	Cold Start	Hot Start	No Start	Cold Start	Hot Start	No Start
5174	1.983	0.080	0.420	25.365	3.329	6.102	1.194	0.288	0.519
5177	1.926	0.030	0.369	19.936	4.789	10.408	1.905	0.420	0.781
5181	1.312	0.006	0.047	13.031	2.769	3.789	0.953	0.289	0.326
5182	1.133	0.025	0.018	9.143	0.686	0.426	0.291	0.016	0.023
5183	1.734	0.084	0.210	20.005	2.601	5.981	0.489	0.146	0.116

Table 8-3. X-axis Intercept of EPA Sample Test Vehicles

Cycle	**Vehicle ID**	**HC**	**CO**	**NOx**
LA92	5174	231.04	261.69	-36.94
	5177	207.82	161.98	1647.21
	5181	158.97	205.39	356.88
	5182	136.12	159.80	-44.25
	5183	235.74	270.43	469.23
ST01	5174	308.92	229.77	-2751.64
	5177	204.94	160.38	123.48
	5181	143.26	147.09	261.58
	5182	96.21	181.92	-380.97
	5183	209.85	193.62	-98.16
Mean		195.25		
Standard Deviation		51.84		

Table 8-4. Calibrated Model Coefficients for Cold Start Linear Model

Vehicle Class	Y axis value					Slope				
	Fuel	HC	CO	CO_2	NO_x	Fuel	HC	CO	CO_2	NO_x
LDV1	0.00073	22.98	128.02	1442.17	17.73	3.65E-06	0.115	0.640	7.211	0.089
LDV2	0.00070	21.06	186.75	1442.48	16.30	3.50E-06	0.105	0.934	7.212	0.081
LDV3	0.00072	19.21	205.89	1537.00	13.96	3.58E-06	0.096	1.029	7.685	0.070
LDV4	0.00069	23.77	212.53	1162.10	20.32	3.47E-06	0.119	1.063	5.811	0.102
LDV5	0.00108	31.29	330.70	2031.74	16.75	5.38E-06	0.156	1.653	10.159	0.084
LDT1	0.00051	19.18	176.37	1452.83	10.98	2.57E-06	0.096	0.882	7.264	0.055
LDT2	0.00089	26.57	248.25	1954.17	27.34	4.43E-06	0.133	1.241	9.771	0.137
HE1	0.00093	27.91	82.84	1973.51	17.32	4.66E-06	0.140	0.414	9.868	0.087
HE2	0.00158	57.08	1159.21	4058.35	17.95	7.91E-06	0.285	5.796	20.292	0.090
HE3	0.00092	44.03	178.56	1857.98	18.08	4.61E-06	0.220	0.893	9.290	0.090
HE4	0.00110	55.81	770.71	1207.54	17.32	5.52E-06	0.279	3.854	6.038	0.087

Table 8-5. Additional Fuel Consumption and Emissions Attributed to Cold Start Operation for FTP Cycle Bag1

Vehicle Class	Fuel (liters)		HC (mg)		CO (mg)		CO_2 (mg)		NO_x (mg)	
LDV1	0.0729	13.7%	2297.6	75.6%	12801.9	52.3%	144217.5	12.1%	1773.5	42.0%
LDV2	0.0699	13.1%	2106.1	88.6%	18675.2	79.5%	144248.1	11.7%	1629.9	55.9%
LDV3	0.0716	12.5%	1920.7	94.9%	20588.7	92.1%	153699.6	11.8%	1395.6	67.3%
LDV4	0.0693	13.3%	2376.6	89.9%	21252.8	70.1%	116210.5	10.0%	2031.9	65.3%
LDV5	0.1076	14.8%	3129.3	81.4%	33069.9	75.8%	203173.7	12.6%	1675.3	37.1%
LDT1	0.0515	6.6%	1918.1	83.8%	17637.2	72.0%	145283.2	8.2%	1097.5	35.0%
LDT2	0.0887	12.4%	2656.6	66.4%	24824.9	51.4%	195416.9	12.4%	2734.4	48.6%
HE1	0.0932	15.4%	2791.2	72.3%	8283.9	41.5%	197351.3	14.4%	1732.2	12.0%
HE2	0.1581	18.1%	5708.1	92.7%	115921.1	96.4%	405835.1	22.1%	1795.0	25.4%
HE3	0.0923	12.1%	4403.5	37.6%	17856.3	10.2%	185797.6	12.7%	1807.9	38.9%
HE4	0.1105	17.1%	5580.8	40.4%	77070.8	43.6%	120754.2	10.2%	-594.0	-5.1%

Table 8-6. Model Errors for Cold Start Emissions

Vehicle Class	Fuel	HC	CO	CO_2	NO_x	Mean
LDV1	3.22%	13.72%	23.90%	2.59%	13.64%	11.41%
LDV2	0.50%	1.04%	5.59%	1.50%	10.32%	3.79%
LDV3	2.29%	0.36%	2.65%	0.50%	3.88%	1.94%
LDV4	2.30%	20.73%	16.52%	1.19%	20.22%	12.19%
LDV5	0.13%	2.09%	9.79%	0.30%	13.72%	5.21%
LDT1	9.66%	0.68%	4.21%	6.66%	10.13%	6.27%
LDT2	1.40%	13.85%	5.85%	1.16%	2.36%	4.92%
HE1	3.36%	35.39%	24.66%	2.73%	4.21%	14.07%
HE2	8.81%	4.37%	8.06%	2.25%	10.18%	6.74%
HE3	0.32%	9.35%	3.26%	1.63%	11.50%	5.22%
HE4	2.71%	11.18%	8.47%	1.21%	6.24%	5.96%

Table 8-7. Model Errors for Hot Start Emissions

Vehicle Class	Fuel	HC	CO	CO_2	NO_x	Mean
LDV1	3.82%	33.28%	52.15%	2.98%	18.21%	22.09%
LDV2	1.64%	7.39%	24.91%	1.66%	20.18%	11.16%
LDV3	0.59%	1.05%	31.37%	0.53%	5.70%	7.85%
LDV4	2.05%	113.09%	51.34%	1.35%	43.78%	42.32%
LDV5	0.74%	15.51%	33.15%	0.38%	16.78%	13.31%
LDT1	3.70%	1.23%	11.03%	3.47%	15.07%	6.90%
LDT2	2.37%	22.92%	4.66%	2.73%	3.81%	7.30%
HE1	4.06%	69.58%	36.63%	3.22%	4.19%	23.54%
HE2	4.60%	35.84%	126.31%	3.99%	12.86%	36.72%
HE3	1.07%	12.74%	0.88%	1.89%	16.50%	6.62%
HE4	3.33%	16.35%	13.93%	1.37%	5.78%	8.15%

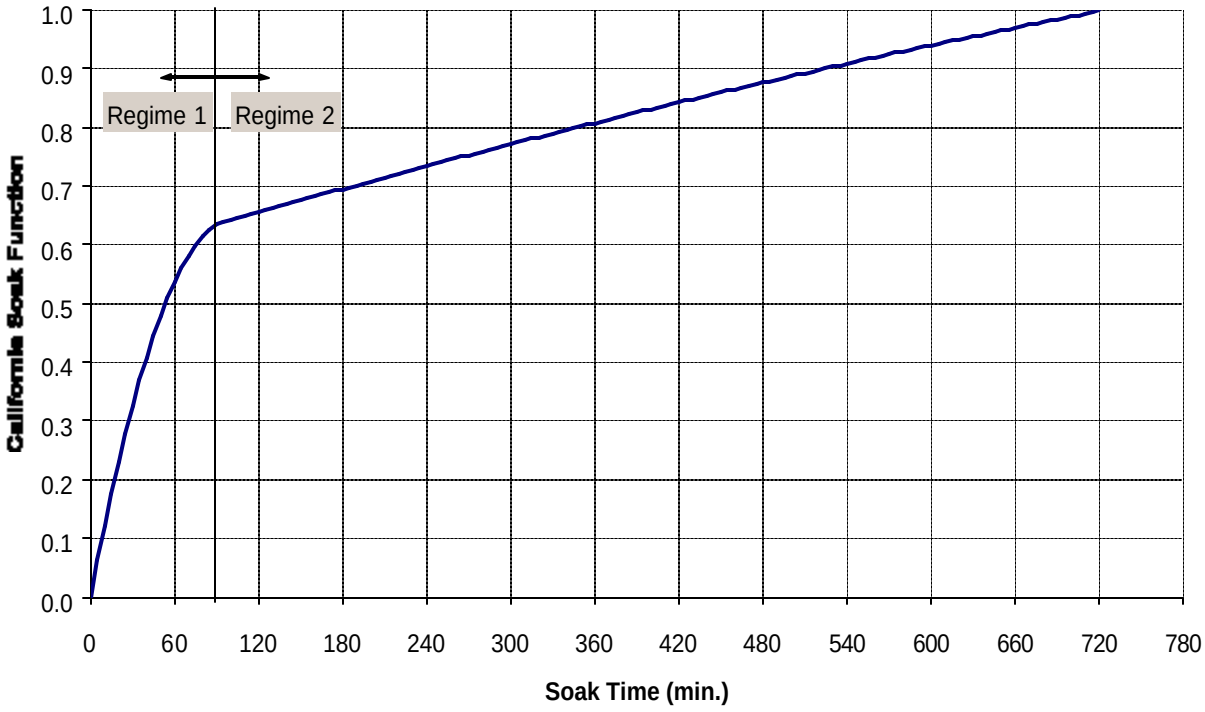

Figure 8-1. HC California Soak Function for a Catalyst-Equipped Vehicle

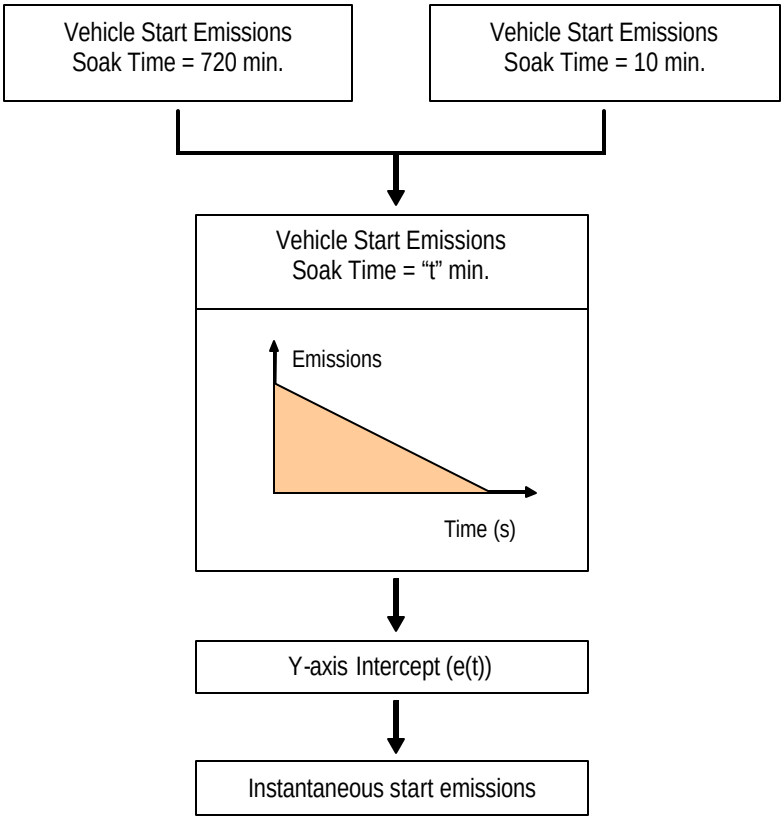

Figure 8-2. Proposed Framework for Estimating Vehicle Start Emissions

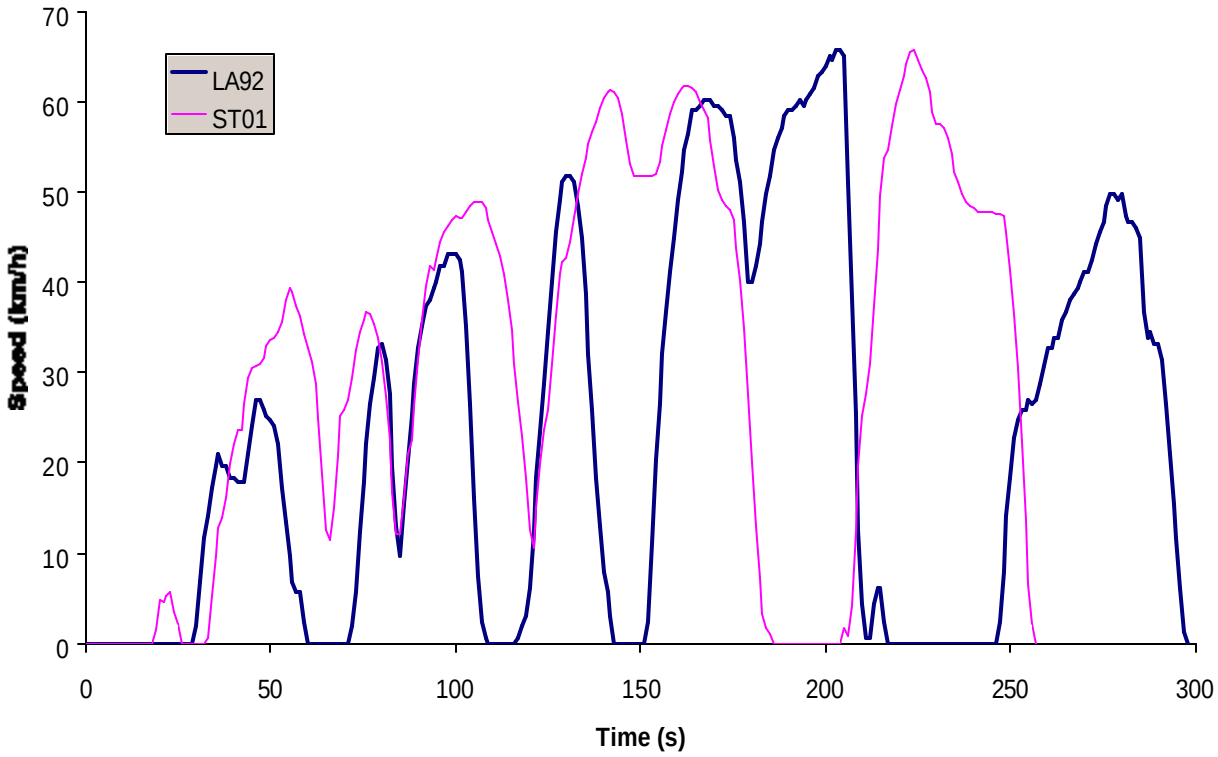

Figure 8-3. Speed Profiles for LA92 and ST01 Drive Cycles

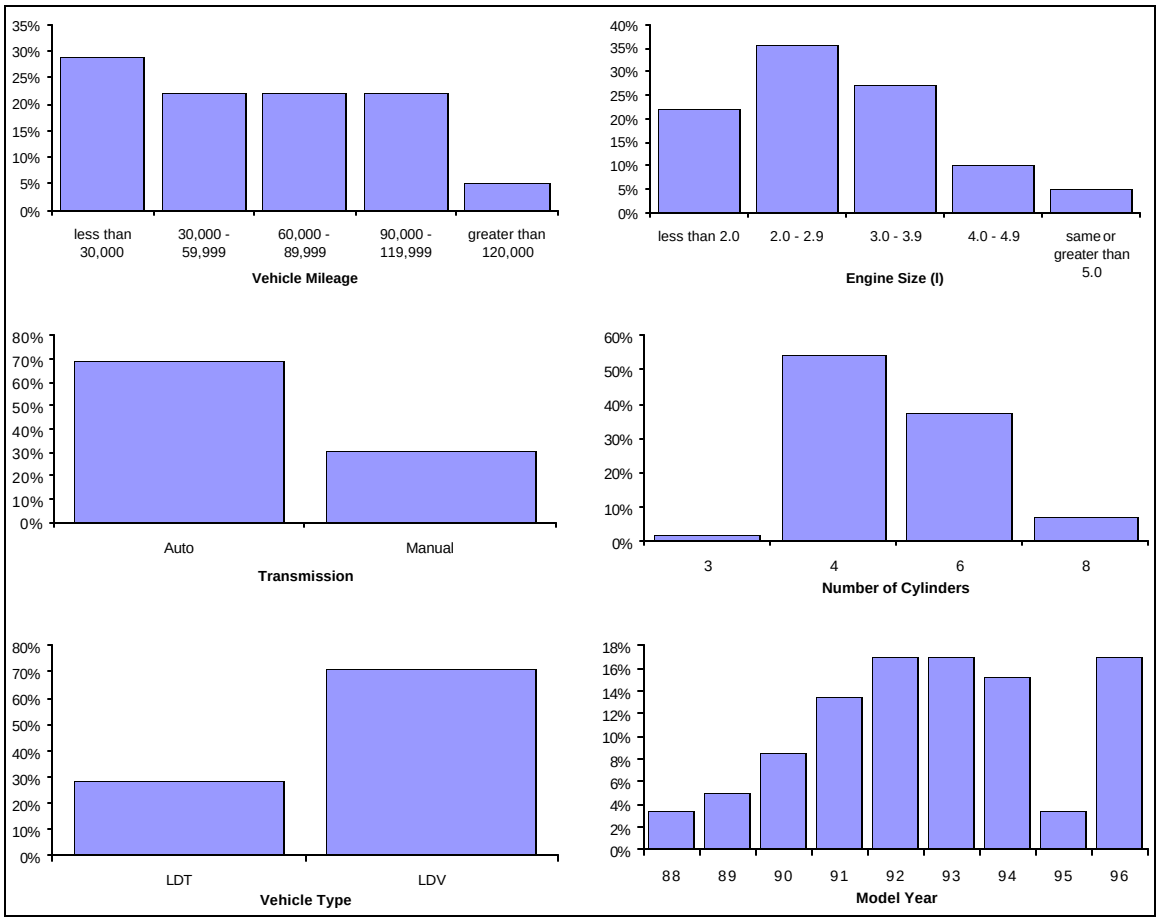

Figure 8-4. EPA Test Vehicle Characteristics

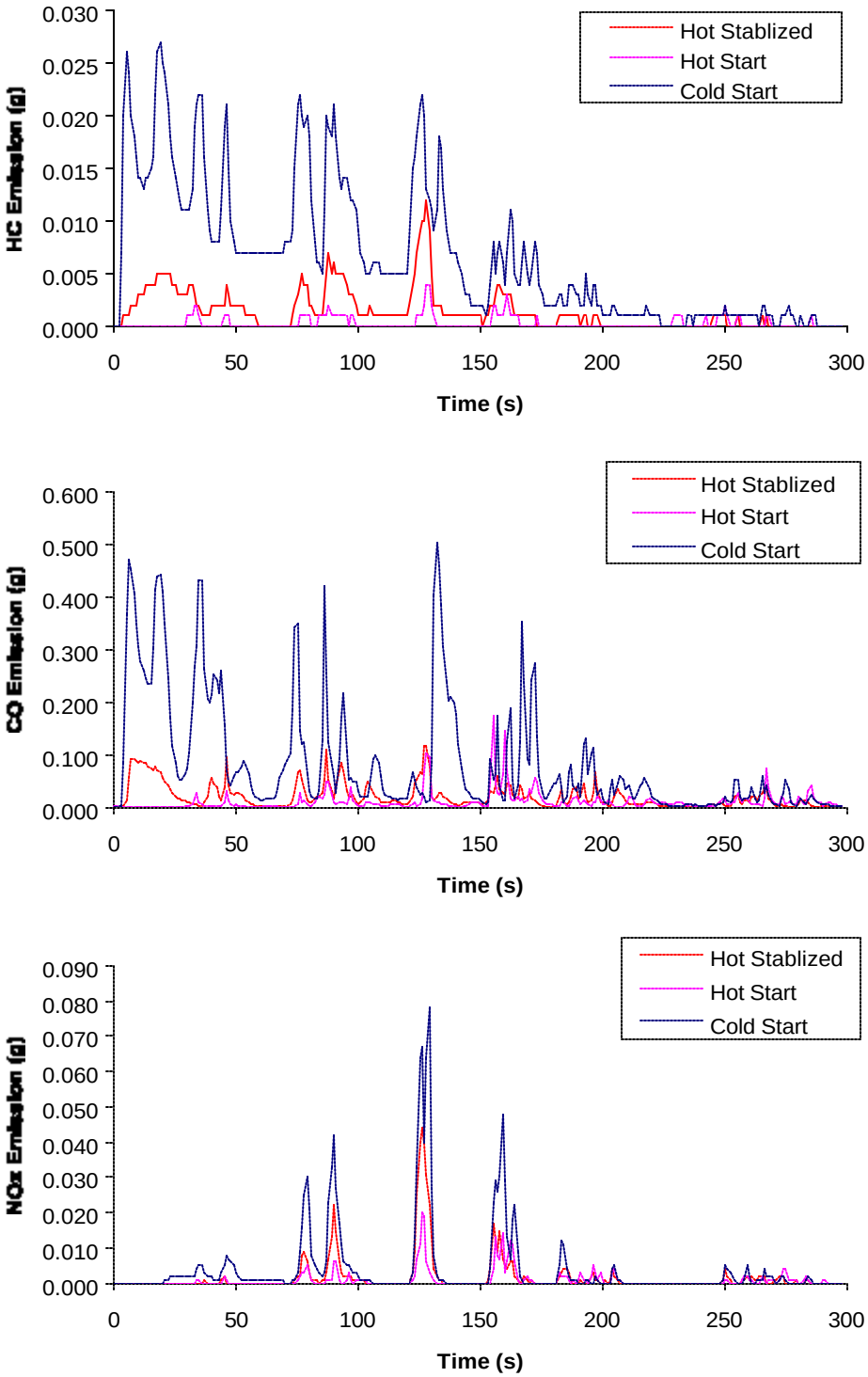

Figure 8-5. Microscopic Engine Start Emissions for a Sample Vehicle (Vehicle 5174)

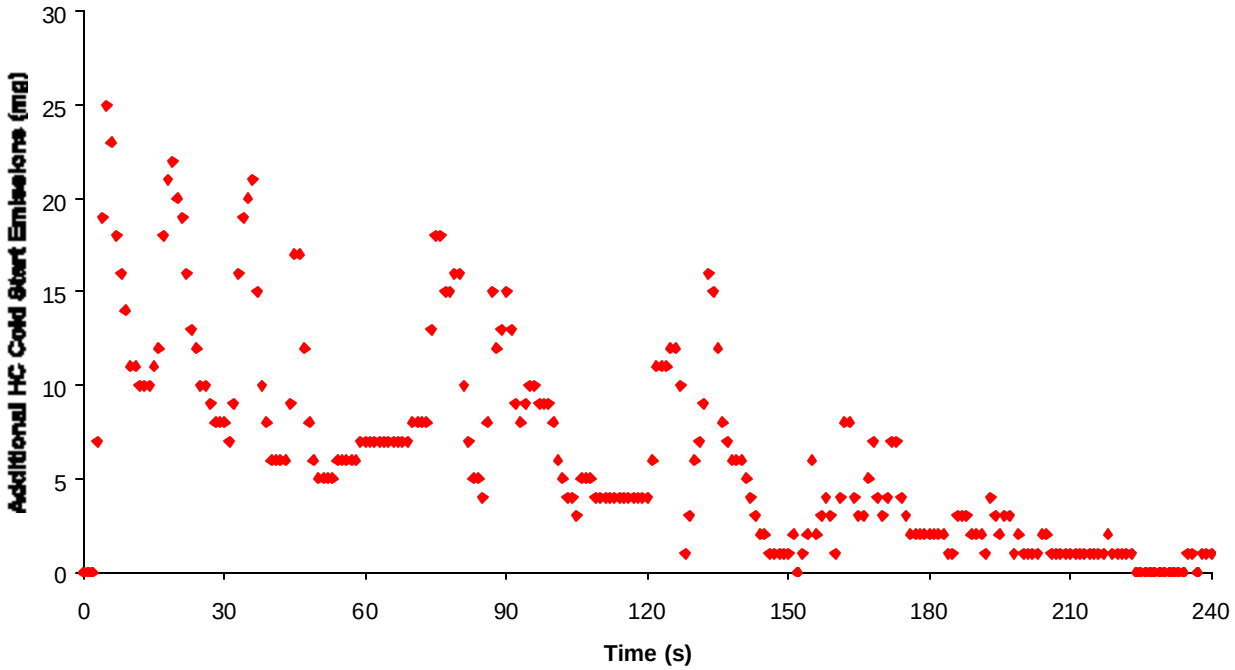

Figure 8-6. Additional HC Emissions Attributed to Cold Start Operation (Emission Difference between Cold Start and Hot Stabilized Conditions)

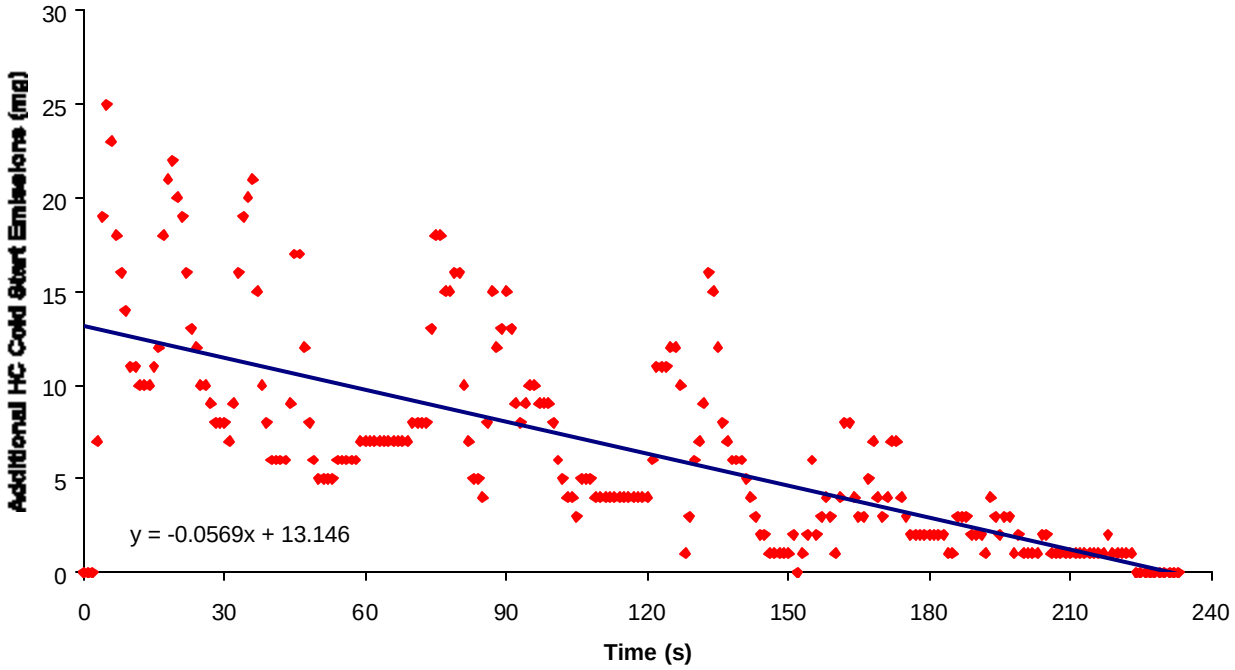

Figure 8-7. Regression Model Cold Start Emission Model for Sample Vehicle (Vehicle 5174)

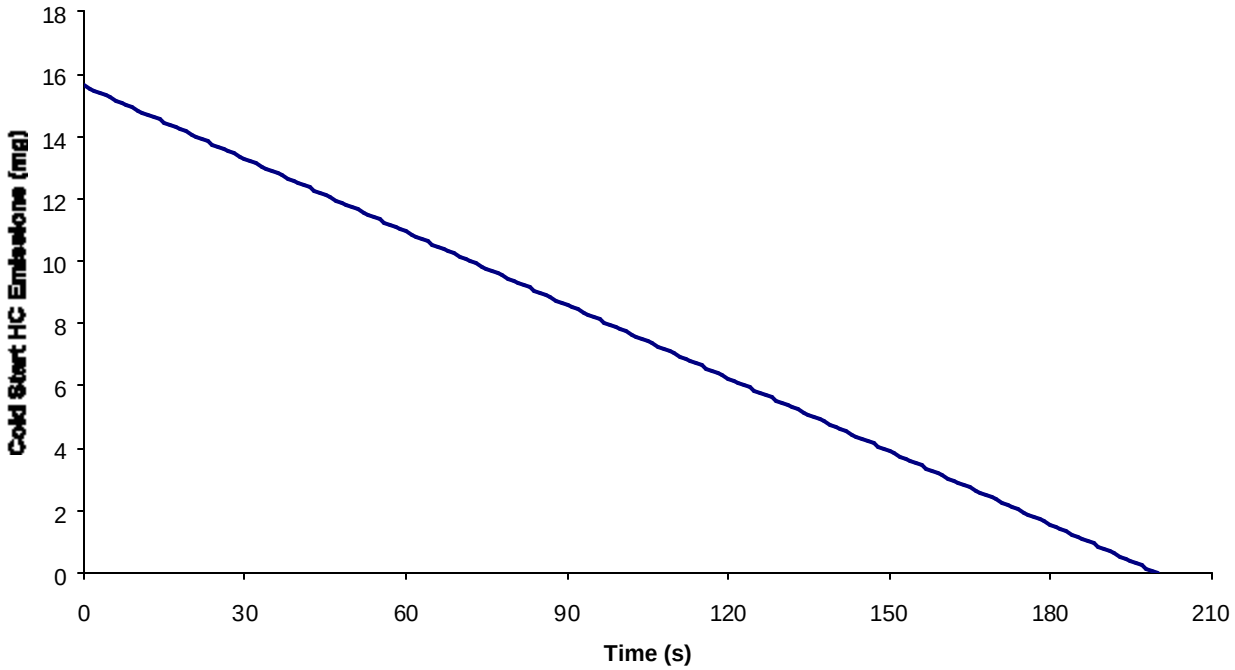

Figure 8-8. Proposed Linear Decay Function in Cold Start Emissions for Sample Vehicle

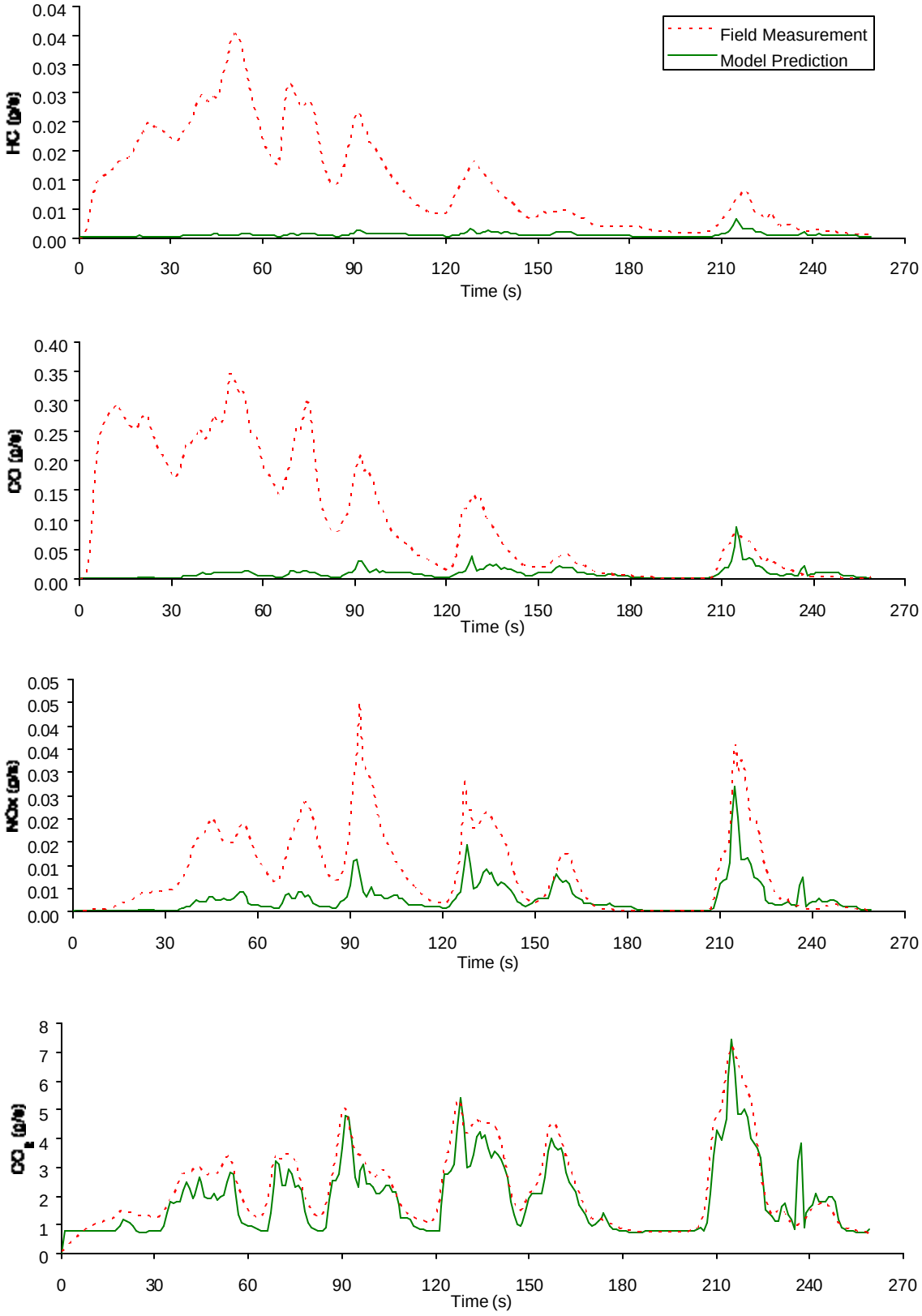

Figure 8-9. Instantaneous Hot Stabilized Emission Variation

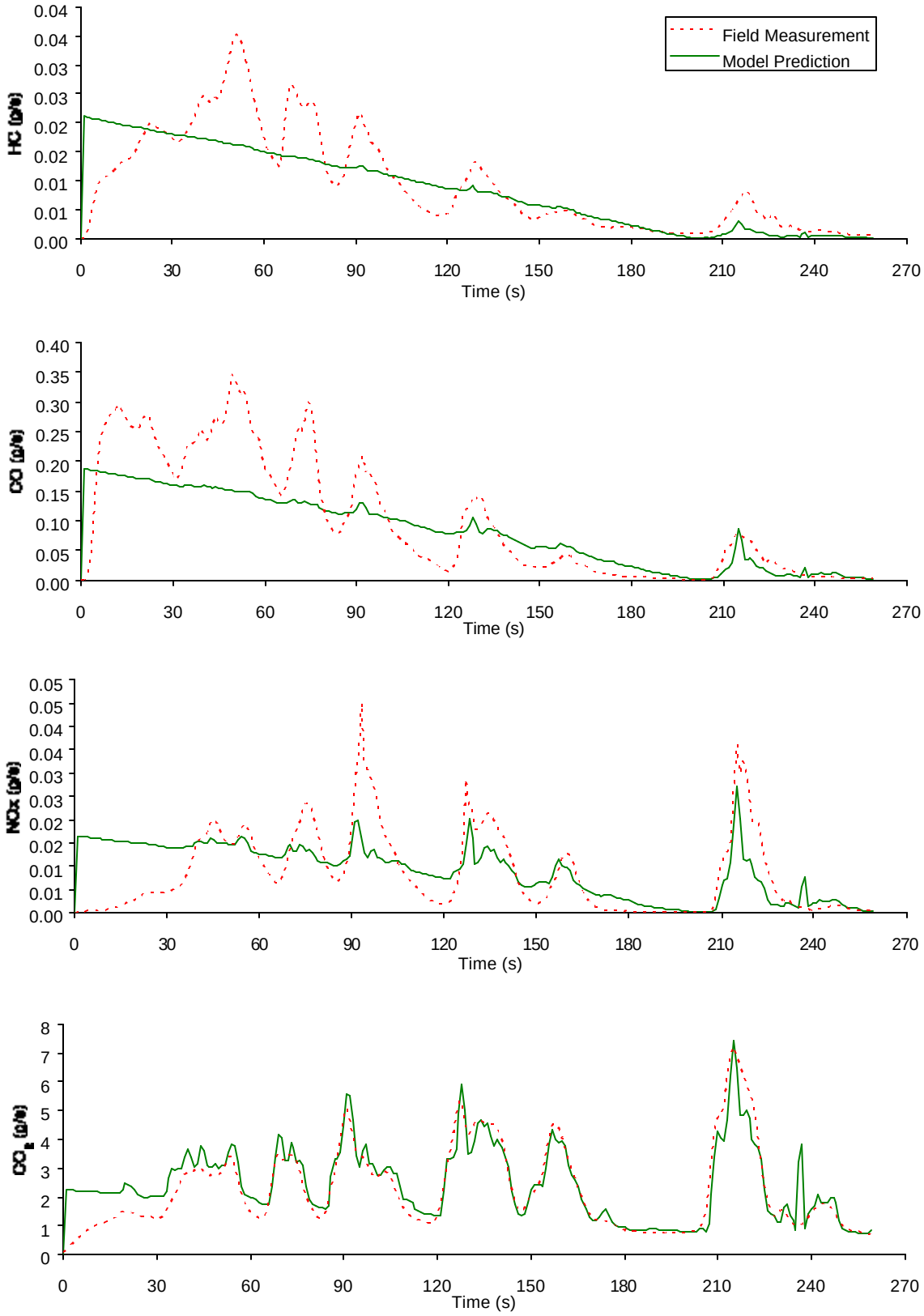

Figure 8-10. Instantaneous Cold Start Emission Validation (Smoothing Factor = 1.0)

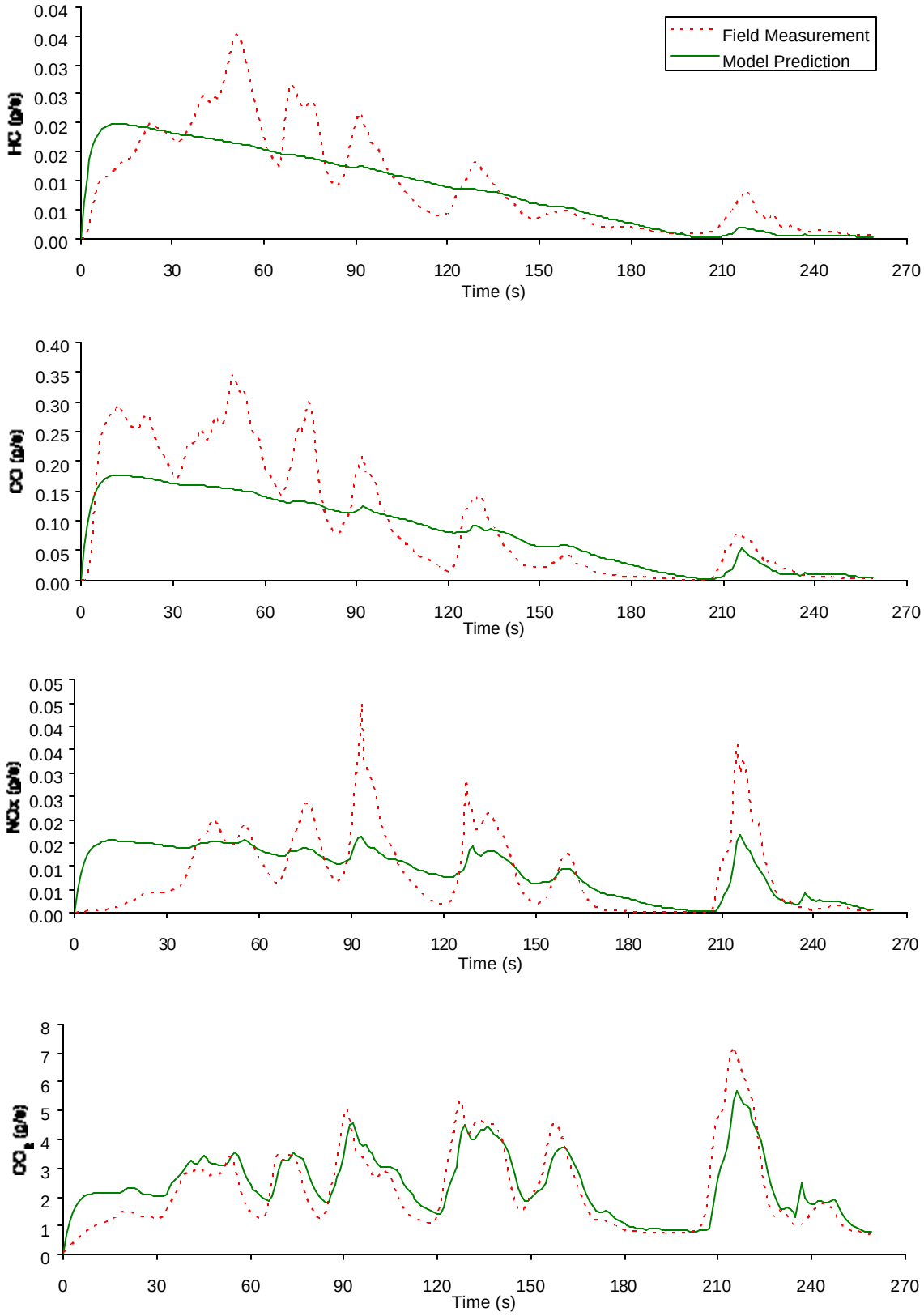

Figure 8-11. Instantaneous Cold Start Emission Validation (Smoothing Factor = 0.3)

CHAPTER 9. CONCLUSIONS AND RECOMMENDATIONS FOR FURTHER RESEARCH

9.1 CONCLUSIONS

The research presented in this thesis developed a framework for modeling vehicle emissions microscopically. In addition, the framework is utilized to develop the VT-Micro model using a number of data sources. Key input variables to the VT-Micro model include instantaneous vehicle speed and acceleration levels. Based on the research presented in this thesis, the following conclusions can be drawn:

a. The power based models that were proposed earlier, namely the Post and Akcelik models, do not provide good MOE estimates when compared to field data. Instead, a log-transformed dual-regime 3rd order polynomial model structure, as proposed in this research effort, predicts fuel consumption and emission errors within an acceptable margin of error relative to field data.

b. The state-of-practice CMEM microscopic model exhibits some abnormal behaviors. First, the model estimates identical MOE estimates for speeds of 0 km/h regardless of the acceleration rate. Second, the model estimates constant MOE estimates during deceleration maneuvers. Third, the model generally underestimates MOEs for acceleration maneuvers when compared to EPA field data. Fourth, the CO emission estimates exhibit unrealistic behavior at low speeds and high acceleration levels (sudden drops of emissions). Finally, the NO_x emissions do not exhibit the typical decay in emission rates at high engine loads.

c. The VT-Micro model 1.0, which was developed using ORNL data, produces excellent results for hot stabilized conditions showing a good agreement between raw field data and the model predictions. The fuel consumption and emission models are found to be highly accurate compared to the ORNL data with coefficients of determination ranging from 0.92 to 0.99.

d. The VT-Micro model 1.0 has been demonstrated to be valid for light-duty hot stabilized normal vehicle tailpipe emissions. Specifically, the emission estimates were found to be

within the 95 percent confidence limits of field data and within the same level of magnitude as the MOBILE5a model. The proposed VT-Micro model was found to reflect differences in drive cycles and in a fashion that was consistent with field observations. Specifically, the model accurately captures the increase in emissions for the Ramp cycle, with its associated aggressive acceleration maneuvers, in comparison with other drive cycles.

e. The research also presents a framework for developing microscopic emission models for assessing the environmental impacts of transportation projects. The framework develops emission models by aggregating data using vehicle and operational variables. Specifically, statistical CART algorithms for aggregating vehicles into homogenous categories are utilized as part of the framework. In addition, the framework accounts for temporal lags between vehicle operational variables and vehicle emissions. Finally, the framework is utilized to develop the VT-Micro model version 2.0 utilizing EPA's second-by-second chassis dynamometer data for a total of 60 light duty vehicles and trucks. A total of 5 LDV and 2 LDT categories are developed as part of this research effort.

f. The model validation of the VT-Micro model 2.0 demonstrates that the emissions estimated are consistent with EPA field data for both aggregate and instantaneous emissions with errors ranging between 0 to 17 percent.

g. Without a consistent high emitter criteria standard, it is impossible to estimate accurate mobile source emissions. When similar vehicles are tested, the emission rates are very different depending on the test cycle when test conditions such as temperature, test fuel, etc. is identical. Depending on the test cycle and emission cut-point standards, a vehicle can be a high emitter or a normal vehicle. Therefore, it is recommended that each test cycle needs its own emission cut-point to classify emitter states. In this study, a scale factor method was applied to the EPA MOBILE6 drive cycles in order to obtain emission cut points for each cycle. Using the scale factor method, it is possible to utilize different drive cycles to characterize high emitting vehicles. For example, the low speed New York cycle may be tested in very contaminated urban areas while the Arterial LOS A cycle can be utilized for suburban or rural areas.

h. The VT-Micro 3.0 model is developed to include microscopic high emitter emission models that estimate second-by-second mobile source emissions in hot stabilized conditions using instantaneous vehicle speed and acceleration levels as input variables. The emission models were developed using the EPA second-by-second emission data, which include off-cycle emissions and aggressive driving behaviors. The high emitting vehicles in the database are categorized by vehicle characteristics/technologies using the criteria utilized within the CMEM model, thus creating four high emitter groups.

i. The high emitter models were found to produce vehicle emissions consistent with EPA data at the aggregate and instantaneous level of resolution. Specifically, the average relative error over all 15 drive cycles was 3, 5, 10, and 1 percent for HC, CO, NO_x, and CO_2 emissions, respectively.

j. Aggregate cold start emissions (soak time of 720 minutes) are computed as the difference in measured emissions in the FTP bag1 and HR505 drive cycles. In addition, vehicle start emissions for a soak time of 10 minutes are computed as the difference between field measurements for the FTP bag3 and HR505 drive cycles. The state-of-practice approach for estimating aggregate vehicle start emissions is to utilize the 10-minute and 720-minute soak time emission rates as boundary conditions for computing a soak time dependent function. The research presented in this thesis extends the state-of-practice aggregate approach to develop a microscopic framework that is consistent with the state-of-practice macroscopic approach for estimating vehicle start emissions.

k. The proposed framework demonstrates that a 200-second decay interval in vehicle start emissions is a reasonable assumption. Furthermore, a linear decay function appears to capture the decay in cold start emissions.

l. The cold start emission model estimates were validated by comparing against aggregate and instantaneous field data. The results indicated that aggregate emission estimates were within 14 percent of field measurements for all four emissions considered (HC, CO, NO_x, and CO_2). Furthermore, instantaneous emission predictions were found to generally follow field measurements.

The ultimate expansion of this model is its implementation within a microscopic traffic simulation environment in order to evaluate the environmental impacts of alternative ITS and non-ITS strategies. Also, the model can be applied to estimate vehicle emissions using instantaneous GPS speed measurements (Rakha *et al.*, 2000a). Currently, the VT-Micro model has been implemented in the INTEGRATION software for the environmental assessment of operational-level transportation projects.

9.2 RECOMMENDATIONS

The following areas of research should be pursued to expand the applicability of the models developed in the context of microscopic traffic simulation:

a. More field data are required using on-board instrumentation to expand the model and to cover a wider range of the current on-road vehicle fleet.

b. The environmental impact of heavy-duty vehicles cannot be ignored in the modeling process. Data on heavy-duty vehicle emissions are required to develop similar microscopic models.

c. Models should introduce other important pollutants such as particulate matters.

d. Further research is required to characterize how vehicle start emissions vary as a function of a number of factors including ambient temperature, relative humidity, aggressiveness of the drive cycle, and the vehicle soak time.

e. This model is developed for standard temperature condition, 75 degrees F. Therefore, it is not suitable for emissions estimation for other hot or cold areas. The effect of ambient temperature and relative humidity on vehicle emissions should be studied.

f. Further research is required to characterize the variability in vehicle emissions as a function of different variables including the ambient temperature, relative humidity, vehicle speed, vehicle acceleration, acceleration position, and other state variables.

g. On-line emission estimation techniques should be considered to expand the model.

h. Alternative data sources, including remote sensing emission data and bag emissions, should be investigated in estimating vehicle emissions.

i. Current VT-Micro model utilize two regimes. Complexity of model with different regimes should be investigated.

REFERENCES

Ahn, K., Rakha, H., Trani, A., and Van Aerde, M. (2002) Estimating vehicle fuel consumption and emissions based on instantaneous speed and acceleration levels, *Journal of Transportation Engineering*, 128(2), 182-190.

Ahn, K., Trani, A., Rakha, H., and Van Aerde, M. (1998) Microscopic fuel consumption and emission modeling, , Presented at 77th Annual Meeting of the Transportation Research Board, Washington, D.C.

Akcelik, R. (1989) Efficiency and Drag in the Power-Based Model of Fuel Consumption, *Transportation Research* 23B, 376-385.

Akcelik, R. (1985) An Interpretation of the parameters in the Simple Average Travel Speed Model of Fuel Consumption, *Australian Road Research* 15, 46-49.

An, F., Barth, M., Scora, G., and Ross, M. (1998). Modeling Enleanment Emissions for Light-Duty Vehicles, *Transp. Res. Rec. 1641*, 48-57.

An, F., and M. Ross (1993a) Model of Fuel Economy with applications to Driving Cycles & Traffic Management, Presented at 72nd Annual Meeting of the Transportation Research Board, Washington, D.C.

An, F., and M. Ross (1993b) A Model of Fuel Consumption and Driving Patterns, SAE 930328

An, F., M. Ross, and A. Bando. (1993c) *How To Drive To Save Energy and Reduce Emissions in Yore Daily Trip*, RCG/Hagler, Bailly, Inc., Arlington, Va., And The University of Michigan, Ann Arbor, 10 PP.

Baker, M. (1994) *Fuel Consumption and Emission Models for Evaluating Traffic Control and Route Guidance Strategies*, Mater thesis, Queen's University, Kingston, Ontario, Canada

Barth, M., An, F., Younglove, T., Scora, G., Levine, C., Ross, M., and Wenzel, T. (2000) *Comprehensive modal emission model (CMEM), version 2.0 user's guide.*

Barth, M., Norbeck, J., and Ross, M. (1998) National Cooperative Highway Research Program Project 25-11 Development of a Comprehensive Modal Emissions Model, Presented at the 77th Annual Meeting of the Transportation Research Board, Washington, D.C.

Barth, M., An, F., Norbeck, J., and Ross, M. (1996) Model Emission Modeling: A Physical Approach, *Transp. Res. Rec. 1520*

Breiman, L., Friedman, J.H., Olshen, R.A., and Stone, C.J. (1984) *Classification and regression trees*, Wadsworth International Group, CA.

Brzezinski, D.J., Enns, P, and Hart, C. (1999a) Facility-Specific Speed Correction Factors, MOBILE6 Stakeholder Review Document (M6.SPD.002), US EPA, Ann Arbor, Michigan.

Brzezinski, D.J., Glover, E., and Enns, P. (1999b) The Determination of Hot Running Emissions From FTP Bag Emissions, MOBILE6 Stakeholder Review Document (M6.STE.002), US EPA, Ann Arbor, Michigan.

Carlson, T.R., Austin, T.C. (1997) Development of Speed Correction Cycles, MOBILE6 Stakeholder Review Document (M6.SPD.001), Prepared for EPA by Sierra Research, Inc., Ann Arbor, Michigan.

Chang, M., Evans, L., Herman, R., and Wasielewski P. (1979) Gasolin Consumption in Urban Traffic, *Transp. Res. Rec.* 599

Davis, S.C. (1994) *Transportation Energy Data Book: Edition 14*, ORNL-6798. Center for Transportation Analysis, Energy Division, Oak Ridge National Laboratory, Tenn., May.

DeCorla-Souza, P. (1993) Travel and Emissions Model Interactions, Presented at Transportation-Air Quality Conference, Washington, D.C., 23-26

Ding, Y. (2000) *Quantifying The Impact Of Traffic-Related and Driver-Related Factors On Vehicle Fuel Consumption And Emissions*, Mater thesis, Virginia Polytechnic Institute and State University, Blacksburg, VA

Enns, P. and Brzezinski, D.J. (2001) Comparison of Starting Emissions in the LA92 and ST01 Test Cycles, Draft. MOBILE6 Stakeholder Review Document (M6.STE.001), US EPA, Ann Arbor, Michigan.

Enns, P., J. German, and J. Markey, (1993) EPA's Survey of In-Use Driving Patterns: Implications for Mobile Source Emission Inventories, Office of Mobile Sources, U.S. EPA.

EPA (2001a) *User's Guide to Mobile 6 Draft, Mobile Source Emission Factor Model*, Ann Arbor, Michigan.

EPA (2001b) State Implementation Plans, (http://www.epa.gov/ARD-R5/sips/) Access date: May, 06, 2001

EPA (1997a) Development of Speed Collection Cycles. Draft. M6. SPD.001, Prepared by Sierra Research, Ann Arbor, Michigan.

EPA (1994a) Automobile Emissions: An Overview, U.S. Environmental Protection Agency Report No. EPA 400-F-92-007. August (http://www.epa.gov/omswww/05-autos.htm) Access date: May, 06,2000

EPA (1994b) Milestones in Auto Emissions Control, U.S. Environmental Protection Agency Report No. EPA 400-F-92-014. August (http://www.epa.gov/omswww/12-miles.htm) Access date: May, 06, 2001

EPA (1993a) Automobile and Carbon Monoxide, U.S. Environmental Protection Agency Report No. EPA 400-F-92-005. January

EPA (1993b) Federal Test Procedure Review Project: Preliminary Technical Report. Office of Air and Radiation, May

EPA (1993c) *MOBILE 5A User Guide*, Ann Arbor, Michigan.

Fisk, C. S. (1989) The Australian Road Research Board instantaneous model of fuel consumption Transportation Research. 23B, 373-376.

Glover, E.L. and Koupal, J.W. (1999) Determination of CO basic emission rates, OBD and I/M effects for tier1 and later LDVs and LDTs, MOBILE6 Stakeholder Review Document (M6.EXH.009), US EPA, Ann Arbor, Michigan.

Glover, E., Carey, P., Enns, P. and Brzezinski, D.J. (1998) Determination of Start Emissions as a Function of Mileage and Soak Time for 1981-1993 Model Year Light-Duty Vehicles, Draft. MOBILE6 Stakeholder Review Document (M6.STE.003), US EPA, Ann Arbor, Michigan.

Guensler, R. et al. (1998) Overview of the MEASURE Modeling Framework, Presented at the 77th Annual Meeting of the Transportation Research Board, Washington, D.C.

Guensler, R., S. Washington, and D. Sperling. (1993) A Weighted Disaggregate Approach To Modeling Speed Correction Factors, Presented at the 72nd Annual Meeting of the Transportation Research Board, Washington, D.C., 44pp.

Heinsohn, R.J. and Kabel, R.L. (1999) Sources and Control of Air Pollution, Prentice Hall, pp 101

Hellman, K.H. and Heavenrich, R.M. (2001) Light-Duty Automotive Technology and Fuel Economy Trends; 1975 through 2001, EPA420-R-01-008, U.S. EPA.

Horowitz, J.L., (1982) *Air Quality Analysis for Urban Transportation Planning*, MIT Press, Cambridge, Mass., 387 pp.

Howitt, A.M. and Moore E.M. (1999) Implementing the Transportation Conformity Regulations, *TR News No 202* May-June, TRB National Research Council, Washington, D.C.

Insightful Corporation (2001) *S-Plus 6 guide to statistics volume 1 and volume 2*, Seattle, WA.

Johnson, J.H. (1988) *Automotive Emissions. Air Pollution, the Automobile, and Public Health. Health Effects Institute*, National Academy Press, Washington, D.C.

Koupal, J.W. and Glover, E.L. (1999). Determination of NOx and HC basic emission rates, OBD and I/M effects for tier1 and later LDVs and LDTs. MOBILE6 Stakeholder Review Document (M6.EXH.007). US EPA, Ann Arbor, Michigan.

LeBlanc, D., M.D. Meyer. F.M. Saunders, and J.A. Mulholland (1994) Carbon Monoxide Emissions from Road Driving: Evidence of Emissions due to Power Enrichment, Presented at the 73rd Annual Meeting of the Transportation Research Board, Washington, D.C., 23pp.

Lewis, R.J. (2000). An introduction to classification and regression tree (CART) analysis. Paper presented at the 2000 Annual Meeting of the Society for Academic Emergency Medicine, San Francisco, CA.

Minnesota Pollution Control Agency (1998) State Implementation Plans, http://www.pca.state.mn.us/air/sip.html, St. Paul, MN.

Murrell, D. (1980) *Passenger Car Fuel Economy: EPA and Road*, U.S. EPA, Jan., 305 PP

National Research Council (2000) *Modeling Mobile-Source Emissions*, National Academy Press, Washington, D.C.

National Research Council (1997) *Improving Transportation Data for Mobile Source Emission Estimates*, National Academy Press, Washington, D.C.

National Research Council (1995) *Expanding Metropolitan Highways: Implications for Air Quality and Energy Use*, National Academy Press, Washington, D.C.

Nizich, S.V., T.C. McMullen, and D.C. Misenheimer (1994). National Air Pollutant Emissions Trends, 1900-1993. EPA-454/R-94-027. Office of Air Quality Planning and Standards, Research Triangle Park, N.C., Oct,. 314 PP.

Pidgeon, W. M. and Dobie, N. (1991) The IM240 Transient I/M Dynamometer Driving Schedule and The Composite I/M Test Procedure, EPA-AA-TSS-91-1, http://www.epa.gov/otaq/im240rpt.htm, Asscess: Oct/24/2001

Post, K. Kent, J.H. Tomlin, J. and Carruthers, N. (1984) Fuel consumption and emission modeling by power demand and a comparison with other model, *Transpn. Res.* 18A, 191-213.

Rakha, H., Medina, A., Sin, H., Dion, F., Van Aerde, M., and Jenq, J. (2000a). Traffic signal coordination across jurisdictional boundaries: Field evaluation of efficiency, energy, environmental, and safety impacts. *J. Transp. Res. Rec.*,1727, 42–51.

Rakha, H., Van Aerde, M., Ahn, K., and Trani, A. (2000b). Requirements for evaluating traffic signal control impacts on energy and emissions based on instantaneous speed and acceleration measurements, *J. Transp. Res. Rec.*, 1738, 56–67.

Rakha, H., Ahn, K., and Trani, A. (in press). Comparison of MOBILE5a, VT-MICRO, and CMEM models for hot-stabilized light duty gasoline vehicles. Being considered for publication in the *Transportation Research: Part D.*

Richardson, A.J., and Akcelik, R. (1981) Fuel consumption Models and Data Needs for the design and Evaluation of Urban Traffic System, *Australian Road Research Board*, ARR 124, September

Singer, B.C., Kirchstetter, T.W., Harley, R.A.., Kendall, G.R., and Hesson, J.M. (1999) A Fuel-Based Approach to Estimating Motor Vehicle Cold Start Emissions, *Journal of the Air & Waste Management Association* 49, 125-135., Pittsburgh, PA.

U.S. DOT. (1997) Transportation Conformity: A Basic Guide for State and Local Officials. (http://www.bts.gov/NTL/data/fhwaconf.pdf)

U.S. DOT and EPA (1993) Clean Air Through Transportation: Challenges in Meeting National Air Quality Standards. Aug.

Venigalla, M., Miller, T., and Chatterjee, A. (1995) Alternative Operating Model Fractions to Federal Test Procedure Mode Mix for Mobile Source Emissions Modeling, *Transp. Res. Rec.*, 1472

Ward's Communications (1996) *Ward's Automotive Yearbook*. 58th Edition, Intertec Publishing., Southfield, MI.

Ward's Communications (1996) *Ward's Automotive Reports* Vol. 70, No. 51, December, Intertec Publishing., Southfield, MI.

Wayson, R., Cooper, CD., Brenner, ML., Kim, B., and Datz, A. (1998) Determination of Hot and Cold Start Percentages for the State of Florida to be Used in Mobile Source Emissions, Presented at 77th Transportation Research Board, Washington, D.C.

Washington, S., wolf, J., and Guensler, R. (1997) Binary Recursive Partitioning Method for Modeling Hot-Stabilized Emissions from Motor Vehicles, *Transp. Res. Rec. 1587*, 96-105

Wenzel, T. and Ross, M. (1998) Characterization of Recent-Model High-Emitting Automobiles, *Society of Automotive Engineers*, Paper No. *981414*.

West, B., McGill, R., Hodgson, J., Sluder, S., Smith, D. (1997) Development of Data-Based Light-Duty Modal Emissions and Fuel consumption Models, *Society of Automotive Engineers*, Paper No. 972910

Wolf, J., Guensler, R., Washington, S., and Bachman, W. (1999) High-Emitting Vehicle Characterization Using Regression Tree Analysis *Transp. Res. Rec.*,1641.

APPENDIX

APPENDIX A

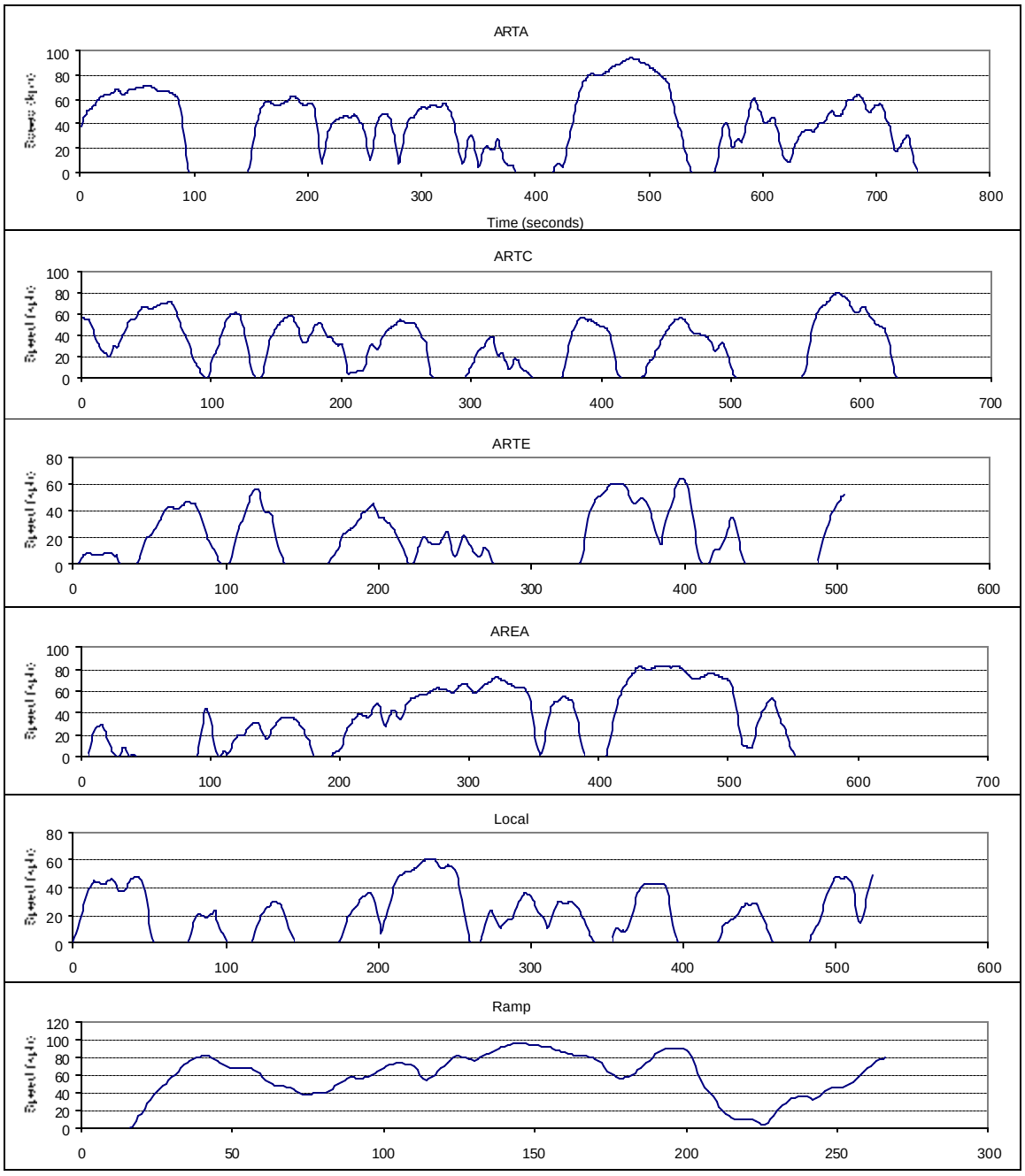

Figure A-1. Driving cycles of arterial and local road ways

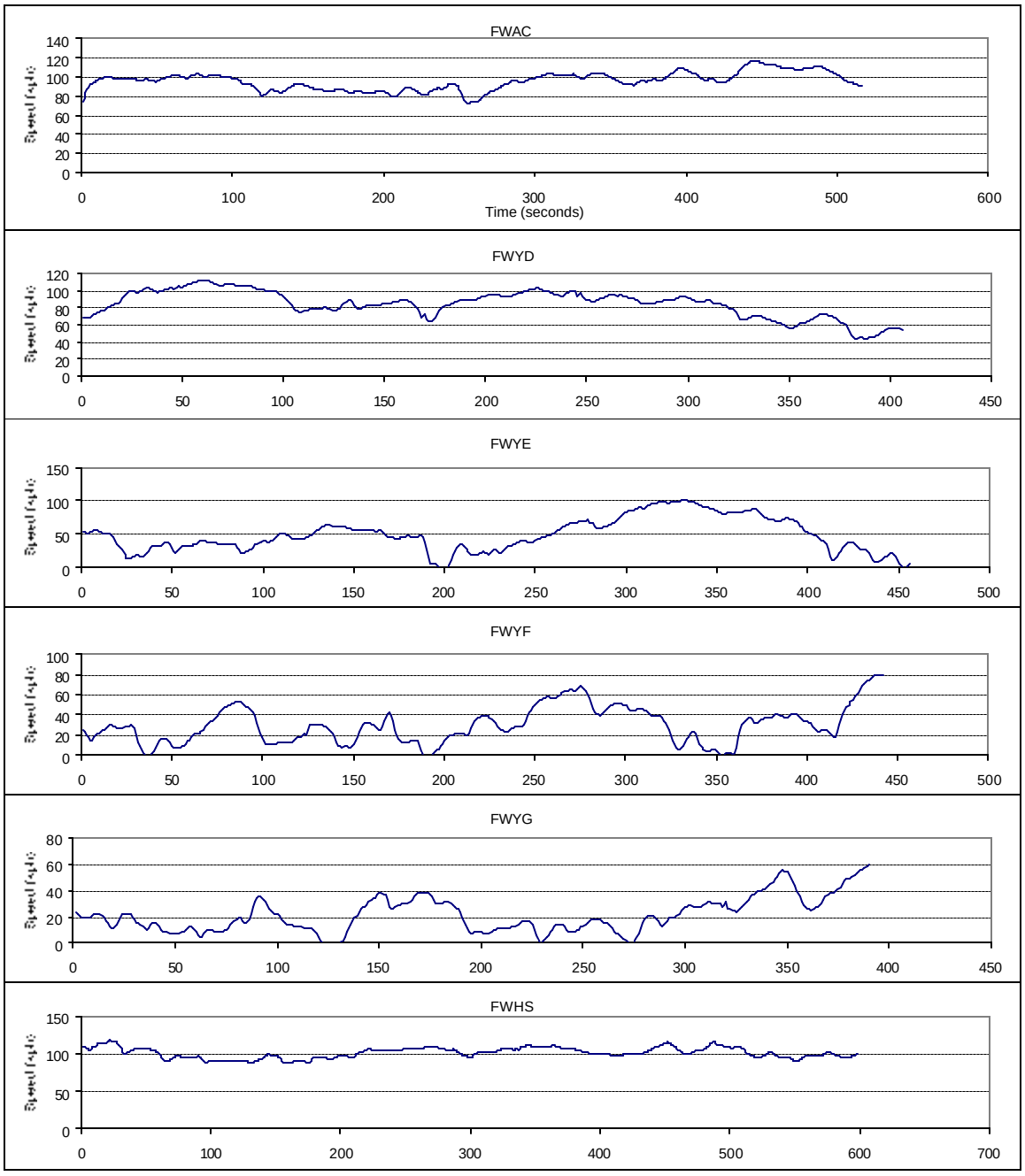

Figure A-2. Driving cycles of freeways

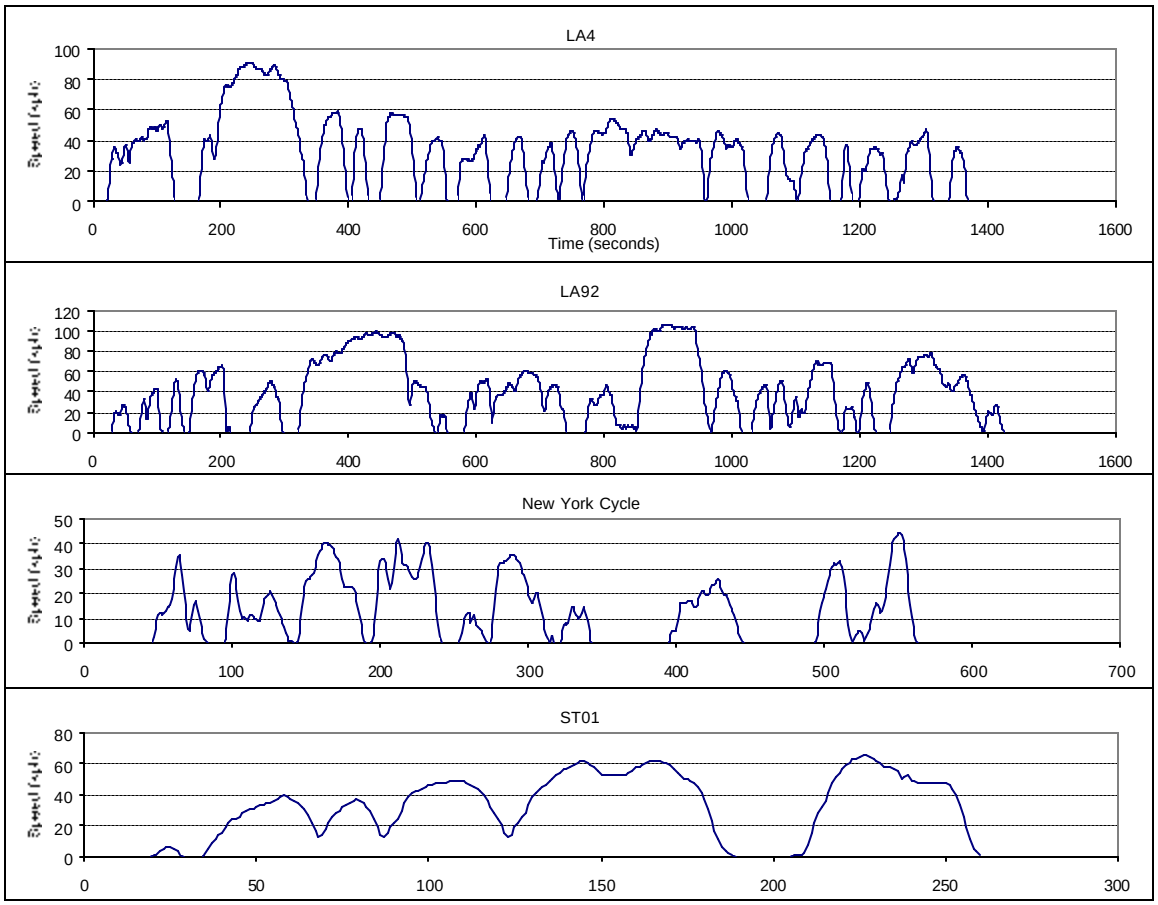

Figure A-3. Driving cycles of additional cycles

APPENDIX B

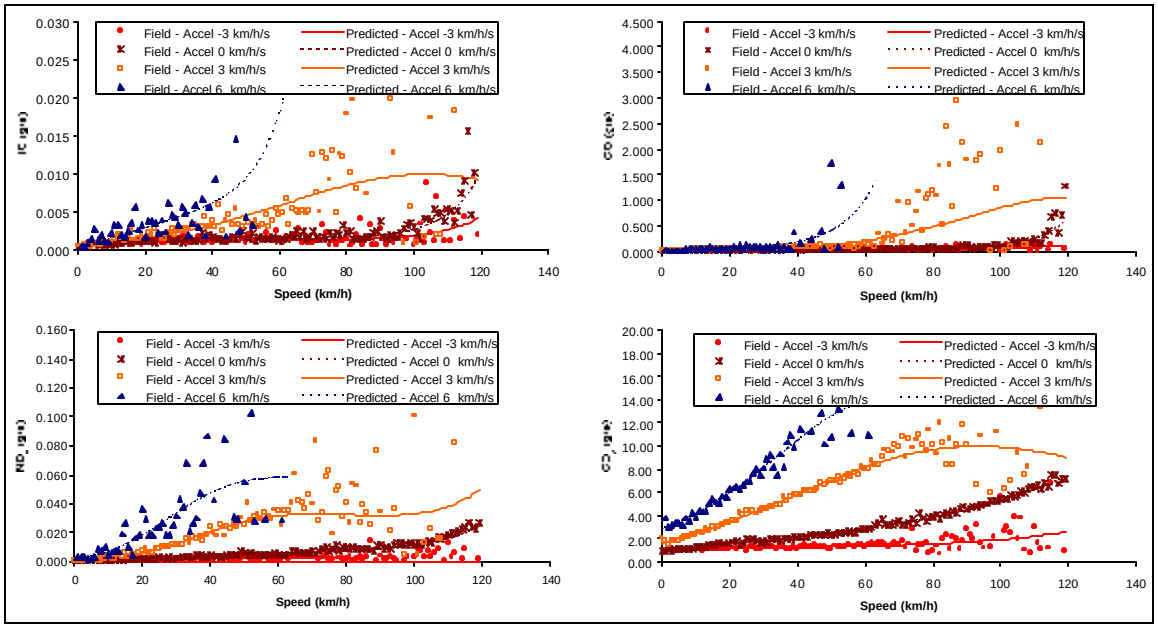

Figure B-1. Model Prediction (LDT2)

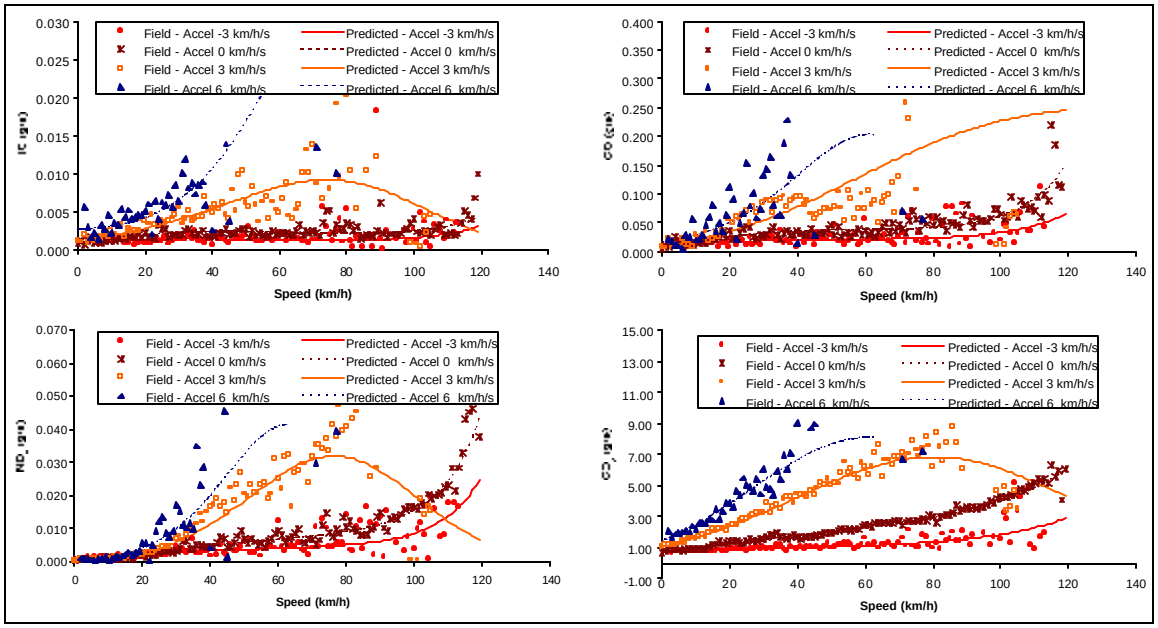

Figure B-2. Model Prediction (LDV1)

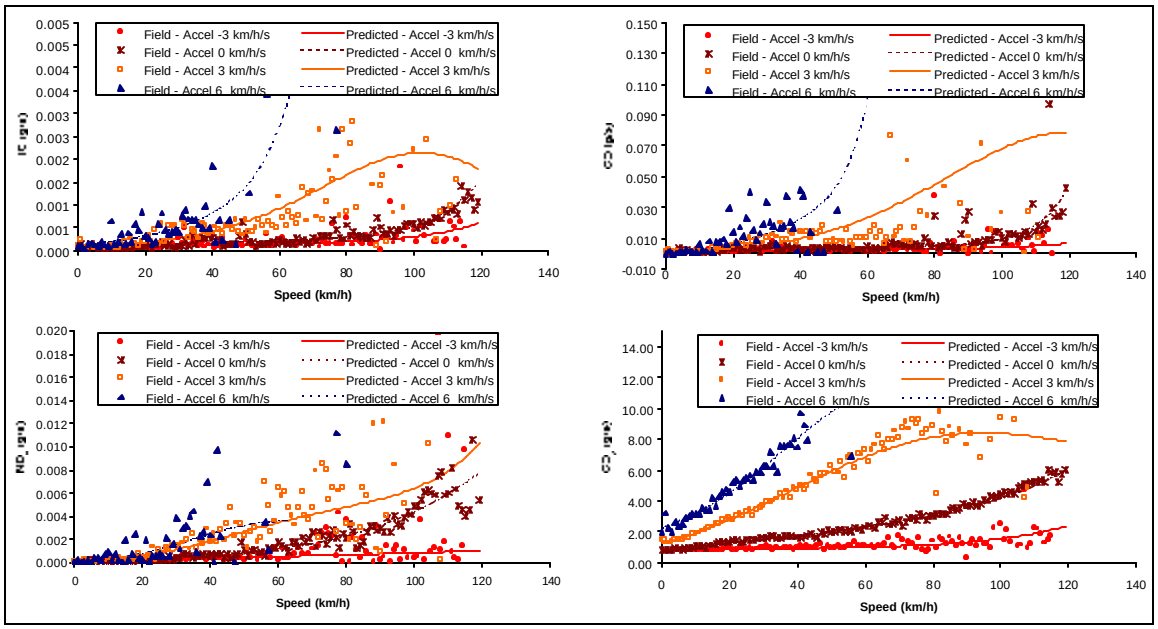

Figure B-3. Model Prediction (LDV3)

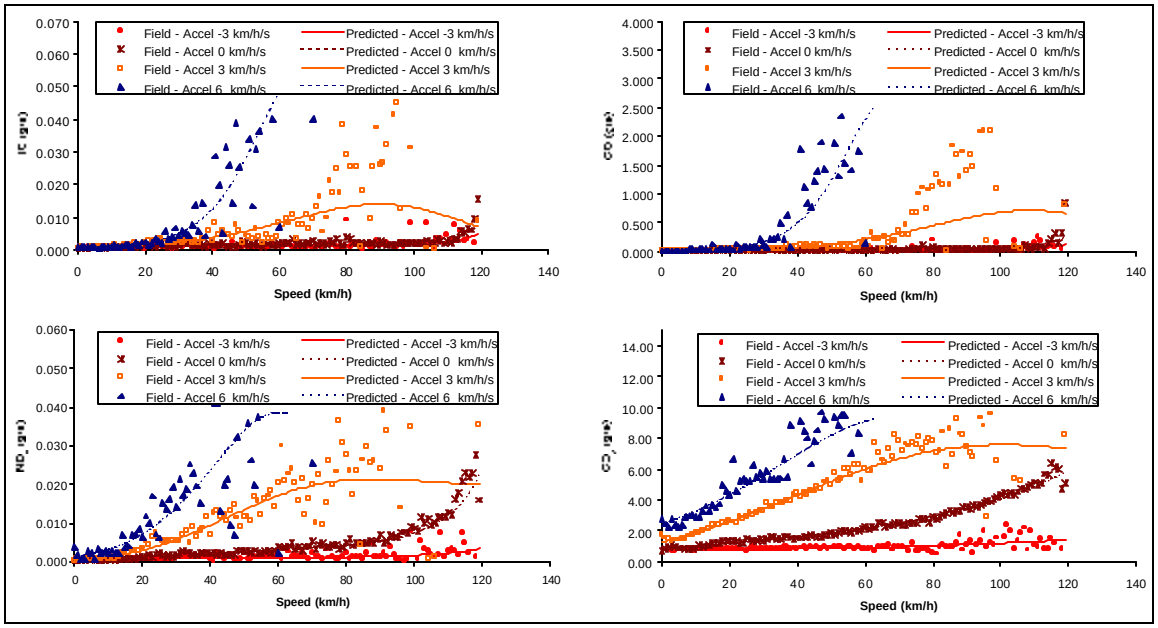

Figure B-4. Model Prediction (LDV4)

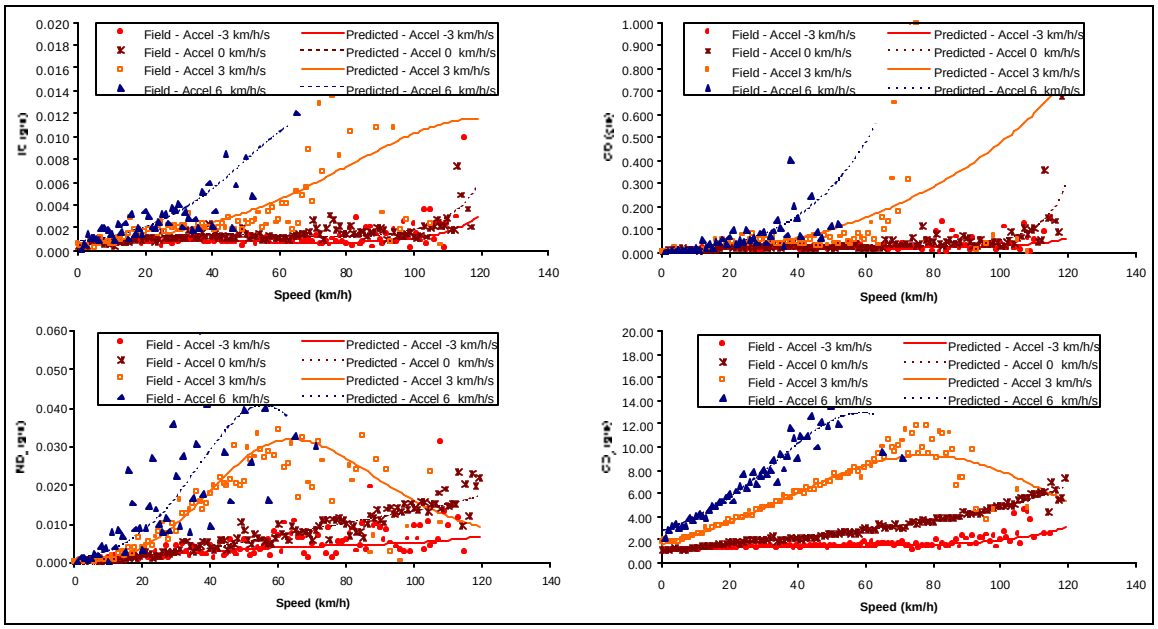

Figure B-5. Model Prediction (LDV5)

APPENDIX C

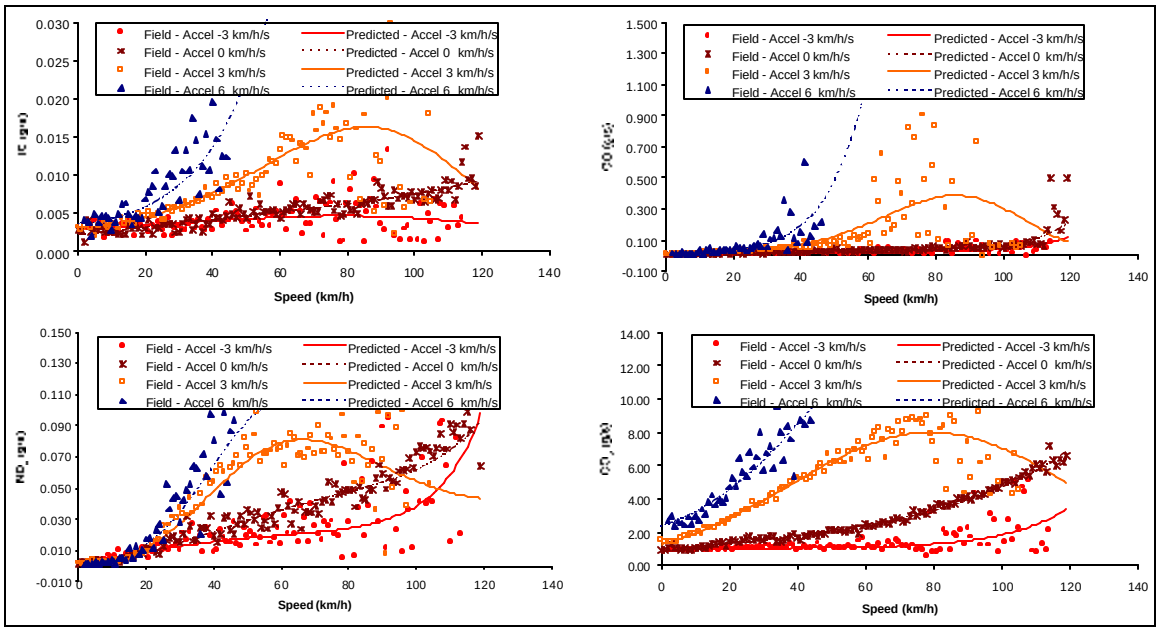

Figure C-1. Model Prediction (Vehicle Category High Emitter Group 1)

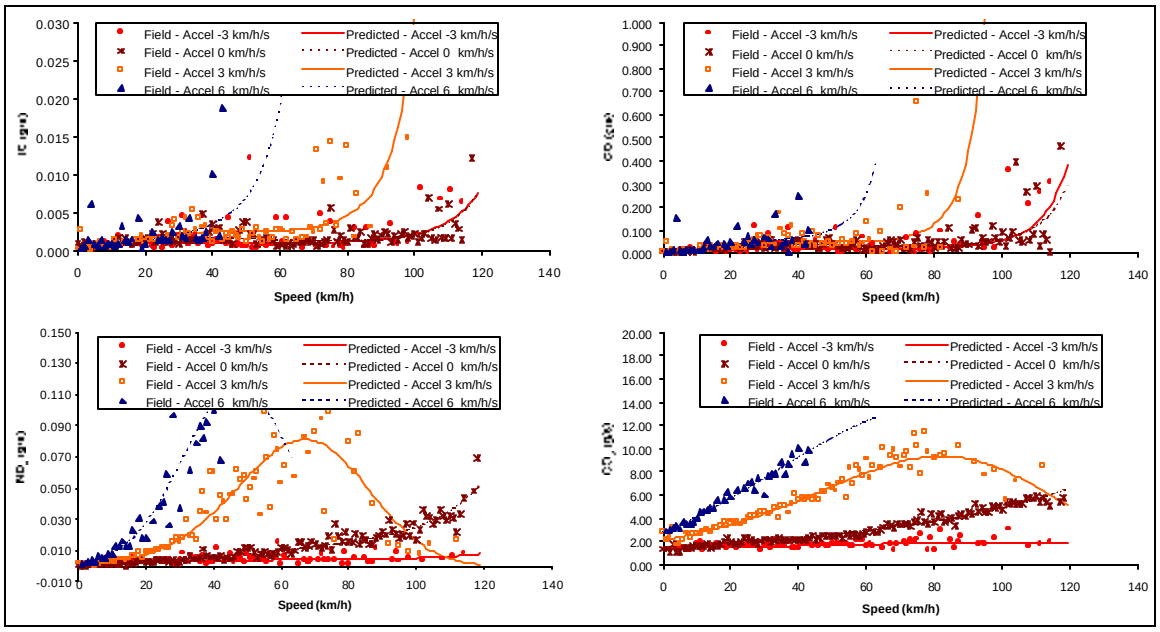

Figure C-2. Model Prediction (Vehicle Category High Emitter Group 2)

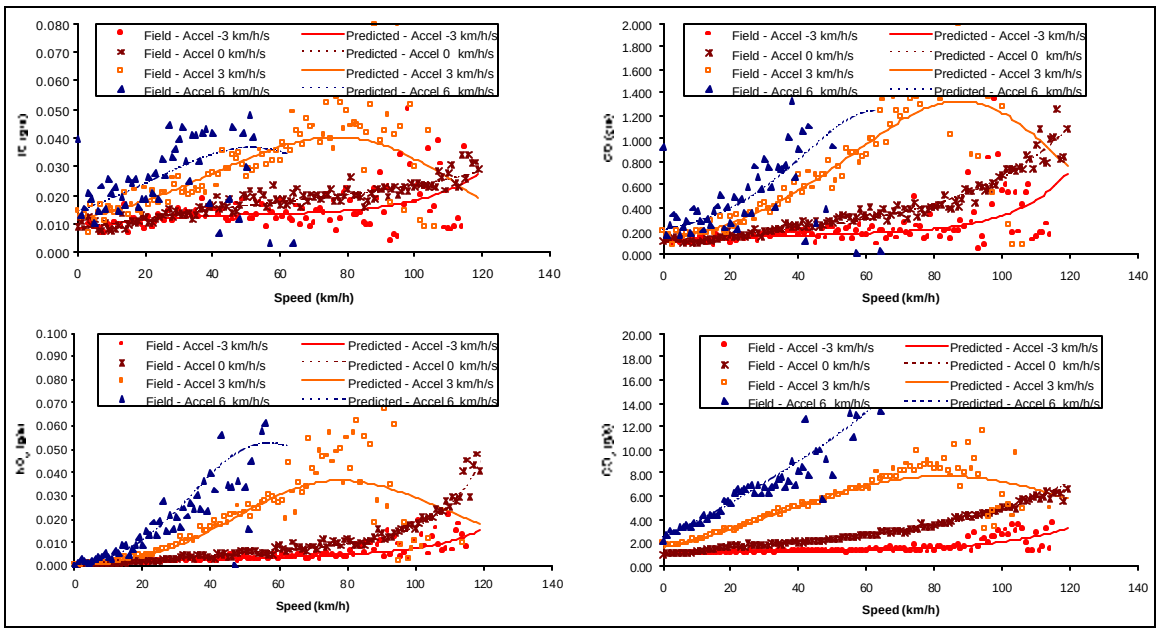

Figure C-3. Model Prediction (Vehicle Category High Emitter Group 3)

VITA

Kyoungho Ahn was born on February, 1971 in Cheongju, Korea. He received a Bachelor of Engineering degree in the department of Urban Engineering from Chungbuk National University in Korea in 1996. In 1996, he began studies at Virginia Polytechnic Institute and State University. He completed a Master of Science degree in the department of Civil and Environmental Engineering (Transportation Major) in 1998. In May 2002, he received the Doctor of Philosophy Degree in Civil and Environmental Engineering (Transportation Major). While progressing toward the completion of his degrees, he worked as a graduate research assistant in the Virginia Tech Transportation Institute (previous the Center for Transportation Research) at Virginia Tech.